USGS
science for a changing world

Prepared in cooperation with the U.S. Department of Agriculture, U.S. Forest Service, Gifford Pinchot National Forest

A Multidecade Analysis of Fluvial Geomorphic Evolution of the Spirit Lake Blockage, Mount St. Helens, Washington

Scientific Investigations Report 2020–5027

U.S. Department of the Interior
U.S. Geological Survey

Cover. Oblique aerial view to south of Mount St. Helens and Spirit Lake blockage. The blockage occupies the center and left sides of the image below the volcano. Channels on the left side of image drain northeast toward Spirit Lake, those on far right of image drain northwest toward North Fork Toutle River. Photograph by Jon Major taken July 16, 2018.

A Multidecade Analysis of Fluvial Geomorphic Evolution of the Spirit Lake Blockage, Mount St. Helens, Washington

By Jon J. Major, Gordon E. Grant, Kristin Sweeney, and Adam R. Mosbrucker

Prepared in cooperation with the U.S. Department of Agriculture, U.S. Forest Service, Gifford Pinchot National Forest

Scientific Investigations Report 2020–5027

U.S. Department of the Interior
U.S. Geological Survey

U.S. Department of the Interior
DAVID BERNHARDT, Secretary

U.S. Geological Survey
James F. Reilly II, Director

U.S. Geological Survey, Reston, Virginia: 2020

Suggested citation:
Major, J.J., Grant, G.E., Sweeney, K., and Mosbrucker, A.R., 2020, A multidecade analysis of fluvial geomorphic evolution of the Spirit Lake blockage, Mount St. Helens, Washington: U.S. Geological Survey Scientific Investigations Report 2020-5027, 54 p., https://doi.org/10.3133/sir20205027.

ISSN 2328-0328 (online)

Contents

Figures

Tables

Conversion Factors

International System of Units to U.S. customary units

Multiply	By	To obtain
	Length	
centimeter (cm)	0.3937	inch (in.)
millimeter (mm)	0.03937	inch (in.)
meter (m)	3.281	foot (ft)
kilometer (km)	0.6214	mile (mi)
kilometer (km)	0.5400	mile, nautical (nmi)
meter (m)	1.094	yard (yd)
	Area	
square meter (m^2)	0.0002471	acre
square kilometer (km^2)	247.1	acre
square meter (m^2)	10.76	square foot (ft^2)
square kilometer (km^2)	0.3861	square mile (mi^2)
	Volume	
cubic meter (m^3)	264.2	gallon (gal)
cubic meter (m^3)	0.0002642	million gallons (Mgal)
cubic meter (m^3)	35.31	cubic foot (ft^3)
cubic meter (m^3)	1.308	cubic yard (yd^3)
cubic kilometer (km^3)	0.2399	cubic mile (mi^3)
cubic meter (m^3)	0.0008107	acre-foot (acre-ft)
	Flow rate	
cubic meter per second (m^3/s)	70.07	acre-foot per day (acre-ft/d)
cubic meter per year (m^3/yr)	0.000811	acre-foot per year (acre-ft/yr)
meter per second (m/s)	3.281	foot per second (ft/s)
meter per minute (m/min)	3.281	foot per minute (ft/min)
meter per hour (m/h)	3.281	foot per hour (ft/h)

Multiply	By	To obtain
meter per day (m/d)	3.281	foot per day (ft/d)
meter per year (m/yr)	3.281	foot per year ft/yr)
cubic meter per second (m^3/s)	35.31	cubic foot per second (ft^3/s)
cubic meter per day (m^3/d)	35.31	cubic foot per day (ft^3/d)
	Mass	
gram (g)	0.03527	ounce, avoirdupois (oz)
kilogram (kg)	2.205	pound avoirdupois (lb)
metric ton (t)	1.102	ton, short [2,000 lb]
metric ton (t)	0.9842	ton, long [2,240 lb]

Datum

Vertical coordinate information is referenced to the North American Vertical Datum of 1988 (NAVD 88).

A Multidecade Analysis of Fluvial Geomorphic Evolution of the Spirit Lake Blockage, Mount St. Helens, Washington

By Jon J. Major,[1] Gordon E. Grant,[2] Kristin Sweeney,[3] Adam R. Mosbrucker[1]

Executive Summary

The eruption of Mount St. Helens on May 18, 1980, began with an immense landslide (debris avalanche) followed by a catastrophic, laterally directed pyroclastic density current (commonly called the "lateral blast" but herein called the "blast PDC"), and by subsequent pyroclastic flows. This suite of volcanic events reconfigured the Spirit Lake basin, blocked its outlet, and reset the fluvial landscape of upper North Fork Toutle River (NFTR) valley. Consequently, Spirit Lake basin effectively became a tub with no drain. To mitigate a potentially catastrophic breaching of the lake blockage, the U.S. Army Corps of Engineers bored a 2.5-km-long tunnel through bedrock to provide an outlet. The tunnel has performed its intended function and kept the lake at a safe level since becoming operational in 1985. However, episodic maintenance and repairs have required extended tunnel closures that have allowed the lake to rise occasionally to potentially problematic levels. Within this context, alternative lake outlets are being considered and evaluated. Here, we discuss characteristics of the blockage and geomorphic evolution of the drainage network on and near the blockage to provide additional landscape context for potential outlet options.

The Spirit Lake blockage is a composite of volcanic deposits that have variable thicknesses and degrees of resistance to erosion. The 1980 debris avalanche filled upper NFTR valley with more than 150 meters (m) of a heterogeneous sand-and-gravel mixture of shattered volcanic rock. Few particles in this deposit are larger in diameter than a few meters. Thus, the deposit is not strongly resistant to erosion if sufficient stream capacity to transport sediment is applied. The part of the debris-avalanche deposit that impounds Spirit Lake is overlain by a veneer of pyroclastic deposits that range in composition from rocky bits of sand and gravel to pumiceous gravel and silt. The sequence of pyroclastic deposits, emplaced during the May 18 and subsequent eruptions in 1980 and which ranges from individual deposits less than 1 m thick to a stratigraphic sequence nearly 40 m thick, has physical compositions that vary both laterally and vertically owing to overlapping of units. During emplacement of the pyroclastic flows, large billowing clouds of ash lofted upward and subsequently settled. These "ashcloud" deposits are very fine grained (mostly very fine sand and silt) and are interspersed stratigraphically within the pyroclastic-deposit sequence.

The profound landscape change caused by the cataclysmic eruption hydrologically disconnected upper NFTR basin on several scales. It severed hydrologic connection between the upper and lower parts of the basin, between hillsides and the valley floor, and between the volcano and the valley, and it isolated Spirit Lake. Landscape changes also temporarily altered streamflow magnitude and frequency within upper NFTR Basin. Basin reconnection required establishment of a new drainage network. Drainage development in upper NFTR basin began within hours after emplacement of the debris-avalanche deposit when several ponds on its surface, formed by groundwater seepage into depressions, enlarged and breached. Though channel initiation began within hours of deposit emplacement, it took nearly 3 years to fully integrate a new drainage network. By the mid-1980s, the drainage system was defined and well-established; since then, channels have enlarged, and their beds have coarsened. However, this drainage network lacks an overland outlet for Spirit Lake, as outflow passes through the tunnel, bypasses the blockage, and returns to NFTR downstream from Coldwater Lake.

Initial channel development on the blockage and farther downstream occurred during a period of enhanced runoff when the hydrologic regime that translates precipitation input to streamflow output was radically changed compared to pre-eruption conditions. For several years after the eruption, post-eruption streamflow peaks for a given precipitation input were larger than those before the eruption by a few percent to a few tens percent. Initially, channels upstream from Elk Rock, 20 kilometers (km) downstream from the volcano, incised swiftly by as much as tens of meters and widened by hundreds of meters. By the mid-1980s, rates and magnitudes of channel erosion had diminished, but since then channel widening has persisted more than channel incision. Furthermore, by the mid- to late 1980s geomorphic evolution across upper NFTR basin became more event-driven, requiring moderate- to

[1]U.S. Geological Survey

[2]U.S. Forest Service, Pacific Northwest Research Station

[3]University of Portland

large-magnitude daily mean streamflow (greater than 150 cubic meters per second, m^3/s, as measured below the U.S. Army Corps of Engineers' sediment retention structure 40 km downstream from the volcano) to do much geomorphic work beyond nibbling channel margins.

Overall channel positions appear to have been influenced primarily by basin topography and secondarily by geologic constraints. The overall position of the post-eruption drainage system bears strong resemblance to the pre-eruption drainage network. Despite thick valley fill, an overall topographic low abuts the base of the south face of Johnston Ridge—and both the pre-eruption and post-eruption courses of upper NFTR occupy that part of the landscape. Truman channel, an informal name for the watercourse that abuts Johnston Ridge closer to Spirit Lake and lies along the pre-eruption course of NFTR, was formed chiefly by water pumped from Spirit Lake from 1982–85. Its location was dictated largely by the location of the pumped outflow. Location of Loowit Creek channel, which drains the Mount St. Helens crater and cuts across the Pumice Plain, has been influenced largely by topography, but also by both pre- and post-eruption geology. Differential resistance to erosion among debris-avalanche and assorted pyroclastic-flow deposits, as well as the location of a pre-1980 lava flow, appears to have influenced channel position. Overall evolution of Loowit Creek channel has also been influenced by development of a fan of flood and debris-flow deposits formed at the base of the volcano's lower north flank. Near the apex of that fan, which lies along the blockage drainage divide, Loowit Creek channel and Step creek channel, another (informally named) drainage from the crater, are shallow (about 1 m), and Loowit Creek has switched its course from one side of the drainage divide to the other on several occasions. It presently (2020) flows westward toward NFTR, but with only modest sediment deposition on that fan it might easily switch and flow again toward Spirit Lake.

In most mountainous landscapes, channel adjustments typically occur in response to sediment transport during rainfall- or snowmelt-driven hydrologic events, such as floods, debris flows, and landslides. At Mount St. Helens, major hydrologic events also can be, and have been, driven by volcanic eruptions. With extensive glacier ice now covering much of the volcano's crater floor, there is potentially a readily available source of water during future eruptions. If liberated, a large volume of meltwater could cause extensive erosion of the Spirit Lake blockage and potentially initiate geomorphic instabilities along both perennial and ephemeral channels, which could have significant impact on channel stabilities.

Although the location of the drainage network in upper NFTR basin is largely settled, and the network now evolves mainly through persistent, low-magnitude erosion of channel banks, significant event-driven channel incision, particularly along Loowit Creek channel, still occurs. Single-storm incision of up to many meters occurred as recently as 2006. Furthermore, the swift and substantial incision of Truman channel (20 m of incision over a span of weeks to months), when pumping from Spirit Lake introduced a 5.1 m^3/s flow, vividly illustrates the exceptional mobility of sediment in this landscape and that even modest streamflow has abundant transport capacity under the right conditions. Our documentation of substantial erosion, channel avulsion, and patterns of channel evolution following emplacement of the Spirit Lake blockage illustrates the geomorphically dynamic character of upper NFTR basin. The considerable mobility of sediment in this landscape can establish geomorphic instabilities such as knickpoints or knickzones (abrupt steps in channel bottom profile) that can migrate rapidly headward and potentially trigger additional instabilities in smaller channels tributary to main-stem channels. These instabilities are most likely to occur when moderate to large amounts of concentrated surface runoff are introduced to parts of the landscape not adjusted to such flows.

The erosional susceptibility documented here has significant implications—and cautionary ramifications—for an open-channel outlet for Spirit Lake. The most logical location for an open-channel outlet is along or near the present alignment of Truman channel. But that channel has equilibrated to a mean streamflow of 5.1 m^3/s. Streamflow of substantially greater magnitude, almost certain because discharge would be unregulated and vary with lake level, is very likely to induce additional channel incision and widening unless the channel is heavily armored, especially given the overall 3-percent gradient (125-m elevation drop over 4 km) from Spirit Lake to the Truman channel-NFTR confluence. Furthermore, if water somehow escaped such an open channel and breached across the blockage drainage divide, it would largely flow over landscape lacking channels adjusted to such flow. Because this landscape is very susceptible to erosion, such a situation could generate geomorphic instabilities with possibly catastrophic consequences. A rigorous analysis of this risk is difficult owing to many uncertainties, chief among them the actual location and design of an open channel. Nevertheless, such risk could be reduced by careful design and engineering that accounts for the hydrogeomorphic behavior of this landscape.

Introduction

Volcanic eruptions can affect landscapes in many ways (Pierson and Major, 2014) and consequently alter erosion and the fluxes of water and sediment. Hydrologic and geomorphic responses to volcanic disturbances are varied in both space and time, and, in some instances, can persist for decades to centuries. Understanding the broad context of how landscapes respond to eruptions can help inform how they may evolve, and therefore provides context for managing and mitigating hazards associated with future volcanic and hydrologic events. To provide a lens through which to view the landscape of upper North Fork Toutle River (NFTR) basin as it exists today (2020)—the basin most heavily affected by the cataclysmic May 18 and later 1980s eruptions of Mount St. Helens—we first briefly discuss landscape effects and responses to volcanism broadly, then focus more sharply on specific geomorphic changes caused by the 1980s Mount St. Helens eruptions.

In this way, we provide context for the landscape changes caused by the eruptions as they relate to potential hydrological hazards associated with Spirit Lake, an iconic landform at the northern foot of the volcano, which was transformed by the cataclysmic 1980 eruption and had its outlet blocked. Here, we provide detailed analyses of geomorphic evolution of upper NFTR valley immediately north of the volcano. These analyses are presented to provide context for considerations of potential outlets for Spirit Lake, a landform which might be viewed as a "sleeping giant" on this landscape: a giant capable of causing catastrophic downstream consequences if water is released uncontrollably from the lake.

Hydrogeomorphic Disturbance by Eruptions and Landscape Responses—General Context

Volcanic eruptions can fundamentally alter the hydrologic and geomorphic (hydrogeomorphic) conditions of a landscape (Pierson and Major, 2014). Changes in hydrology and sediment delivery from watersheds following volcanic eruptions owe to many factors. For example, eruptions can remove or damage vegetation allowing more water to fall directly on the ground surface, and complex sequences of volcanic activity—pyroclastic flows, debris avalanches, tephra falls, and lahars (volcanic debris flows)—can bury areas surrounding volcanoes with loose, unconsolidated sediment. Commonly after explosive eruptions, hillsides blanketed by tephra-fall deposits have fine-grained (silt to fine sand) surfaces that inhibit infiltration, channels can be deeply filled with sediment, and drainages can be blocked by thick sediment accumulations (fig. 1). Such fundamental alteration of the hydrogeomorphic conditions of the landscape commonly enhances runoff of rainfall and snowmelt for several years (for example, Major and Mark, 2006; Pierson and Major, 2014) and spawns exceptional sediment delivery. As a result, landscapes surrounding volcanoes are subject to some of the highest erosion rates and sediment yields on Earth following eruptions. Sediment yields after eruptions can exceed those from nonvolcanic river systems by several orders of magnitude (Gran and Montgomery, 2005; Gran and others, 2011; Pierson and Major, 2014).

Typically, erosion rates and consequent sediment delivery peak in the months to years following an eruption and then decline (Collins and Dunne, 1986; Major and others 2000, 2016; Hayes and others 2002; Gran and others, 2011). Initially, extraordinary sediment delivery results from runoff erosion of hillside tephra and erosion of new channel fill. Commonly, erosion of hillside tephra diminishes within a few years after rills and gullies stabilize (for example, Collins and Dunne, 1986, 2019), but channel erosion persists (Gran and others, 2011; Pierson and Major, 2014; Major and others, 2019). After the most easily erodible channel sediment is depleted, sediment delivery diminishes greatly from peak levels, but it can remain higher than pre-eruption levels because of persistent, but lower magnitude, channel modification. In some instances, extraordinary sediment delivery can be rejuvenated when landslides that lag eruptions increase delivery of hillside sediment (Swanson and Major, 2005; Korup and others, 2019), if lakes impounded by volcanic sediment breach and reinvigorate channel erosion (for example, White and others, 1997), or when substantial hydrologic events (floods and debris flows) perturb quasi-stable channel conditions and effectively reset the recovery clock (for example, Tunnicliffe and others, 2018). As a result, the hydrogeomorphic legacy of a large eruption (one that deposits perhaps more than 1 km^3 of sediment on a landscape) can last for decades, and possibly centuries, creating exceptionally long-term channel- and sediment-management challenges (Gran and others, 2011; Major and others, 2000, 2018, 2019; Sclafani and others, 2018).

Major factors driving sediment-delivery rates and temporal patterns are the establishment and equilibration of the drainage network. Establishment of the drainage network in a landscape substantially reset by an eruption occurs in both a downstream direction, as overland flow incises tephra-mantled hillsides and creates rills and gullies that coalesce into larger channels, and an upstream direction as channels initiate and develop knickpoints or knickzones that migrate upstream. Once channels are established, they can further degrade, aggrade, or widen as a function of the imposed flow regime and pattern of upstream sediment delivery. Hence, evolving channels can undergo complex patterns and durations of response depending on the relations between sediment supply and sediment-transport capacity (for example, Schumm, 1999; Simon and Rinaldi, 2006; Nicholas, 2013; Major and others, 2019; Renshaw and others, 2019). When this relation is in balance, channels are in a state of equilibrium and change slowly; when this relation is out of balance, channels adjust, and geometric adjustments can be swift, dramatic, and persistent. Furthermore, channel evolution rarely follows the simple, sequential trajectory commonly portrayed in channel and stream evolution models (for example, Schumm and others, 1984; Simon and Hupp, 1986, 1987; Cluer and Thorne, 2014). Rather, channel evolution can follow nonsequential trajectories that involve varying combinations of degradation, aggradation, widening, and narrowing (Cluer and Thorne, 2014; Major and others, 2019; Renshaw and others, 2019).

Although channel adjustments typically occur in response to rainfall and snowmelt events, channel evolution can be accelerated dramatically if water stored on the landscape in lakes or ponds is released suddenly (Janda and others, 1984; White and others, 1997; Manville and others, 2007). Under these circumstances, channel adjustments that might ordinarily have taken months to decades to occur may occur over the course of hours to days. Such lake-breakout events can lead to floods and debris flows (lahars) that can be extremely destructive (for example, Janda and others, 1984; Manville and others, 2007; Gudmundsson, 2015). A breakout of an ancestral Spirit Lake, Washington, following an eruption of Mount St. Helens about 2,600 years ago, spawned the largest lahar documented in the Toutle River basin geologic record (Scott, 1988). That lahar, about 10 times greater in magnitude than the largest one triggered by the 1980 eruption (Janda and

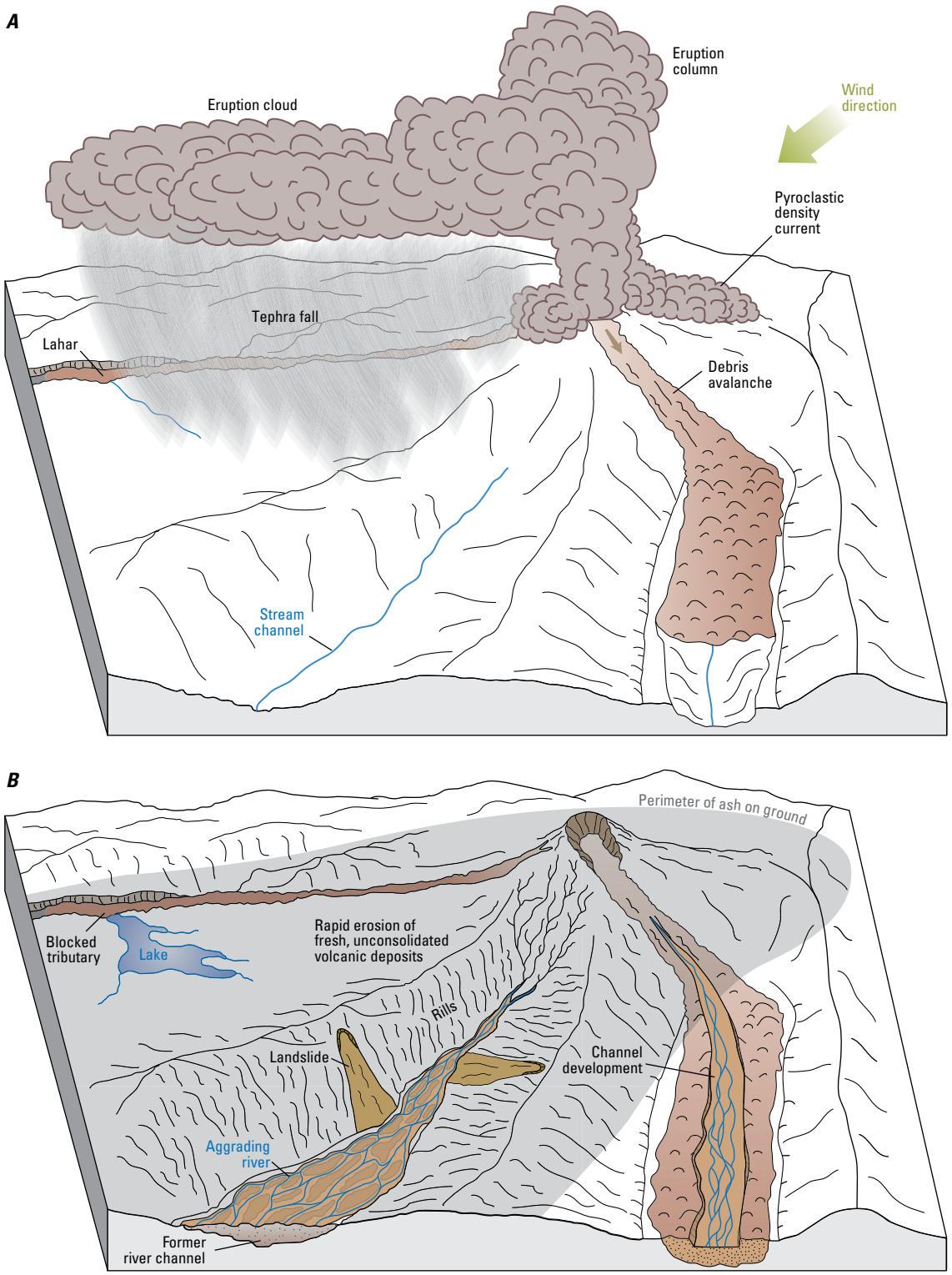

Figure 1. Diagram illustrating explosive eruption processes and subsequent landscape responses. *A*, Volcanic processes from or related to an explosive eruption, including tephra fall, pyroclastic density current, debris avalanche, and lahar. *B*, Landscape changes and responses to disturbances caused by eruption processes shown in panel *A* include rapid erosion of fresh tephra by rills and landslides, erosion of channel fill and development of new channel networks, channel aggradation and formation of braided channel patterns, and impoundments of channel-margin lakes. From Pierson and Major (2014).

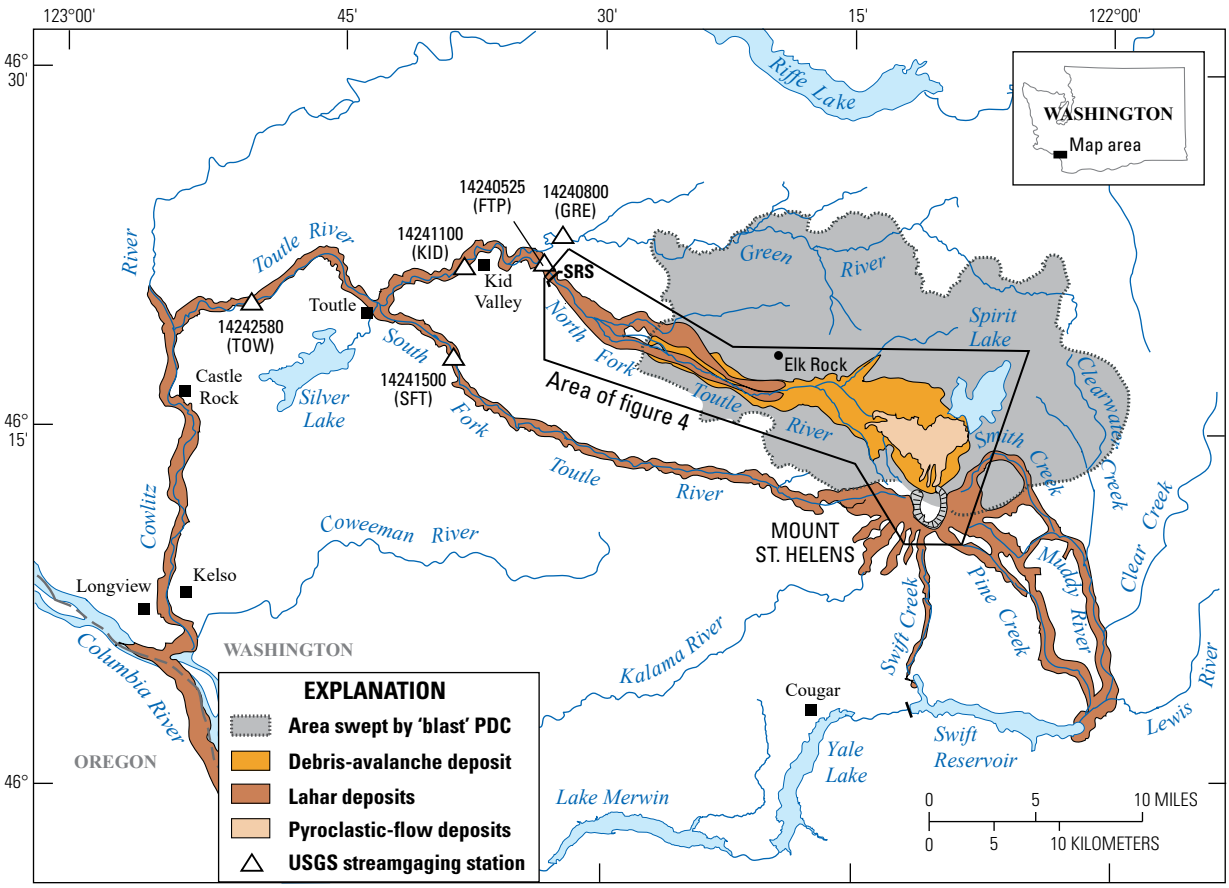

Figure 2. Distribution of volcanic disturbance zones of 1980 Mount St. Helens eruption and locations of gaging stations. PDC, pyroclastic density current; SRS, sediment retention structure. Gaging stations: GRE, Green River above Beaver Creek near Kid Valley (USGS streamgage 14240800); FTP, North Fork Toutle River below SRS near Kid Valley (USGS streamgage 14240525); KID, North Fork Toutle River at Kid Valley (USGS streamgage 14241100); SFT, South Fork Toutle River at Toutle (USGS streamgage 14241500); TOW, Toutle River at Tower Road near Silver Lake (USGS streamgage 14242580).

others, 1981; Fairchild, 1987), inundated the present sites of Castle Rock, Kelso, and Longview, Washington (fig. 2).

Catchments affected by severe volcanic disturbance may never recover to pre-eruption geomorphic conditions (that is, with regard to hydrologic and sediment fluxes)—or at least not for many human generations. Rather, they can attain a degree of quasi-stability and ecological function under different equilibrium conditions, and they can remain on the verge of precarious threshold (tipping point) conditions having prolonged societal consequences. One important lesson that has been learned from studies at many volcanoes over the past several decades is that volcanically disturbed channels are highly sensitive to erosion and can remain so for decades depending on the magnitude of initial disturbance.

Landscape Disturbance by the 1980 Mount St. Helens Eruption—Context for Spirit Lake Blockage

The landscape around Mount St. Helens has been disturbed and modified repeatedly for millennia. Mount St. Helens, as we see it, is a youthful volcano that sits on rugged, older volcanic terrain that has been modified by glacial, volcanic, and fluvial processes. Much of the area immediately around the volcano has been filled and smoothed by volcanic debris shed over millennia (fig. 3; Clynne and others, 2005, 2008). The distribution of sediment shed by the volcano shows clearly that Spirit Lake is a landform modulated by eruptive disturbance and volcanic deposits (Mullineaux and Crandell, 1962; Crandell, 1987; Hausback and Swanson, 1990). Before the May 18, 1980, eruption, upper NFTR channel, the outlet for Spirit Lake, formed along the edge of volcanic fill that abuts Johnston Ridge (fig. 3). The 1980 eruption added to this volcanic fill, and once again affected Spirit Lake (see Lipman and Mullineaux, 1981; W. Meyer and others, 1986; Grant and others, 2017).

The May 18, 1980, eruption consisted of a suite of volcanic processes (see papers in Lipman and Mullineaux, 1981). It began with catastrophic failure of the volcano's north flank, producing a massive landslide known as a debris avalanche. That failure simultaneously unroofed a magmatic intrusion high within the edifice, generating a devastating, laterally directed pyroclastic density current (herein called the "blast

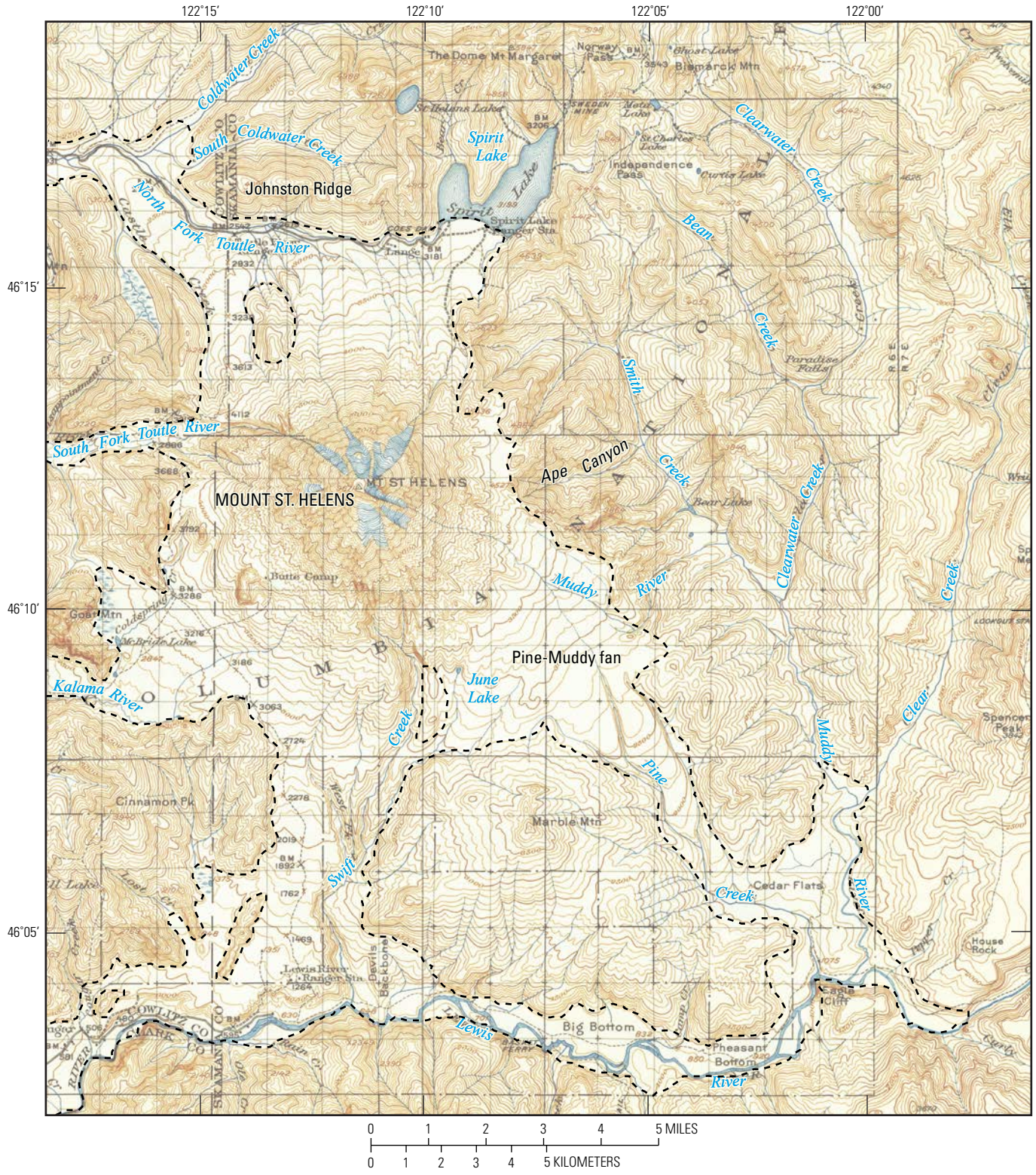

Figure 3. Topographic map of the Mount St. Helens area before the 1980 eruption. Dashed lines denote the approximate limit of the volcanic sediment apron that surrounds the volcano. Fragmental deposits derived from Mount St. Helens extend down all drainages (adapted from Clynne and others, 2008). Note the location of Spirit Lake, the pre-1980 location of North Fork Toutle River, and the pre-1980 locations of channels draining the north flank of the volcano.

PDC"). These events were followed by lahars (volcanic debris flows), a billowing eruption column that delivered widespread tephra fall (mostly east of the volcano), and pyroclastic flows when parts of that eruption column collapsed. Subsequent eruptions through summer 1980 produced additional pyroclastic flows that added to the volcanic fill in upper NFTR valley.

These volcanic processes transformed Spirit Lake basin and blocked the lake's outlet (W. Meyer and others, 1986; Glicken and others, 1989). The Spirit Lake blockage is a composite of volcanic deposits (fig. 4). It is composed principally of an extraordinarily thick (locally more than 150 m deep) mass of sediment emplaced by the debris avalanche, sediment that consists of shattered parts of the volcanic edifice, a deposit from the consequent gravel-and-sand-rich, laterally directed blast PDC (herein called the "blast deposit"), and deposits from subsequent pumiceous pyroclastic flows (Lipman and Mullineaux, 1981; Glicken and others, 1989). During emplacement of the pyroclastic flows, large billowing clouds of ash lofted from the basal flows and subsequently settled. These ashcloud deposits are very fine grained (mostly silt to fine sand), of variable thickness, and are interspersed stratigraphically within the pyroclastic-flow-deposit sequence (Glicken and others, 1989). Composition and stratigraphy of the blockage is described in greater detail in the section on geomorphic and stratigraphic context of upper NFTR basin. Greater details of the respective deposits can be found in Lipman and Mullineaux (1981), Glicken (1996), and Brand and others (2014, 2016).

Mitigation of the Blockage Hazard

Transformation of Spirit Lake basin, and blockage of its outlet, caused the lake level to rise. Uncontrolled rise would have eventually allowed the lake to breach the blockage, likely leading to a catastrophic flood and lahar downstream as happened during an eruptive period about 2,600 years ago (Scott, 1988). To prevent such a catastrophe and to modulate and manage the level of Spirit Lake, water was pumped from Spirit Lake over the crest of the blockage while a suitable outlet was designed and constructed. Pumping to stabilize and lower the lake level began in late 1982, was continuous through August 1983, and then intermittent through early

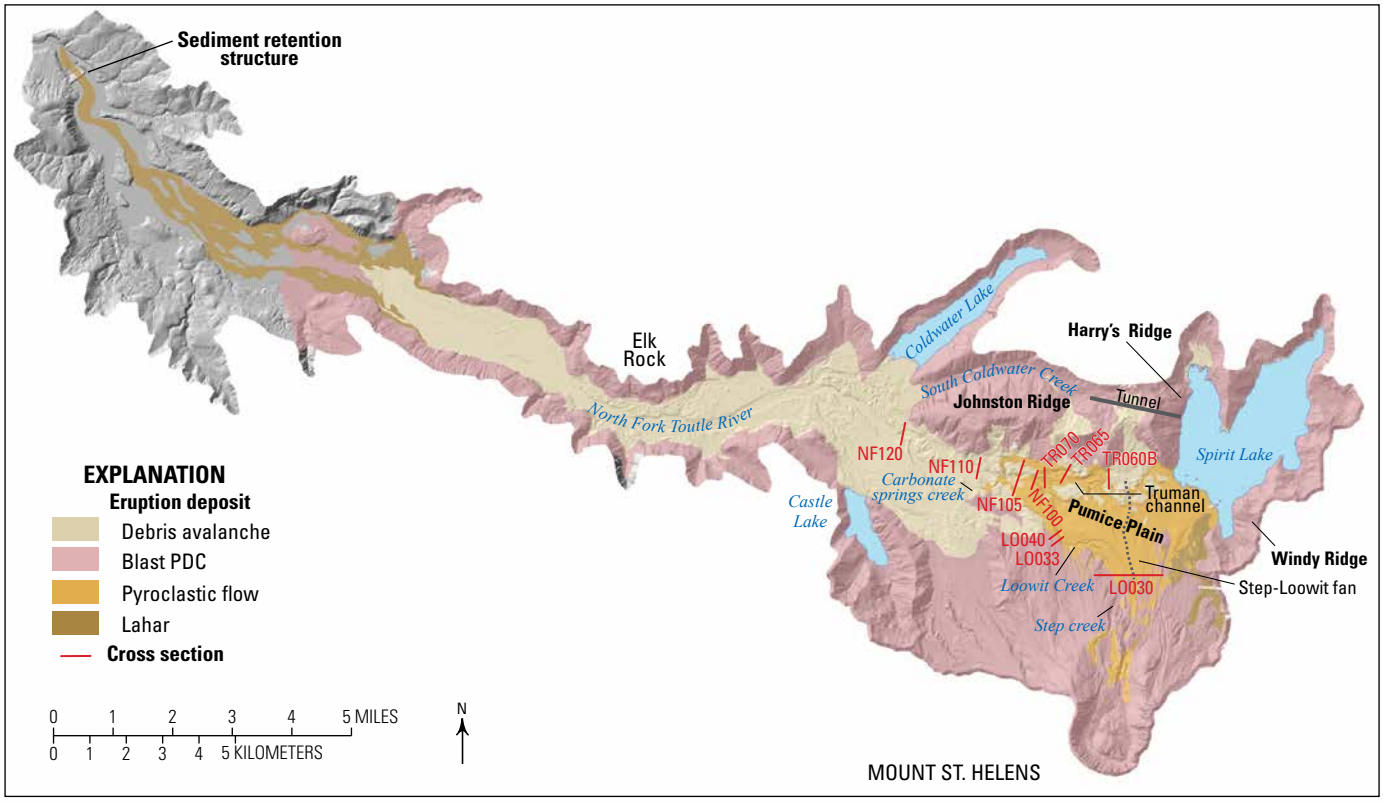

Figure 4. Simplified surface geologic map of 1980 eruption deposits in upper North Fork Toutle River basin (adapted from Lipman and Mullineaux, 1981) draped over digital terrain model derived from a 2009 airborne lidar survey. Locations of cross sections used for channel-evolution analysis are shown. The Spirit Lake blockage is defined as the region bounded on the east by Spirit Lake, on the west by Loowit Creek, on the north by the base of Johnston Ridge, and on the south by Step-Loowit fan. Dashed line highlights drainage divide along the blockage crest.

1985 (Paine, 1984). To provide an outlet for the lake, the U.S. Army Corps of Engineers bored a tunnel through bedrock that bounds the western shore of Spirit Lake (Sager and Chambers, 1986). The tunnel began full operation in May 1985. Water from the lake presently flows through the tunnel, into South Coldwater Creek valley, and re-enters NFTR downstream from Coldwater Lake (fig. 4). Since 1985, the tunnel has maintained the lake at a safe operating level, though it has required episodic closures to repair sections that have deteriorated (Britton and others, 2016).

Episodic closures of the Spirit Lake tunnel have caused the water level to rise to elevations near that having the potential to compromise tunnel integrity and functionality (Grant and others, 2017). At times of such elevated lake levels, the potential for breaching the blockage and causing an uncontrolled release of lake water is heightened. Thus, the U.S. Forest Service (the agency that owns the tunnel) and U.S. Army Corps of Engineers (the agency responsible for tunnel inspections and conducting repairs) are evaluating alternative long-term options for managing the security of Spirit Lake. Within that context, a risk assessment of various alternative outlet options was conducted (Grant and others, 2017).

Scope and Objectives of this Report

As part of a re-evaluation of options for managing the long-term security of Spirit Lake, alternative strategies for maintaining safe lake levels are being considered by the U.S. Forest Service and other interested parties (Grant and others, 2017; National Academies of Sciences, Engineering, and Medicine, 2017). This report documents hydrogeomorphic evolution and functioning of upper NFTR basin, focusing on development and evolution of the drainage network, to provide additional information for understanding potential ramifications of various alternative outlet strategies, especially of an open channel across the Spirit Lake blockage. The analyses herein provide additional insights that complement the more formal, semi-quantitative risk assessment of outlet alternatives for Spirit Lake provided by Grant and others (2017).

Post-eruption evolution of the drainage network in upper NFTR basin has been mediated by the size and sequencing of hydrologic events driven by storms, eruptions, and anthropogenic manipulations, and by the composition, structure, and architecture of the underlying volcanic deposits. Erosion that established and integrated the drainage network was driven mainly by runoff from typical winter precipitation, episodic large storms (especially those caused by intense atmospheric rivers of moisture aimed directly at, and sometimes stalled over, the Pacific Northwest [Neiman and others, 2008, 2011]), lake breakouts (Janda and others, 1984; Simon, 1999), controlled releases of water from Castle and Coldwater lakes, and water pumped from Spirit Lake (Sager and Chambers, 1986). In addition, small volcanic eruptions and large storms during the 1980s generated debris flows and floods that issued from the crater of Mount St. Helens (Waitt and others, 1983; Major and others, 2005; Mosbrucker and others, 2019) and modified the evolving channel network in varied ways.

Although there has been ongoing research on channel response to the 1980 eruption over the past four decades, primarily using repeat surveys of cross sections established by USGS scientists and analyses of aerial photographs (Rosenfeld and Beach, 1983; Janda and others, 1984; Parsons, 1985; Meyer and Martinson, 1989; Simon, 1999; Simon and Klimetz, 2012; Zheng and others, 2014; Major and others, 2019), post-eruption evolution of the channel network at the landscape scale has not been well-addressed. This gap in understanding was highlighted by Grant and others (2017, page 122):

> One of the least well-understood dynamics of the Mount St. Helens landscape is the propensity for substantial geomorphic change along channels draining the north flank of the volcano. Recent surveys document as much as 15 m (50 ft) of vertical incision along some reaches of the Loowit channel during single storm events… Yet, other reaches of the same channel are comparatively stable. Understanding controls on both vertical and lateral stability of channels in this area will provide information essential to determining the feasibility of establishing and maintaining an alternative outlet across the debris blockage without exacerbating the risk of an uncontrolled lake release owing to geomorphic instability.

In this report we provide the most comprehensive examination to date of the geomorphic evolution of upper NFTR basin and its linkages to hydrology, topography, and geology. Our analysis is based primarily on interpretations and measurements from remote sensing, including orthorectified stereoscopic photographs from 1980 to 2015, high-resolution lidar (airborne laser scanning) data from 2003, 2007, 2009, and 2017, and oblique aerial photographs from 2018. We complement these remote-sensing analyses with repeat surveys of cross sections made over the past nearly 40 years. Our goals are to: (1) analyze fluvial processes in the upstream reaches of NFTR and across the Spirit Lake blockage to evaluate the susceptibility of the blockage to fluvial erosion and related rapid geomorphic changes that could affect an open-channel outlet or other management actions; (2) develop a process-based understanding of how the geometry and location of the channel network evolved; and (3) relate channel network development to hydrological events, overall topography, and the surface geology of the blockage.

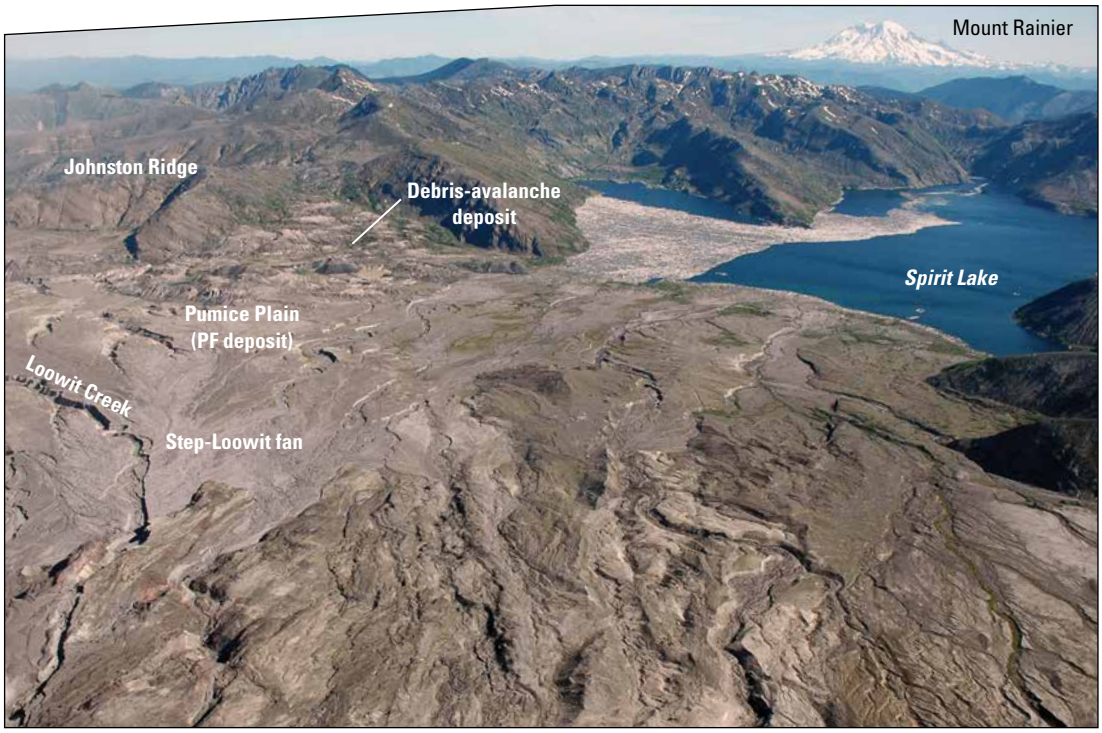

Figure 5. Oblique aerial view of Spirit Lake blockage looking north from vantage over northeast side of volcano (just east of crater mouth). Tan, subdued topography of Pumice Plain is comprised of pyroclastic-flow (PF) deposits that overlie debris-avalanche deposit. Eroded terrain in foreground is covered mainly by blast pyroclastic density current deposit that overlies thin (less than 15 m) debris-avalanche deposit and pre-1980 deposits and bedrock. U.S. Geological Survey photograph by J. Vallance, June 26, 2007.

Geomorphic and Stratigraphic Context of Upper North Fork Toutle River Basin

The Spirit Lake blockage is a composite of multiple deposits (figs. 4, 5)—it is not a single, homogenous deposit. It is composed of a thick, heterogeneous mixture of shattered rock from the volcano—the debris-avalanche deposit—overlain by a veneer of pyroclastic deposits ranging in composition from rocky bits of sand and gravel to pumiceous gravel and silt with pumice boulders. Field observations indicate there are few, if any, large, coherent, erosion-resistant masses within the blockage. Nearly all rock in the debris-avalanche deposit was shattered at the volcano as the giant rockslide-debris avalanche detached and slid into NFTR valley (Glicken, 1996). Near the surface, few clasts in that deposit are larger in diameter than a couple of meters, which, while large, are unlikely to impede erosion at the scale of the blockage (Grant and others, 2017, p. 112–113). The overlying pyroclastic deposits, including the blast deposit and subsequent pyroclastic-flow deposits (fig. 5), are composed largely of particles ranging in size from cobble gravel to silt, have physical compositions that vary both laterally and vertically owing to overlapping of multiple units, and are of variable thickness. As described by Glicken and others (1989), the blast deposit consists of a lower unit of angular, unstratified, clast-supported rock debris larger than coarse sand, overlain by an upper unit of silt- to sand-sized sediment composed of shattered bits of rock. Its thickness within the Spirit Lake blockage ranges from a few centimeters to as much as 13 m. The overlying pyroclastic-flow and ashcloud deposits are composed mainly of pumice gravel, sand, and silt. Across the blockage, individual deposits range from less than 1 m to as much as 12 m thick, and the stratigraphic sequence of deposits is as much as 40 m thick (Rowley and others, 1981). Cohesion and likely compaction of the pyroclastic-flow deposits (Poland and Lu, 2008; Welch and Schmidt, 2017) to some extent allow them to support nearly vertical walls when eroded. Nevertheless, these pyroclastic deposits are very erodible as shown by rapid channel erosion and by evidence of subsurface piping during very high stands of Spirit Lake before the tunnel was constructed (Glicken and others, 1989).

The surface of the blockage is irregular. Near its northern end at the base of Johnston Ridge, it is particularly irregular and exhibits rugged mounds and depressions where the debris-avalanche deposit is at the surface (figs. 4, 5). Closer to the volcano and along the southern and western parts of the blockage, the topography is smoother, reflective of both the contiguous mantle of pyroclastic sediment that overlies the debris-avalanche deposit there (figs. 4, 5) and a fan of alluvial and debris-flow deposits formed by erosion of the lower northern flank of the volcano.

Both the debris-avalanche and overlying pyroclastic deposits are highly erodible. As we will show, channels near the northern and western edges of the blockage incised tens of meters through the pyroclastic-flow deposits and into the debris-avalanche deposit and widened hundreds of meters within months to a few years. Channels on the Spirit Lake side of the crest are less deeply incised than those to the west. This is because there has been only modest-magnitude streamflow east of the blockage crest, owing largely to runoff from local springs and occasional discharge from the crater following episodic channel avulsions, and because the base level for erosion east of the crest (Spirit Lake) is substantially higher than that to the west (fig. 6). The elevation difference between Spirit Lake and the confluence between Truman channel (an informally named channel that traverses the south base of Johnston Ridge) and NFTR is 125 m (figs. 4, 6); the elevation difference between Spirit Lake and the sediment retention structure (see "Hydrologic Setting of Upper North Fork Toutle River Basin" section)—which sets local base-level control west of the blockage—is 760 m (fig. 4). No coherent channels cross the blockage crest.

Hydrologic Setting of Upper North Fork Toutle River Basin

The hydrologic regime of upper NFTR basin was fundamentally altered by the 1980 eruption. Alteration was caused by razing or removal of vegetation and by extensive sediment deposition on hillsides and within the upper NFTR channel. Like other types of landscape disturbance (such as wildfire), the hydrologic, geomorphic, and ecologic impacts of the eruption affected key components of the hydrologic cycle and influenced the character, magnitude, duration, and timing of runoff (Lettenmaier and Burges, 1981; Major and Mark, 2006; Pierson and Major, 2014).

The 1980 eruption razed (and locally removed) mature forest over hundreds of square kilometers (km^2), broadly deposited tephra that created a fine-grained, nearly impervious surface over more than 1,000 km^2, deposited extensive sediment in river channels, and greatly altered the character of major channels that drain the volcano (Lipman and Mullineaux, 1981; Janda and others, 1984; Simon, 1999; Swanson and Major, 2005; Lisle and others, 2018). In many basins, these effects led to enhanced runoff, greater flood-conveyance efficiency, and peak flows (for a given precipitation input) that were a few percent to many tens percent larger after the 1980 eruption than before it (Leavesley and others, 1989; Major and Mark, 2006). Disruption of upper NFTR valley by the colossal debris-avalanche deposit blocked several channels tributary to NFTR, and the deposit's irregular, hummocky topography and many depressions initially disrupted coherent streamflow. Such profound landscape perturbation severed hydrologic connection between the upper and lower parts of the watershed as well as between the volcano and the valley, and it isolated Spirit Lake. Reconnection required establishment of a new drainage network.

Drainage development on the debris-avalanche deposit began hours after emplacement when groundwater seepage

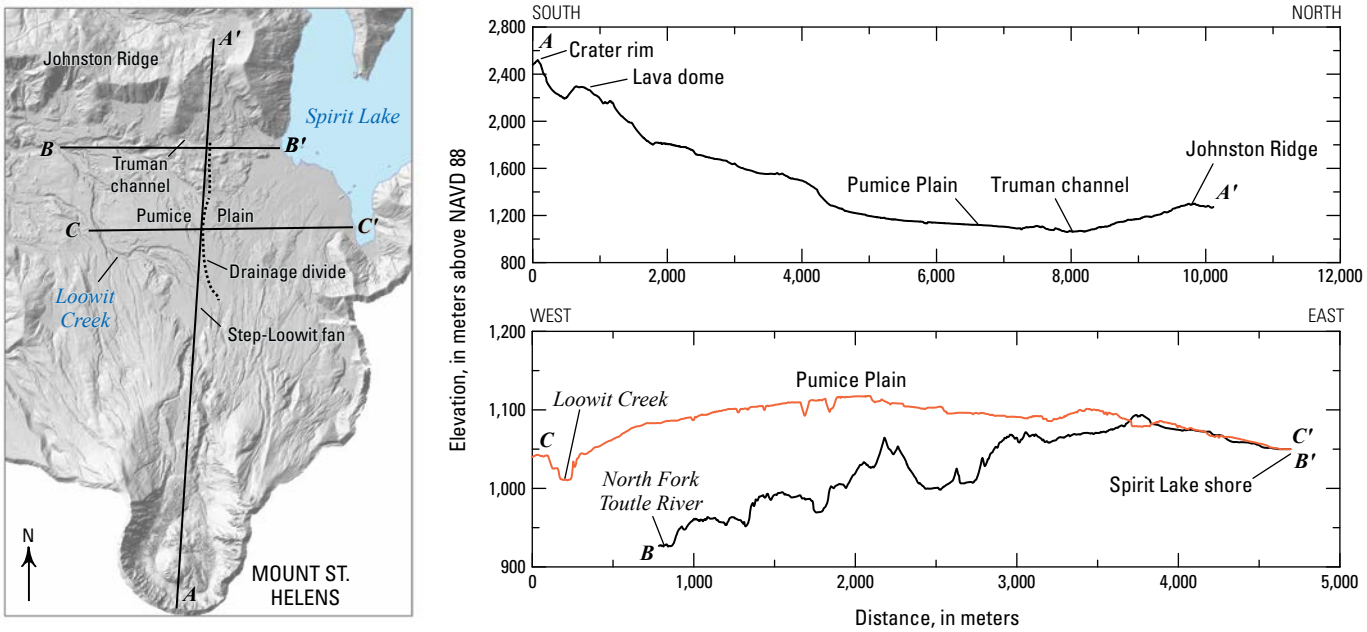

Figure 6. Topographic profiles across the Spirit Lake blockage. *A*–*A*′ is a south to north profile, *B*–*B*′ is a west to east profile across the approximate location of Truman channel (see figure 4), and *C*–*C*′ is a west to east profile across the central part of blockage. Spirit Lake blockage defined as the region bounded on the east by Spirit Lake, on the west by Loowit Creek, on the north by the base of Johnston Ridge, and on the south by Step-Loowit fan. Dashed line depicts blockage drainage-divide. Base map derived from a 2009 airborne lidar survey.

and melting glacier ice in the deposit formed ponds that subsequently enlarged and breached (Janda and others, 1984). As water (and muddy slurry) flowed from one depression to another, it eroded sediment and formed connecting channels. This nascent channel initiation was subsequently augmented in several ways by (1) breakouts of lakes impounded adjacent to the avalanche deposit; (2) controlled releases from the largest impounded lakes (Coldwater and Castle Lakes); (3) pumping water from Spirit Lake across the deposit surface during tunnel construction; (4) meltwater floods and debris flows issuing from the crater; and (5) runoff erosion (Dunne and Leopold, 1981; Rosenfeld and Beach, 1983; Janda and others, 1984; Sager and Chambers, 1986; Paine and others, 1987; Pierson, 1999; Simon, 1999). Although channel initiation on the debris-avalanche deposit began within hours of emplacement, it took nearly 3 years to fully integrate a new drainage network across the deposit (Janda and others, 1984; Meyer, 1995; Simon, 1999). Nevertheless, once sufficient continuous drainage pathways developed, they conveyed enhanced runoff from the basin.

The record of post-eruption daily mean streamflow on NFTR below the U.S. Army Corps of Engineers' large sediment retention structure (SRS) (USGS streamgage 14240525, labeled FTP in fig. 2) illustrates an early phase of enhanced runoff from the basin and highlights significant, episodic hydrologic events (fig. 7; table 1). NFTR streamflow was unregulated through 1988, except for restricted inflow from Spirit Lake through its tunnel. From 1988 to 1998, streamflow was regulated because it passed through a series of culverts in the SRS—a structure designed to trap sediment but pass water (fig. 8). Since 1998, flow has passed over the SRS spillway in run-of-river fashion and is unregulated—there is no deep pool of water impounded. Frequency of moderate to large daily mean streamflow (greater than 150 m^3/s) was greater from 1980–83 than after. From 1981–83, daily mean streamflow of NFTR below the SRS (as recorded at streamgage 14240525, site FTP) exceeded 150 m^3/s seven times. In contrast, from 1984 through 2018, daily mean streamflow exceeded that magnitude of flow only 12 times (supplemental data file DF1). An exceedance probability analysis of annual maximum daily mean streamflow since 1981 (fig. 9) shows that 150 m^3/s streamflow has an annual exceedance probability of about 0.27 (a roughly 4-year recurrence-interval flow). Thus, enhanced runoff was a major factor influencing the geomorphic response of this basin in the immediate aftermath of the eruption.

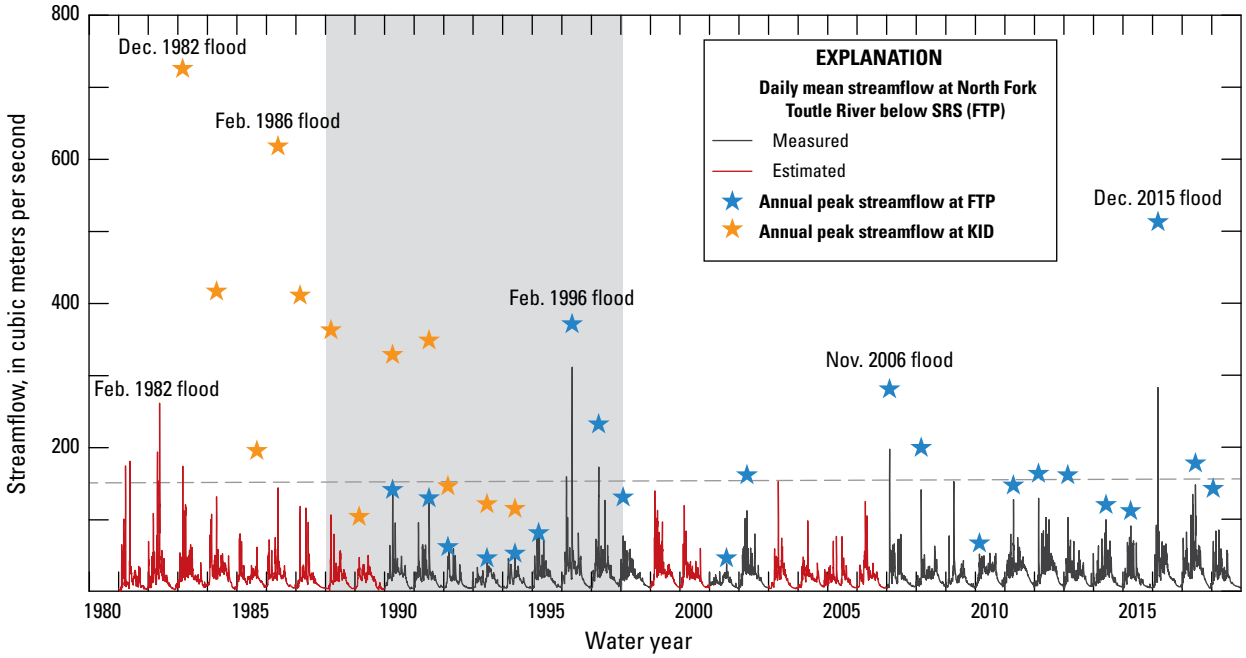

Figure 7. Time series of daily mean streamflow and annual peak streamflow of North Fork Toutle River below the sediment retention structure (SRS) near Kid Valley (USGS streamgage 14240525, FTP, see fig. 2). For periods in which measurements were not available, daily mean streamflow estimated using a regression on the difference between streamflow measured at North Fork Toutle River at Kid Valley (USGS streamgage 14241100, KID, see fig. 2) and at Green River above Beaver Creek near Kid Valley (USGS streamgage 14240800, GRE, see fig. 2) or using regression relations among Toutle River at Tower Road (USGS streamgage 14242500, TOW, see fig. 2), FTP, and the differences between KID and GRE (see supplemental data file DF1). Major floods are annotated. Annual peak streamflow for water year 1982 (963.4 m^3/s), caused by the March 19, 1982, lahar, is not shown. Dashed horizontal line highlights daily mean streamflow of 150 m^3/s, a flow having an annual exceedance probability of 0.27 (a recurrence interval of about 4 years) (see fig. 9). Shaded region shows period when streamflow was regulated by passage through culverts in SRS (see fig. 8).

Table 1. Key hydrogeomorphic events in post-eruption channel development of upper North Fork Toutle River.

[Estimated volume is water (landslide) volume. Q is discharge, where subscript denotes type of measurement or estimate; E, estimated value; m^3/s, cubic meters per second; SRS, sediment retention structure]

Date	Event	Estimated volume (10^3 m^3)	Q_{peak} (m^3/s)[1]	$Q_{daily\ mean}$ (m^3/s)[2]	Q_{peak} (m^3/s)[3]	$Q_{daily\ mean}$ (m^3/s)[4]	Source
Dec. 26, 1980	Flood			174.8 E	No data	238.4	Gage record
Feb. 19, 1981	Flood			181.1 E	No data	297.5	Gage record
Jan. 24, 1982	Flood			194.0 E	No data	379.7	Gage record
Jan. 25, 1982	Flood—Breach of ponds on Coldwater Lake levee	379		95.3 E	No data	176.8	Simon (1999)
Feb. 14, 1982	Flood—Breach of ponds along north side of valley above Coldwater reach	710		120.1 E	No data	212	Simon (1999)
Feb. 16, 1982	Flood			154.3 E	No data	270.6	Gage record
Feb. 20, 1982	Flood—Breach of Jackson Lake adjacent to Elk Rock	2470		261.8 E	[5]960.6	427.9	Simon (1999); gage record
Mar. 19, 1982	Lahar	10,000–13,000		57.5 E	963.4	79.3	Waitt and others (1983); Pierson (1999); gage record
Nov. 5, 1982	Spirit Lake pumping begins at 5.1 m^3/s			24.2 E		41.4	Simon (1999); gage record
Dec. 3, 1982	Flood			174.3 E	725.4	308.9	Gage record
Mar. 10, 1983	High flow			65.9 E	No data	117.6	Gage record
Jul. 13, 1983	High flow—3 days			40.3 E	No data	67.4	Gage record
Jan. 24, 1984	Flood			131.9 E	416.5	265.8	Gage record
Apr. 5, 1985	Spirit Lake pumping ends; tunnel opens						Simon (1999)
Feb. 23, 1986	Flood			144.2 E	617.7	325.9	Gage record
Nov. 24, 1986	Flood			118.6 E	410.9	279.4	Gage record
Jan. 9, 1990[6]	Flood		141.4	138.0	328.7	253.0	Gage record
Feb. 8, 1996	Flood		371.2	311.7			Gage record

Table 1. —Continued

Date	Event	Estimated volume (10^3 m^3)	Q_{peak} (m^3/s)[1]	$Q_{daily\ mean}$ (m^3/s)[2]	Q_{peak} (m^3/s)[3]	$Q_{daily\ mean}$ (m^3/s)[4]	Source
Jan. 1, 1997	Flood		232.4	173.1			Gage record
Jan. 31, 2003	Flood		No data	152.9 E			Reconstructed
Jan. 2006	Landslide near cross section NF110	600					Major and others (2018)
Nov. 7, 2006	Flood and debris flow		280.8	198.1			Gage record
Dec. 9, 2015	Flood		512.9	283.4			Gage record

[1,2]Streamflows estimated for or measured at U.S. Geological Survey gage North Fork Toutle River below SRS near Kid Valley (streamgage 14240525). Station record begins October 1, 1989. See supplemental data file DF1 for estimated streamflow values.

[3,4]Streamflows measured at U.S. Geological Survey gage North Fork Toutle River at Kid Valley (streamgage 14241100). Period of record is June 10, 1980, to September 30, 1994.

[5] Unpublished secondary streamflow peak (K.R. Spicer, U.S. Geological Survey, written commun., 2019).

[6]Streamflow on North Fork Toutle River below SRS was strongly affected by regulation of flow through culverts in SRS. In other basins within Toutle River watershed (South Fork Toutle River and Green River), this flood was a substantial hydrologic event in the streamflow record.

Figure 8. Views of sediment retention structure on North Fork Toutle River looking upstream. *A*, Oblique aerial view. *B*, Water passing through rows of culverts embedded in face of structure (see *A* for location). U.S. Army Corps of Engineers photographs from approximately 1990.

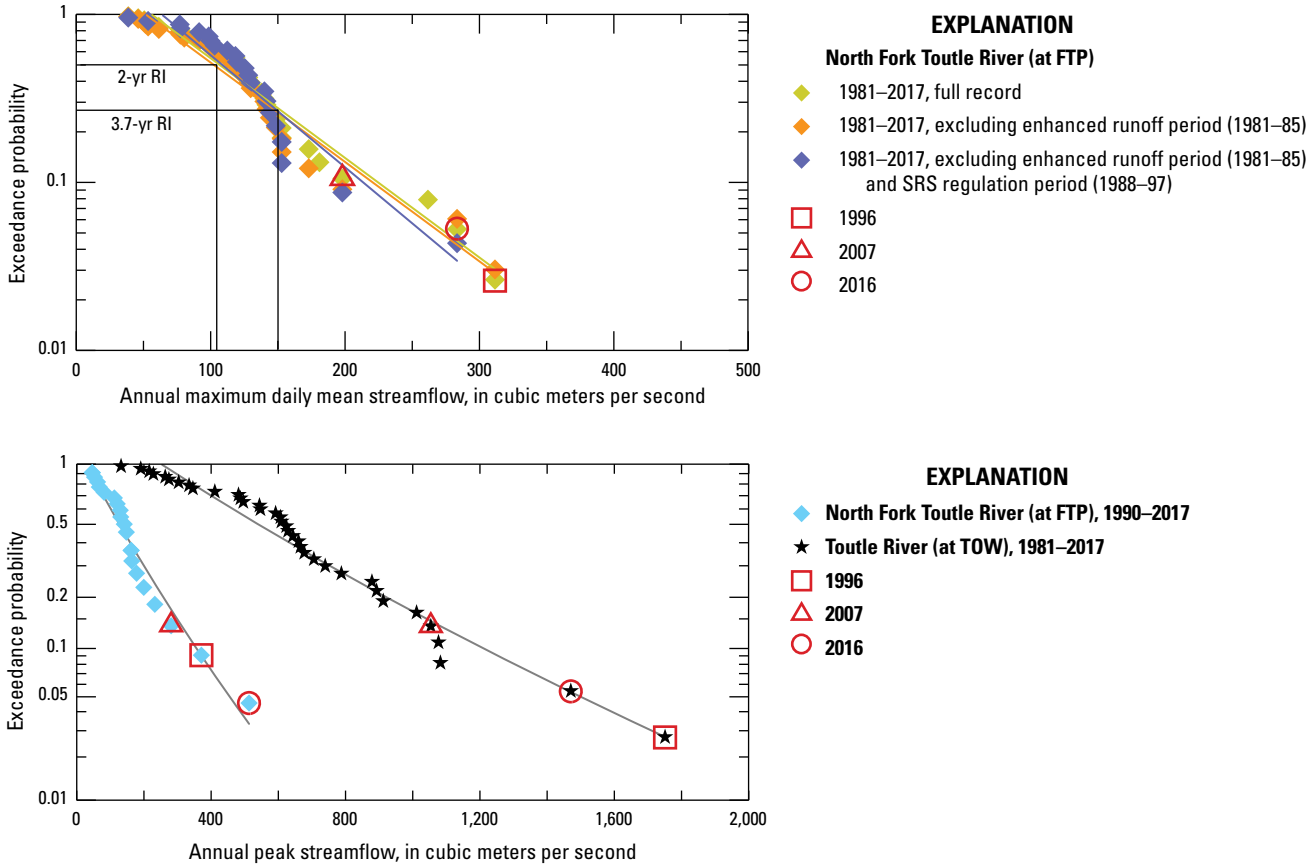

Figure 9. Exceedance probability plots for streamflow at North Fork Toutle River below the sediment retention structure (SRS) (at FTP, USGS streamgage 14240525) and at Toutle River at Tower Road (at TOW, USGS streamgage 14242580). Top, Exceedance probabilities of annual maximum daily mean streamflow. Bottom, Exceedance probabilities of annual peak streamflow.

Fluvial Geomorphic Evolution of Upper North Fork Toutle River Basin

The fundamental framework of the drainage system of upper NFTR basin developed rapidly following the May 1980 eruption. By the mid-1980s, the drainage system was established and defined (see D.F. Meyer and others, 1986; Meyer and Dodge, 1988; Simon, 1999), and since then it has undergone an evolutionary process of enlargement and refinement (for example, Major and others, 2019). Here, we examine the evolutionary trajectory on two different time-scales—first through decadal-scale snapshots of change within the whole basin, followed by a more temporally refined analysis. We also examine evolutionary development on two spatial scales—a landscape scale that encompasses a broad view of the area around the Spirit Lake blockage (and farther downstream for the decadal-scale snapshots of change), and a more discrete, local scale viewed through the lens of repeat surveys of channel cross sections. We first discuss our methods of analysis before presenting results.

Methodology

We examine broad-scale geomorphic changes by creating, and then examining differences between, digital terrain models (DTMs)—digital representations of surface elevation. DTMs were generated from a variety of sources (table 2). Those sources included topographic maps, traditional vertical and low-elevation-oblique aerial photographs, and lidar surveys. These sources comprise a range of scales. Pre-1980 15-minute-quadrangle topographic maps have a scale of 1:62,500; vertical aerial photographs from 1980–85 were acquired at 1:9,600, other vertical aerial photographs have scales of 1:12,000 to 1:14,000, and oblique aerial photos have variable scales; and lidar surveys have horizontal and vertical resolutions ranging from centimeters to meters.

DTMs constructed from aerial photographs were generated using structure-from-motion (SfM) and traditional photogrammetric techniques (for example, Turner and others, 2012; Javernick and others, 2014; Gomez and others, 2015; Bakker and Lane, 2017). For 1980–1996 SfM-derived DTMs, negatives or contact prints were scanned, pre-processed as

needed in Adobe Photoshop software to improve contrast and sharpen detail, oriented to remove as much distortion as possible, and processed in Agisoft Photoscan Pro software using invariant objects (such as logs, large rocks, and other stable landscape features) identified in a georeferenced 2015 DTM as ground control. A calibrated digital camera system was used for the September 2015 aerial photography (table 2), eliminating the need to scan and pre-process imagery prior to DTM construction. For the September 2018 aerial photography, we used a non-calibrated digital camera and acquisition methods described by Mosbrucker and others (2017). DTMs based on lidar surveys are bare-earth surface models—vegetation has been removed using a filtering algorithm. Over much of the area of interest on the Spirit Lake blockage, there is little vegetation other than thin ground cover, although dense riparian vegetation is present locally. Therefore, the DTMs generated from aerial photographs are largely bare-earth models. However, vegetation obscures the ground surface in parts of those photogrammetry-derived models, particularly on and adjacent to hillsides and in areas where springs emerge or where depressions contain ponds, especially since the middle to late 1990s.

Once DTMs were generated, we produced digital terrain models of topographic difference (DoDs) to examine changes in landscape topography between DTMs. The DoDs were created by subtracting surface elevations of grid cells in one DTM from those at identical grid cells in another DTM. The convention adopted here is to subtract elevations in an earlier DTM (DTM1) from those in a subsequent DTM (DTM2) (DTM2 – DTM1). Thus, if the difference in surface elevation at a grid-cell after subtracting DTM1 from DTM2 is positive, then the ground-surface elevation at that cell increased through deposition. Conversely, if the difference in surface elevation at a grid-cell after subtracting DTM1 from DTM2 is negative, then the ground-surface elevation lowered through erosion. Apparent loss of elevation at a grid cell along a river channel can happen if the river incises and lowers the channel bed, or if a channel bank erodes laterally. Removal of bank material can result in very large negative changes in elevation at a grid-cell if banks are tall. Apparent gain of elevation at a grid cell along a river channel can happen if a river deposits sediment on its channel bed or floodplain, if a river debouches from a canyon and deposits a fan of sediment, or if sediment is externally introduced to a channel, such as by a landslide. Thus, DoDs show where erosion and deposition have taken place within the landscape and can identify geomorphic "hot spots" of activity. Here, we focus principally on changes that occur on and around the Spirit Lake blockage resulting largely from fluvial processes that initiated and subsequently sculpted river channels.

A threshold value of change was used to distinguish geomorphic signal from noise and error within each DoD.

Table 2. Available digital terrain models (DTMs), source of topography, and method of creation.

[SfM, structure from motion; lidar, airborne laser scanning]

Year of DTM	Date of topography	Source of topography	Method of creation[1]
Pre-1980	Photography 1952; maps 1953–1958	15-minute topographic maps (Mount St. Helens, Spirit Lake, Elk Rock, Cougar)	Digitized topographic maps
1980	Sept. 5, 1980	Vertical aerial photography; 1:9,600	SfM (1)
1981	July 27, 1981	Vertical aerial photography; 1:9,600	SfM (1)
1982	Sept. 22, 1982	Vertical aerial photography; 1:9,600	SfM (1)
1984	July 7, 1984	Vertical aerial photography; 1:9,600	SfM (1)
1985	July 25, 1985	Vertical aerial photography; 1:9,600	SfM (1)
1987	June 6–11, 1987	Vertical aerial photography; 1:12,000	Traditional photogrammetry (2)
1996	Aug. 29, 1996	Vertical aerial photography; 1:9,600	SfM (1)
1999	Sept. 3, 1999	Vertical aerial photography; 1:14,000	Traditional photogrammetry (2)
2003	Sept. 19–Oct. 2, 2003	Airborne laser scanning	Lidar (3)
2007	Oct. 22–29, 2007	Airborne laser scanning	Lidar (4)
2009	Sept. 16–20, 2009	Airborne laser scanning	Lidar (5)
2015	Sept. 27, 2015	Vertical aerial photography, 1:12,000	SfM (1)
2017	Sept. 2017	Airborne laser scanning	Lidar (6)
2018	Sept. 26, 2018	Oblique aerial photography	SfM (1)

[1]Data sources: (1) Mosbrucker and Sweeney (2019); (2) Mosbrucker (2019); (3) University of Washington libraries (2019); (4) Mosbrucker (2015); (5) Mosbrucker (2014); (6) Mosbrucker (2020).

Owing to photo distortion and challenges identifying and testing adequate ground control, the change-detection threshold was based on empirical trial-and-error that minimized apparent change on areas across each DTM known to be stable. This empirical determination of a threshold value, rather than a more rigorous error-propagation protocol (as described in Brasington and others, 2003; Major and others, 2018; Anderson, 2019, for example), is admittedly coarse and probably masks real geomorphic changes. But because we do not attempt to quantify volumetric changes along channels, and locally use cross-section surveys to quantify amounts of incision and widening, this coarse approach is sufficient to illustrate timing and gross magnitudes of channel change. For most DTMs, the change-detection threshold is set at 2 m (for a few with tighter constraints, it is set at 1 m). However, the DoDs for 1980–81 and 1984–85 required a 4-m threshold. In those DoDs, signals are generally large enough to see distinctive erosion and deposition, but such changes cannot be confidently quantified because the DTMs were distorted, tilted, and could not be co-registered precisely. We include those DoDs for completeness and for what they can tell us heuristically about geomorphic evolution of upper NFTR basin, but more precise quantification of changes between those time periods can be extracted only locally from changes observed in resurveyed cross sections. In several DoDs, apparent erosion and deposition on Harry's Ridge, Windy Ridge, and the ridge bounding the east side of the blockage (for locations, see fig. 4) are largely artifacts owing to distortion, poor georeferenced control along edges of imagery, and, in later years, growth of vegetation. In some instances, apparent erosion and deposition are the result of differencing a photogrammetry-derived DTM (which locally includes vegetation) against a bare-earth, lidar-derived DTM. Such artifacts are especially apparent around emergent springs (for example, the informally named "Carbonate springs"; fig. 4) that support relatively dense riparian vegetation.

Discrete, local changes along major channels in the drainage network are monitored through repeat surveys of channel cross-sections. An initial network of sections was established in the first months to years after the 1980 eruption (D.F. Meyer and others, 1986), and several sections have been resurveyed episodically over the nearly four decades since. Various methods have been used to survey cross-sections. Early surveys used an electronic distance meter (EDM) coupled with a theodolite to measure distances and angles to a rod-mounted prism. In the 1990s, total stations were adopted to measure distances and angles to rod-mounted prisms, and since 2012 reflectorless total-station technology has been adopted. Since 2009, section surveys also have benefitted from integrated global positioning system (GPS) technologies (Mosbrucker and others, 2015).

Cross-section surveys recurred irregularly. In the early 1980s, resurveys were frequent and commonly documented morphological changes after each major storm or other significant hydrological event. Survey frequency declined after 1984, and since the 1990s surveys typically have recurred less than once per year (Mosbrucker and others, 2015).

Each cross-section is georeferenced to monumented endpoints which, since the late 1990s, have been located using GPS. Episodically, monuments lost to erosion were reset. Elevations for cross-section surveys are shown in meters above the North American Vertical Datum of 1988 (NAVD 88) (Mosbrucker and others, 2015), and horizontal distance along a cross section is relative to a left bank monument. In general, elevations from on-the-ground measurements are accurate to within tens of centimeters, and horizontal locations are accurate to within hundreds of centimeters, especially along very long lines that extend many hundreds of meters to more than 1 km (Mosbrucker and others, 2015).

Broad Evolution of Upper North Fork Toutle Basin and Relation to Hydrologic Events

In the first few years after the 1980 eruption, the drainage network in upper NFTR basin evolved swiftly. However, key processes operated largely in spatially disparate reaches. For example, a substantial lake breakout in February 1982 (Jackson Lake; Simon, 1999, fig. 29) produced one of the largest floods and greatest daily mean streamflows in upper NFTR valley (fig. 7; table 2), but it originated far downstream from the Spirit Lake blockage. In contrast, rainfall runoff, debris flows, and water pumped from Spirit Lake from 1982 to 1985 caused significant erosion along Loowit Creek and Truman channels, which bound the west and north sides of the Spirit Lake blockage, respectively (fig. 4).

In the immediate aftermath of the eruption, debris-avalanche and mantling pyroclastic deposits were easily eroded. Measurements of suspended-sediment delivery downstream, when linked to streamflow magnitudes, show that small- to moderate-magnitude streamflow, not just large-magnitude streamflow, transported vast amounts of sediment (Major, 2004). Repeat measurement of cross sections along Loowit Creek channel and upper NFTR channel illustrate rapid evolution—both channel incision and widening—that occurred within the first 5 years after the eruption when the fluvial system was greatly out of equilibrium. Along these channels, vertical incision of 10 meters or more and lateral erosion of 100 meters or more was common (fig. 10).

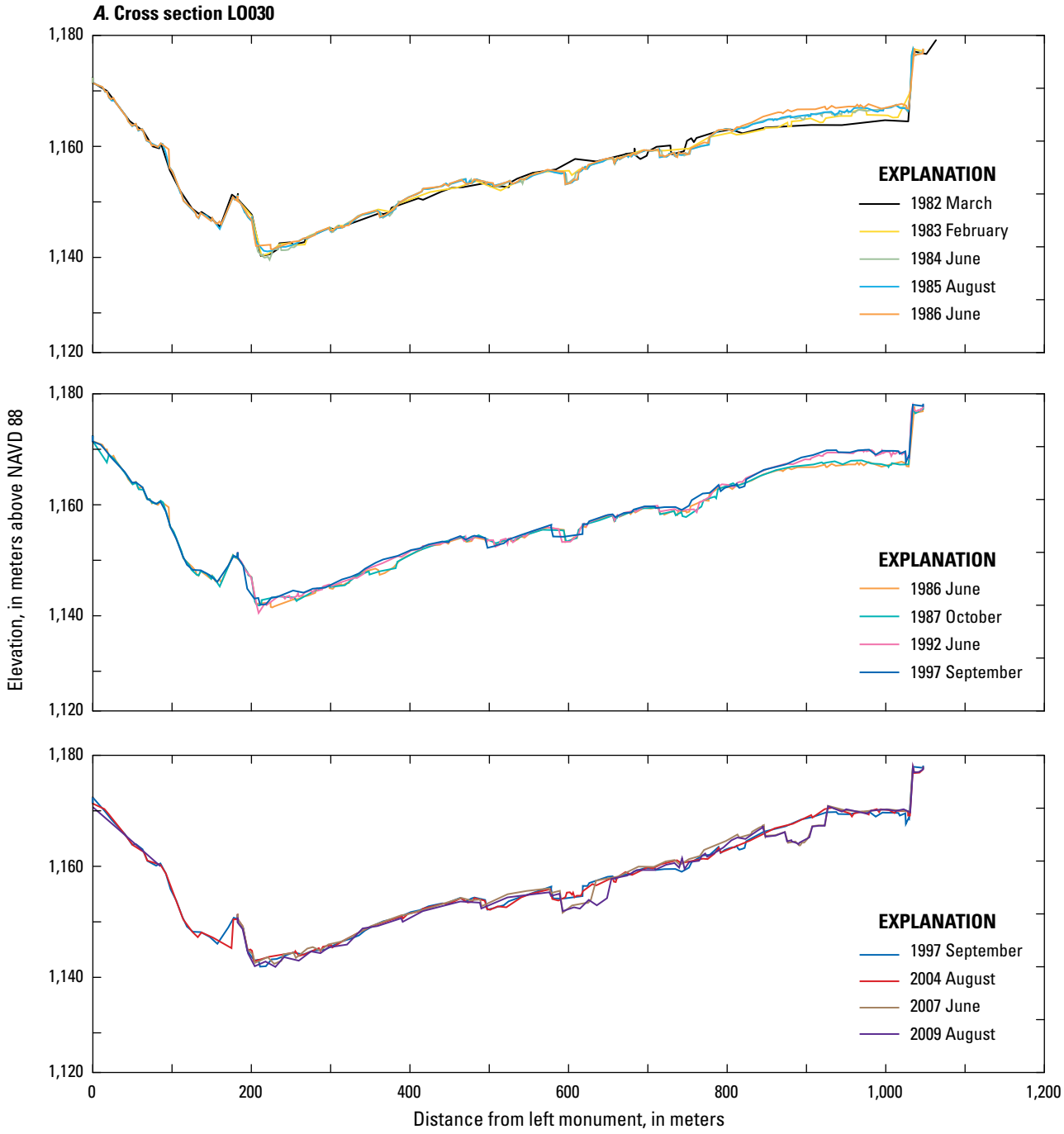

Figure 10 (pages 17–22). Plots of repeat cross-section surveys along Loowit Creek and mainstem North Fork Toutle River channels. See figure 4 for cross section locations. *A*, Cross section LO030; *B*, cross section LO033; *C*, cross section LO040; *D*, cross section NF100; *E*, cross section NF105; *F*, cross section NF110; *G*, cross section NF120. View is looking downstream.

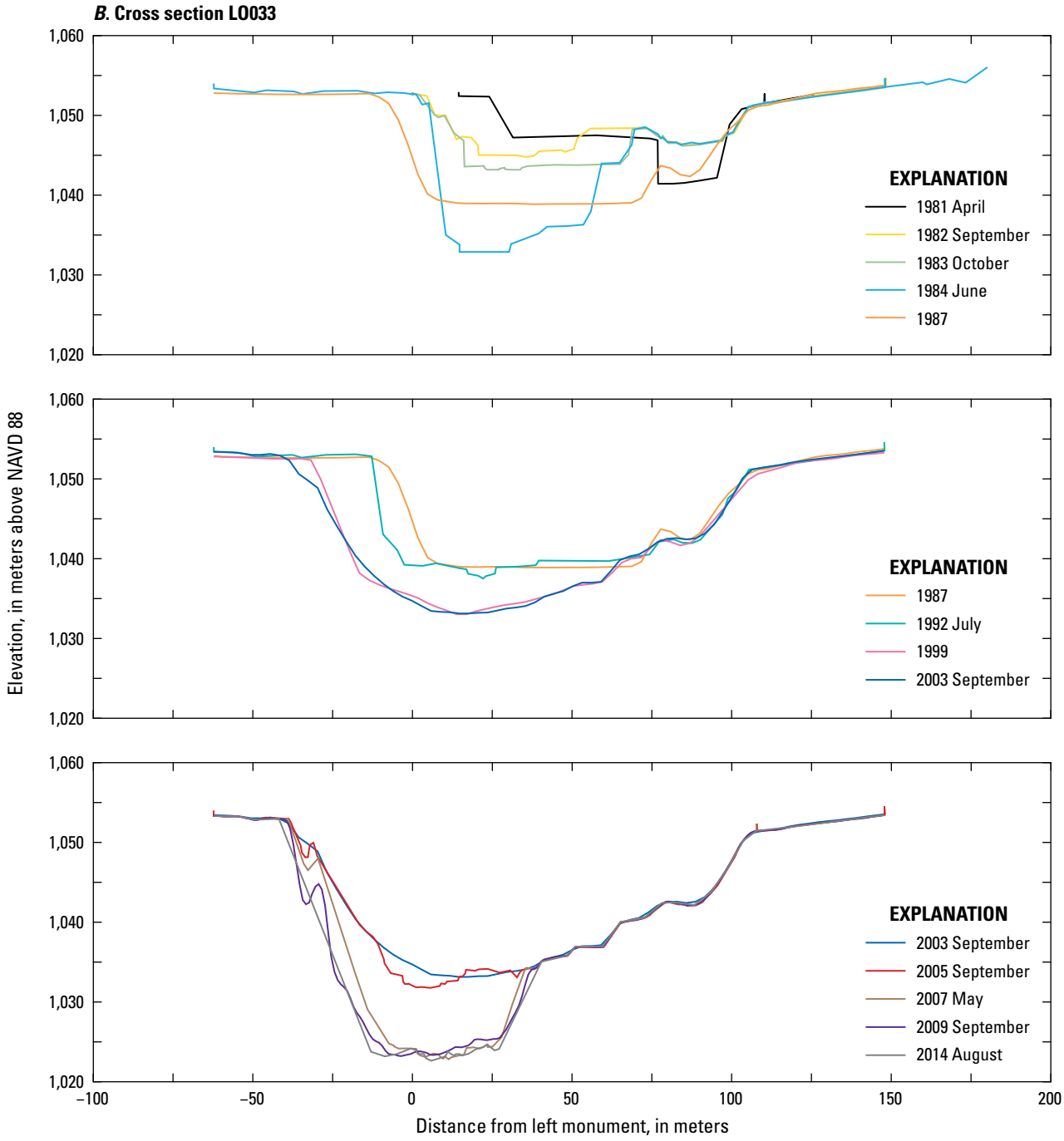

Figure 10 (pages 17–22). Continued

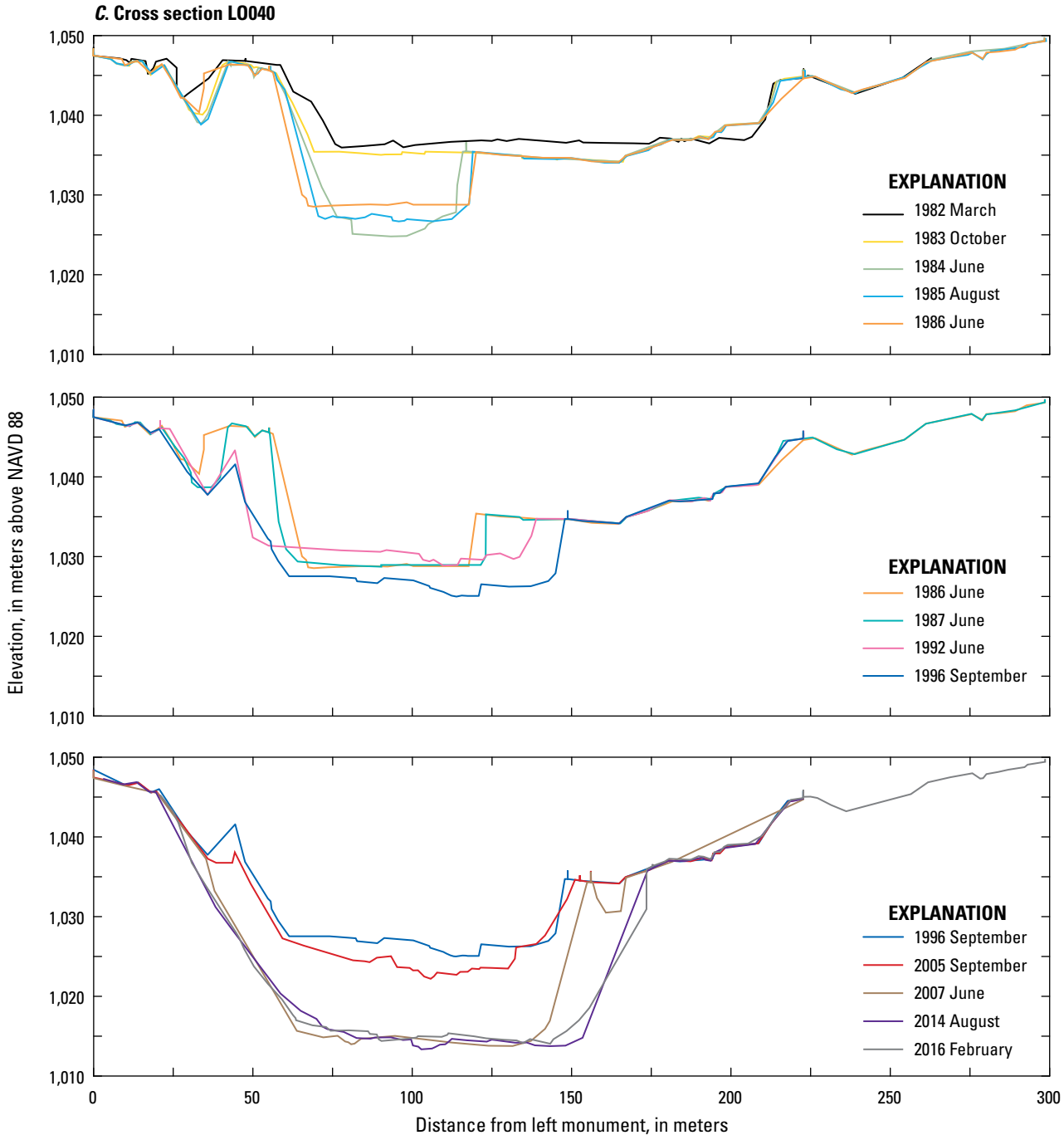

Figure 10 (pages 17–22). Continued

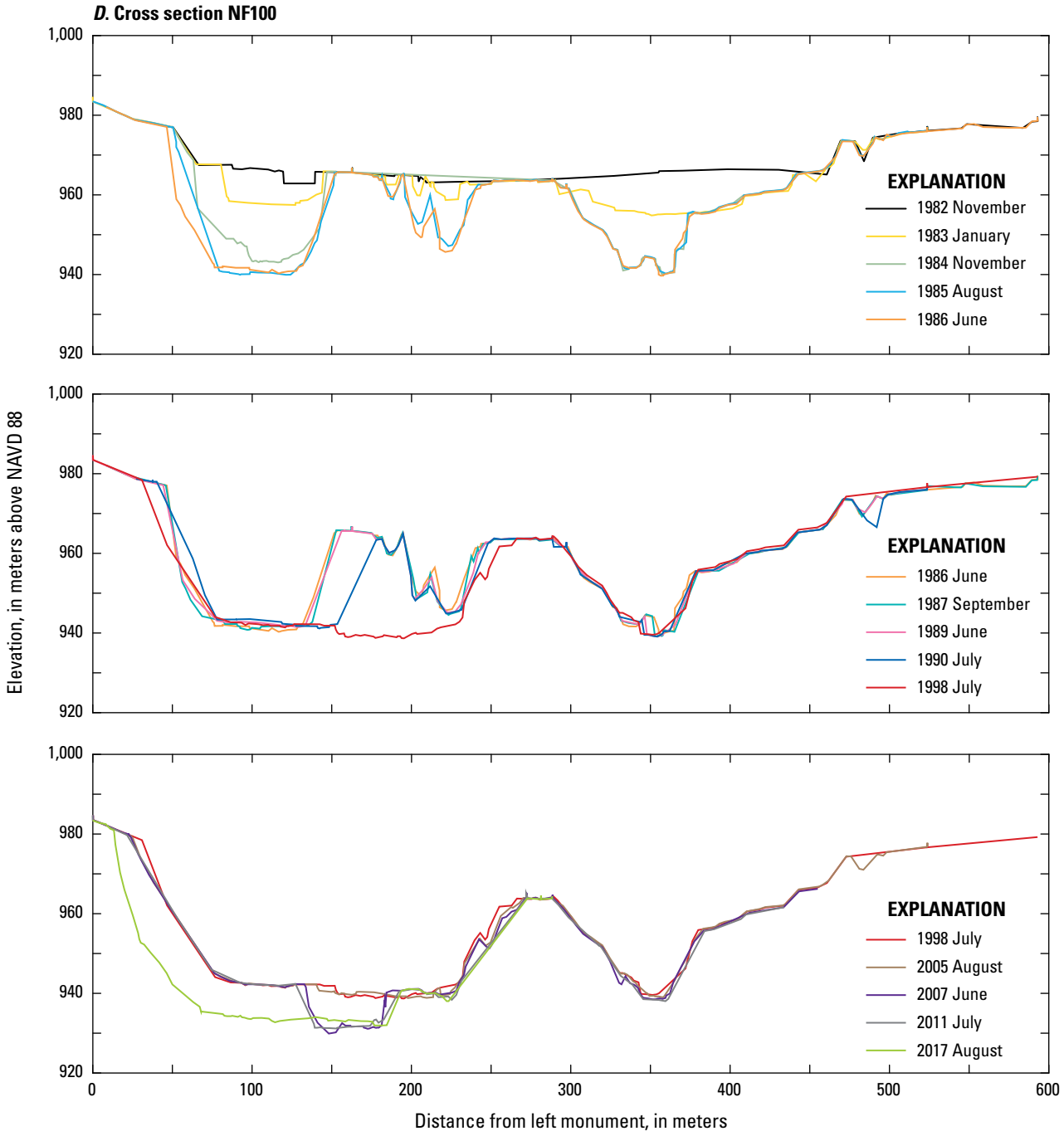

Figure 10 (pages 17–22). Continued

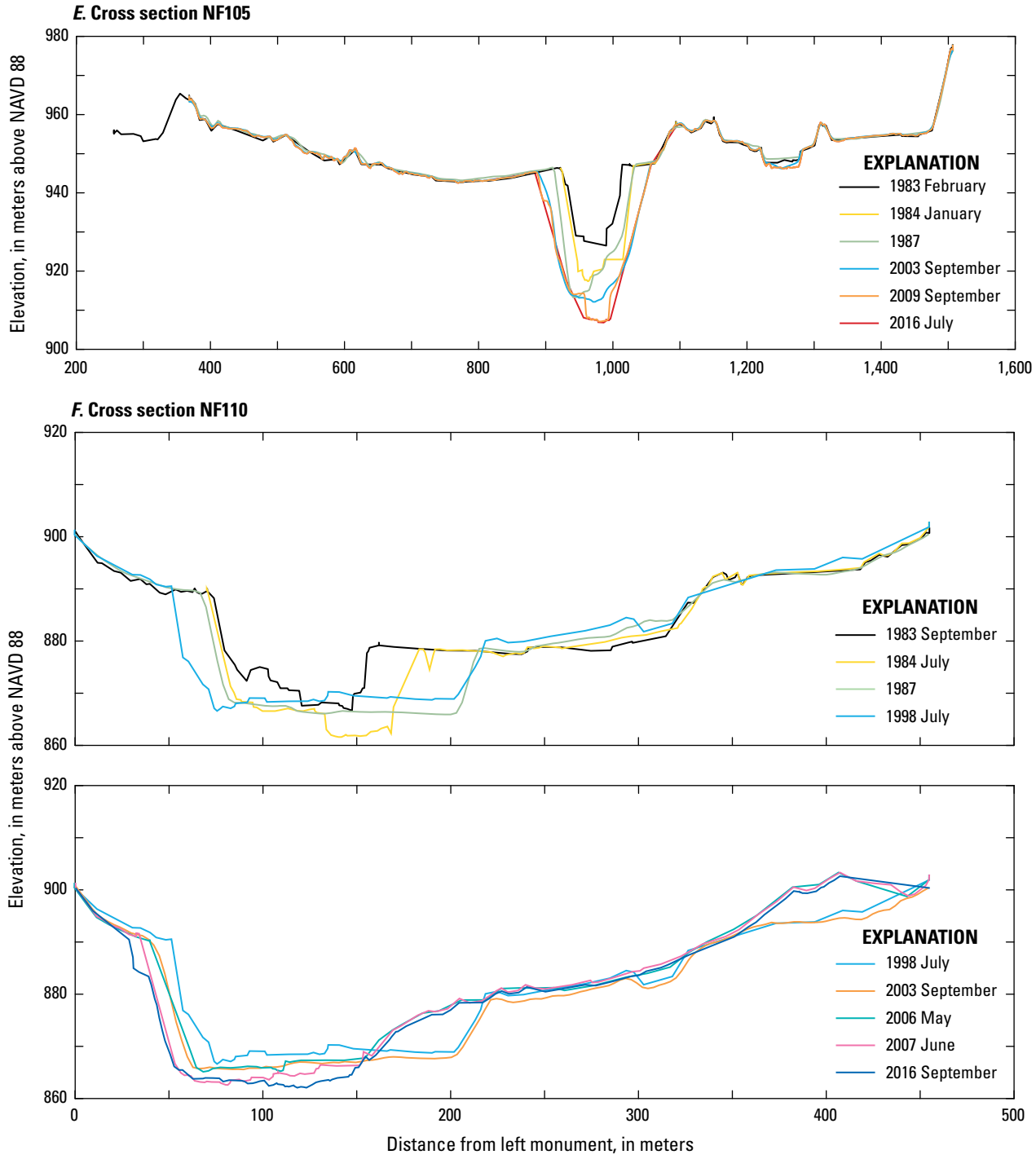

Figure 10 (pages 17–22). Continued

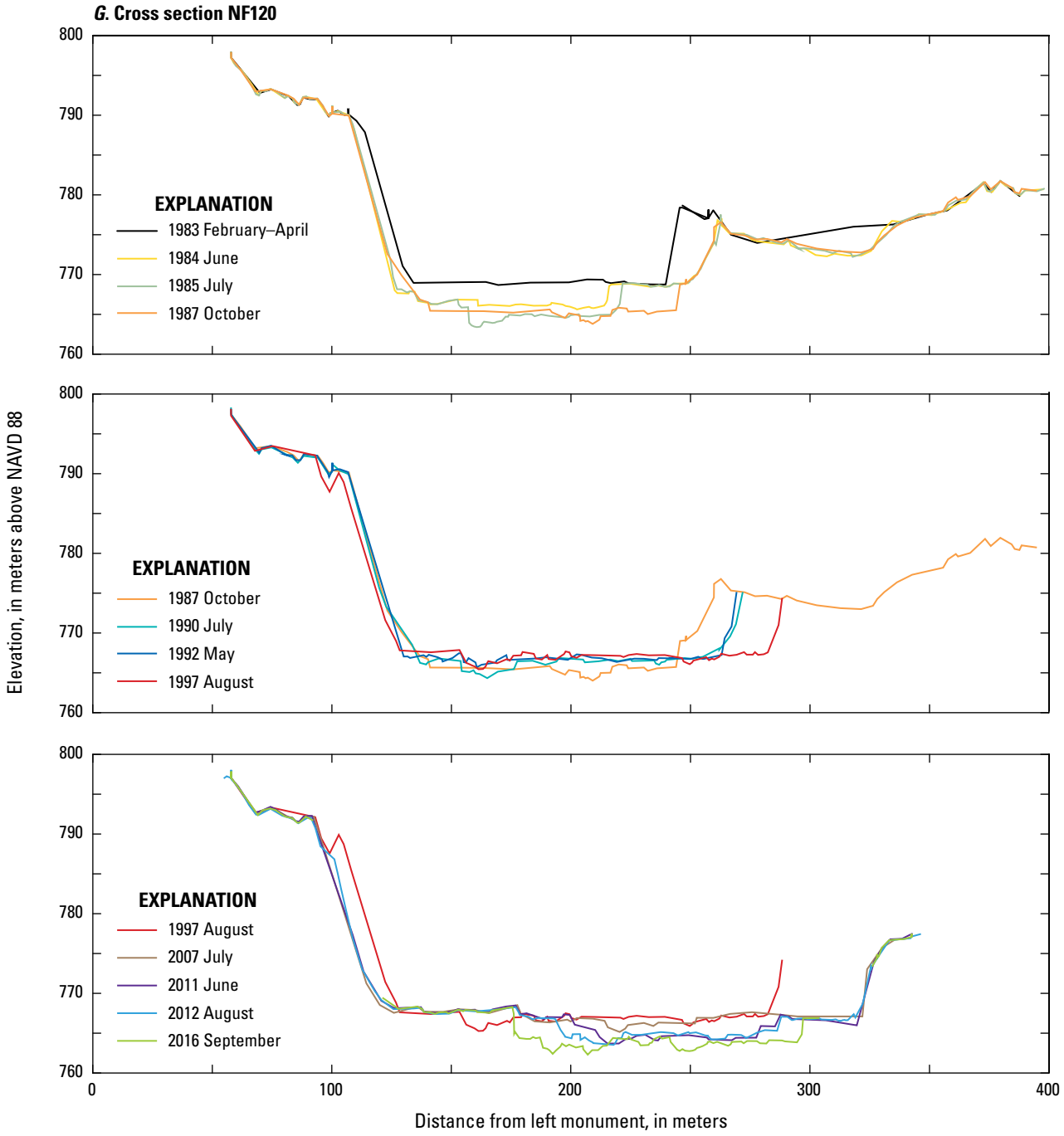

Figure 10 (pages 17–22). Continued

Mobility of this volcanic sediment when initially subject to even modest amounts of water is well illustrated along Truman channel (fig. 11). Along the distal end of Truman channel, just upstream from its confluence with Loowit Creek channel, repeat surveys show considerable incision and widening in late 1982, within a month of water being pumped from Spirit Lake. The channel at cross-section TR065 (fig. 11*B*) incised about 15 m and widened nearly 100 m between late August and late December 1982 (full pumping began on November 5, 1982; Paine, 1984; Glicken and others, 1989). Slightly farther downstream, the channel at cross-section TR070 (fig. 11*C*) incised nearly 15 m between mid-November 1982 and mid-January 1983, and by nearly 20 m by August 1983. Closer to the source of outflow from the pumping operations, at TR060B (fig. 11*A*), the channel incised 11 m between September and December 1982, 7 m of which occurred within 2 weeks of the pumps becoming fully operational (Meyer and Dodge, 1988; Mosbrucker and others, 2015).

As channel geometries evolved and channel beds coarsened (Simon and Thorne, 1996), rates and magnitudes of incision declined (Simon and Thorne, 1996; Zheng and others, 2014). Along Truman channel, geomorphic change effectively ceased once pumping operations halted in spring 1985 and water drained from Spirit Lake through a newly bored bedrock tunnel. Presently, the channel hosts limited local runoff and flow from groundwater seepage and harbors substantial riparian vegetation. Along several locations of upper NFTR and the uppermost reaches of Loowit channel, bed-elevation by the mid- to late 1980s fluctuated around a quasi-static level, though inexorable modest incision persisted locally. In contrast, pervasive lateral erosion persisted. Topographic differences between decade-spanning DTMs show large (multi-meter) magnitudes of vertical elevation change along channel corridors—owing to both vertical and lateral erosion from 1980–87 (fig. 12*A*), and largely to lateral erosion after 1987 (figs. 12*B*, *C*; Major and others, 2018). After 1999,

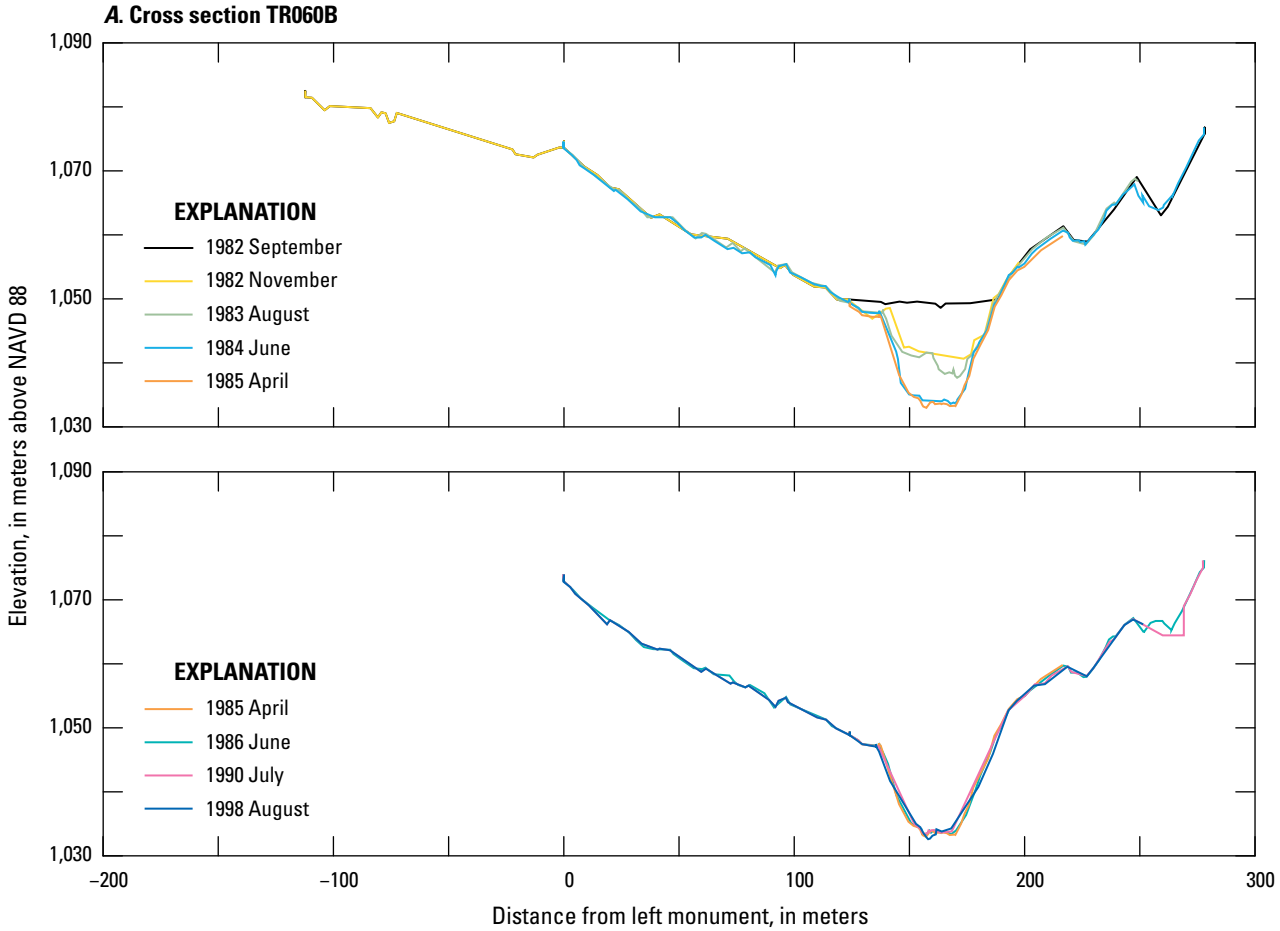

Figure 11 (pages 23–24). Plots of repeat cross-section surveys along Truman channel. See figure 4 for cross section locations. *A*, Cross section TR060B; *B*, cross section TR065; *C*, cross section TR070. View is looking downstream.

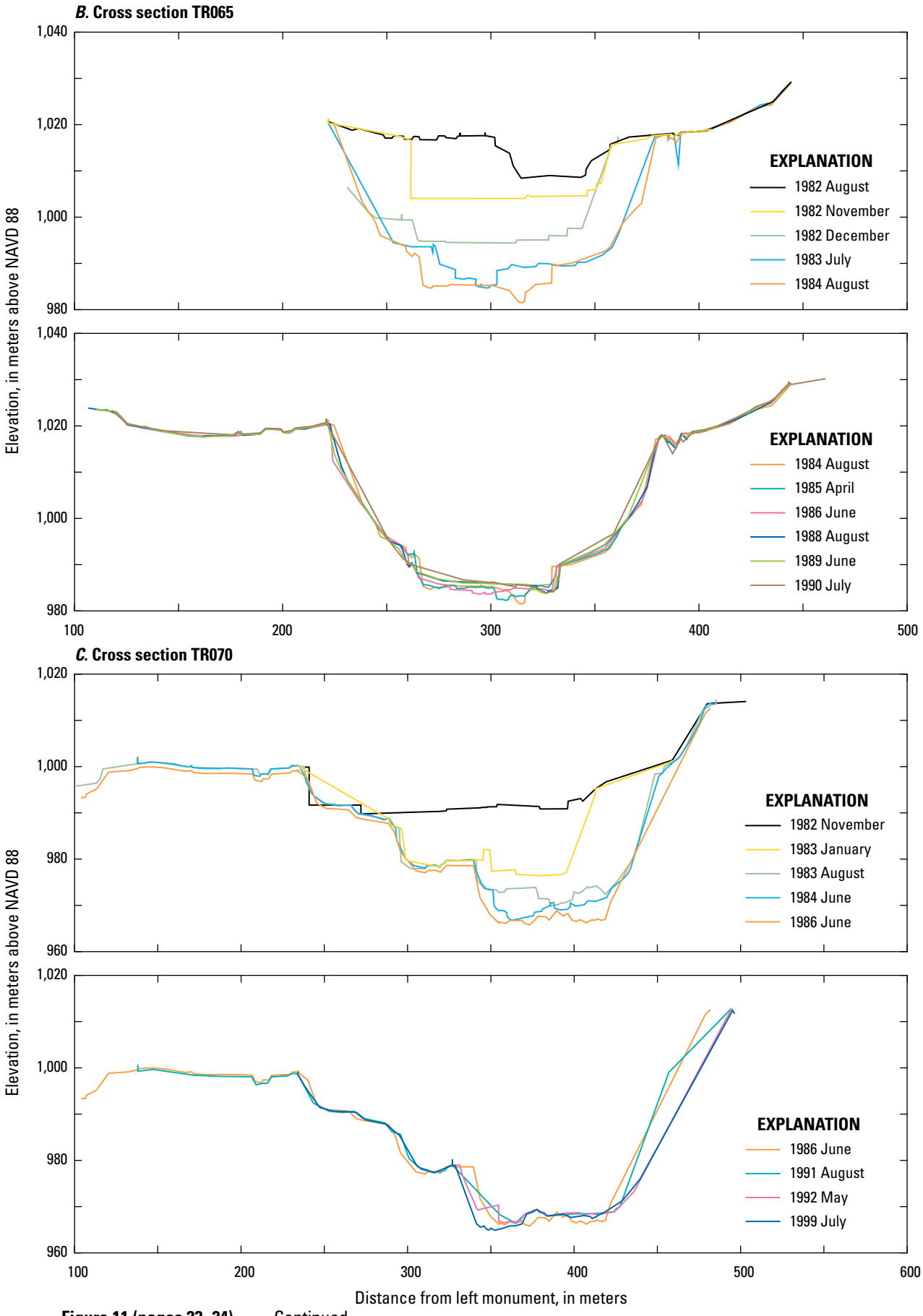

Figure 11 (pages 23–24). —Continued

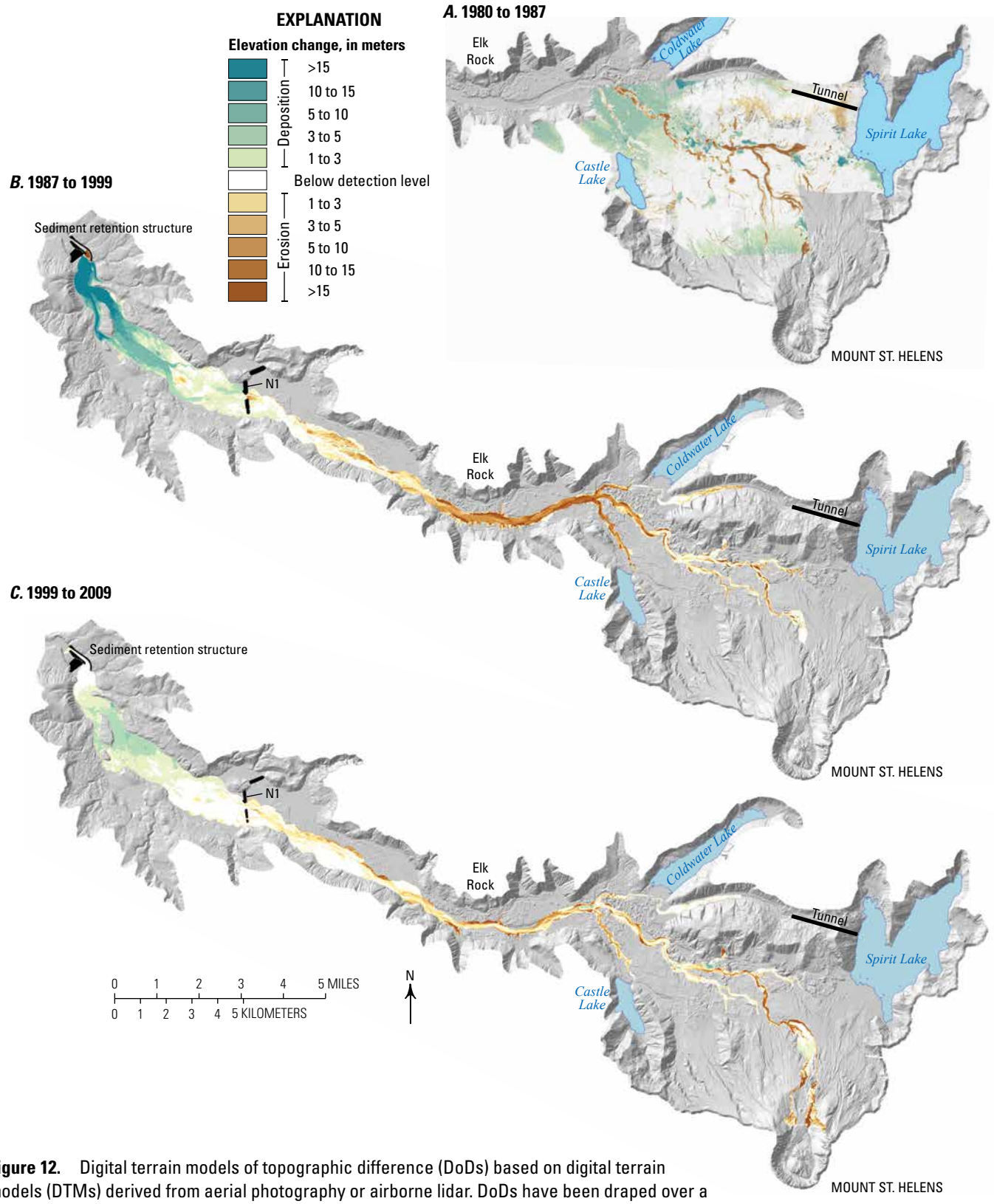

Figure 12. Digital terrain models of topographic difference (DoDs) based on digital terrain models (DTMs) derived from aerial photography or airborne lidar. DoDs have been draped over a shaded-relief topographic model derived from a 2009 airborne lidar survey (table 2). These DoDs provide decadal-scale snapshots of geomorphic changes in upper North Fork Toutle River basin. N1, location of former small retention structure constructed in early 1980s. *A*, DoD from 1980 to 1987. Apparent broad-scale deposition along the western edge of the model is an artifact of poor topographic control and warping along the edge of the 1980 DTM. *B*, DoD from 1987 to 1999. The deep erosion at the sediment retention structure spillway is an artifact of construction activity. *C*, DoD from 1999 to 2009. Parts *B* and *C* are modified from Major and others (2018).

holistic, decadal-scale snapshots of topographic change show that the footprint of substantial erosion had greatly diminished, but that erosional hotspots persisted locally, particularly along upper NFTR and Loowit Creek channels (Major and others, 2018; fig. 12*C*). Reaches of persistent, focused erosion are along the volcano's lower north flank (upstream from cross-section LO030), across the Pumice Plain (between cross-sections LO030 and NF100), and near Coldwater Lake between cross-section NF120 and the Castle Creek/Coldwater Creek confluence (Major and others, 2018) (figs. 4, 12*C*). On the volcano's lower north flank, a few to a few tens of meters of lateral bank erosion can produce many tens of meters of elevation change owing to erosion of very tall banks, especially along upper Loowit Creek and Step creek (informally named). Oblique aerial photographs from late November 2006 indicate some, and perhaps much, of the documented erosion along upper Loowit Creek channel between 1999 and 2009 happened during a large storm in early November 2006 (Major and others, 2018) that delivered 338 mm of rainfall in 5 days (November 5–9) to upper NFTR (Natural Resources Conservation Service, 2019). Those photographs also show a 4.5 million m^3 mass failure on the crater floor, which became a debris flow that traveled down Loowit Creek channel (Mosbrucker and others, 2019).

Following an initial phase of rapid geomorphic change and channel development in the early 1980s under even low- to moderate-magnitude flows, channel evolution became predominantly event driven. Comparing changes in channel geometry documented by measurements of channel cross sections to the hydrological record shows that the most distinctive channel changes from 1990 to 2017 are associated mainly with some of the largest magnitude flows that have occurred since the early 1980s. The three principal hydrological events from 1996 to 2016—a flood in February 1996, a flood and debris flow in November 2006, and a flood in December 2015, as well as a landslide from debris-avalanche sediment perched along the south face of Johnston Ridge in January 2006—left clear imprints on channel morphology, at least as observed through the lens of spatially discrete snapshots of channel geometry. [We note, however, that the elapsed time between surveys makes any impact of the December 2015 flood event less distinctive.] For example, along Loowit Creek channel, high streamflow and a debris flow in November 2006 triggered ~10 m of incision and tens of meters of lateral erosion (cross-sections LO033, LO040; figs. 10*B*, *C*). Farther downstream along the reach of upper NFTR channel that hugs Johnston Ridge, channel incision from this event ranged 3–10 m (cross-sections NF100, NF105, and NF110), with local lateral erosion to tens of meters (figs. 10*D*, *E*, *F*). But floods and debris flows are not the only processes to affect channel evolution. In January 1996, a large mass failure of debris-avalanche material deposited about 600,000 m^3 of sediment in NFTR channel near cross-section NF110 (Major and others, 2018; figs. 4, 10*F*, 12*C*). That deposit forced the river to erode laterally by tens of meters.

In addition to secondary failure of debris-avalanche sediment affecting channel geometry, many debris flows from the crater (of order 100,000 m^3) have deposited considerable sediment on a fan at the base of Loowit and Step canyons (Waitt and others, 1993; Cameron and Pringle, 1990; Pierson and Waitt, 1999; Pringle and Cameron, 1999; Mosbrucker and others, 2019). Such deposition has, over the years, caused Loowit Creek to change course—at times draining directly toward Spirit Lake and at other times draining toward NFTR (fig. 13). Aerial photographs show the Loowit Creek and Step creek channels began to form around November 1980. Since then, Loowit Creek has avulsed multiple times. From 1980 to 1984, the creek flowed toward NFTR. But in 1984, streamflow began to bifurcate with most flowing toward NFTR and some flowing toward Spirit Lake. From 1984 through 1985, bifurcated streamflow discharged both ways in roughly equal proportions. In 1986, bifurcation ceased and streamflow drained toward NFTR, but from 1987 to 1989 streamflow again switched and flowed toward Spirit Lake. Between 1989 and 1994, flow direction switched yet again toward NFTR. Following significant debris-flow deposition in September 1997 (Major and others, 2005), streamflow switched course, and from 1997 to 2002, it drained toward Spirit Lake. The course briefly shifted toward the NFTR in 2002, and again toward Spirit Lake in 2003. The present drainage of Loowit Creek toward NFTR is the result of yet another avulsion in 2004.

The Step-Loowit fan is susceptible to avulsion primarily because its channels are poorly incised at the fan head. Near the fan apex, the nexus of most avulsions (fig. 13), the Loowit Creek channel is about 1 m deep. As a result, it takes little sediment accumulation to cause channel avulsion. Debris flows from the crater commonly deposit sediment fill of 0.5–1 m thick or more. In contrast, channels are more deeply incised farther down the fan and across the Pumice Plain. Thus, avulsions downstream on the fan are less likely. Such physiography has important geomorphic implications (de Haas and others, 2018a,b; Densmore and others, 2019). If avulsion occurs near the fan apex, there is a high probability that streamflow direction will switch completely from one side of the fan to the other, thereby crossing the debris-blockage drainage divide. In contrast, if avulsions happen farther down fan, the change in streamflow direction will be more local and more likely to remain on the same side of the blockage drainage divide.

From 1999 to 2009, reaches of focused erosion along upper NFTR channel were punctuated by reaches of deposition (Major and others, 2018). At the base of the volcano's north flank, but above cross-section LO030 (fig. 4), as much as 4 m of sediment accumulated on the valley floor (fig. 12*C*). Downstream from the fan of landslide debris that filled the channel near cross-section NF110 (fig. 4), fluvial and debris-flow deposits from the large storm in November 2006 left a 6-m-thick fill on the valley floor (fig. 12*C*). Sediment also accumulated on the valley floor farther downstream; in November 2006 deposition displaced the confluence of NFTR and Coldwater Creek several hundred meters downstream (Major and others, 2018).

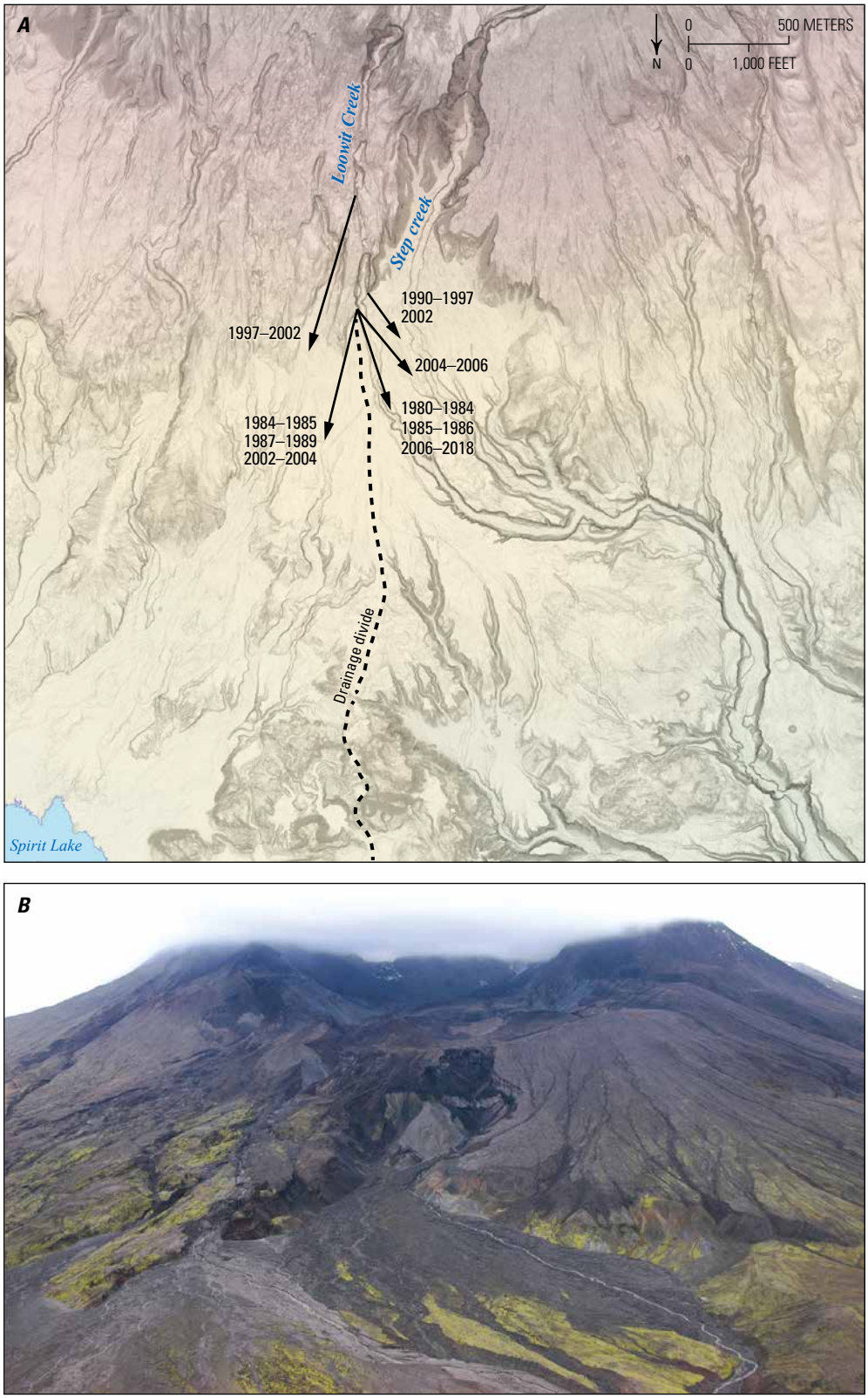

Figure 13. Step-Loowit fan. *A*, Schematic diagram showing history of channel avulsion of Loowit Creek near head of fan. Arrows show predominant flow direction of Loowit Creek for time period indicated. Dashed line shows approximate drainage divide on Spirit Lake blockage. Colors show relative elevation; warmer colors indicate higher elevations. Base map derived from a 2009 airborne lidar survey (table 2). *B*, Oblique aerial view of fan. USGS photograph by John Pallister, October 6, 2004.

The erosion, channel avulsion, and localized channel deposition documented following emplacement of the Spirit Lake blockage illustrate the very dynamic character of upper NFTR basin. Though many channel reaches now appear to be approaching a state of equilibrium with respect to vertical incision and modification of the river's longitudinal profile (Zheng and others, 2014), the sediment composing the fluvial landscape in this valley remains highly susceptible to erosion. Such erosion is especially intense when abundant, concentrated runoff is first introduced to these deposits. It is also clear that even though chronic incision of the drainage system on and around the blockage has largely diminished, large storm events can drive acute incision locally on the order of several meters. Such acute localized incision can set up geomorphic instabilities that may migrate headward as knickpoints or knickzones (abrupt steps in the channel profile).

Fine-Time-Scale Landscape Evolution from 1980 to 2018 and Linkages to Hydrology and Hydrologic Events

Although decadal-scale DoDs provide useful holistic snapshots of the geomorphic evolution of upper NFTR valley, finer-time-scale DoDs permit a better grasp of linkages among topographic change, hydrology, topography, and surface geology. We thus generated DoDs showing annual to multi-year topographic changes but focused on changes on and around the Spirit Lake blockage. These DoDs are generated from DTMs using various data sources (table 2), and they represent varying time intervals. The fine-time-scale DoDs show initial development of the NFTR network as it integrated the upper basin, along with subsequent adjustments and sculpting. They show that early evolution was dominated largely by vertical channel incision and network extension, whereas later changes shifted more toward lateral erosion and greater definition of the emergent drainage network (see also Major and others, 2019).

Pre-1980 to 1980

A DoD of pre-eruption (approximately 1952) to post-eruption (September 5, 1980) elevation change shows the massive accumulation of debris-avalanche and pyroclastic deposits that filled upper NFTR valley, as well as scour on the lower north flank of the volcano caused by passage of the debris avalanche, the blast PDC, and subsequent pyroclastic flows (fig. 14). This DoD represents the initial condition from which the drainage network develops.

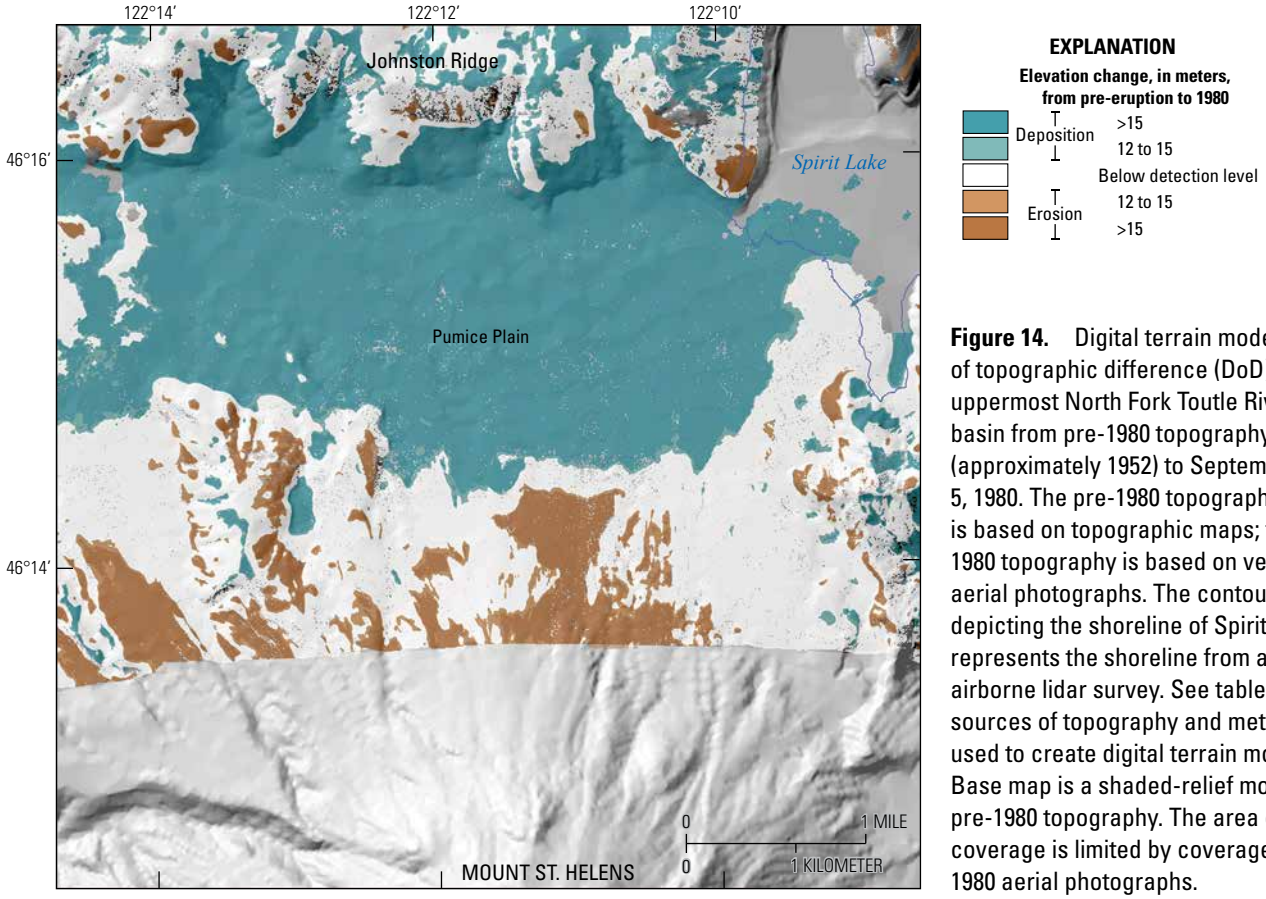

Figure 14. Digital terrain model of topographic difference (DoD) of uppermost North Fork Toutle River basin from pre-1980 topography (approximately 1952) to September 5, 1980. The pre-1980 topography is based on topographic maps; the 1980 topography is based on vertical aerial photographs. The contour depicting the shoreline of Spirit Lake represents the shoreline from a 2009 airborne lidar survey. See table 2 for sources of topography and methods used to create digital terrain models. Base map is a shaded-relief model of pre-1980 topography. The area of DoD coverage is limited by coverage of the 1980 aerial photographs.

1980–81

The DoD representing change from September 5, 1980, to July 27, 1981, illustrates initial development of the nascent drainage network (fig. 15). Despite known distortions, this DoD shows initial erosion of the lower north flank of the volcano in the areas that eventually became the headwaters of Step creek and Loowit Creek, the birth of the debris fan at the mouth of Loowit and Step canyons, nascent development of Loowit Creek channel across the Pumice Plain and the beginning of a drainage channel along the eastern margin and toe of Floating Island lava flow. This DoD also shows closed, sediment-filled depressions along the foot of Johnston Ridge. These depressions are loosely connected, or are beginning to be connected, by small segments of incised channels. When this DoD is compared to a pre-1980 topographic map (fig. 3), it is evident that the nascent drainage network strongly resembles the location of the pre-eruption drainage network. This resemblance indicates fundamental factors such as general topography and gross geology (discussed in "Geomorphic Processes and Relations with Topography and Surface Geology" section) strongly influence the location of drainage channels at Mount St. Helens.

1981–82

Between July 27, 1981, and September 22, 1982, the upper NFTR drainage network expanded and sharpened its definition substantially. This geomorphically active period was characterized by (1) widening along Loowit Creek channel across the Pumice Plain, which enlarged and sharpened the shape of that channel; (2) deposition at the foot of the volcano, which expanded and elevated the Step-Loowit fan; (3) erosion by both surface-water runoff and a lahar in March 1982, which defined a nascent channel at the base of Johnston Ridge along the present-day location of lower Truman channel (see fig. 4); (4) substantial expansion of deposition within a depression at the base of Johnston Ridge known colloquially as the pumice pond, likely as a result of deposition by the March 1982 lahar; (5) breaching of depressions farther downstream, which enlarged and sharpened the definition of small channel segments connecting them, perhaps owing to erosion by the March 1982 lahar; and (6) initiation and enlargement of new channel segments caused by groundwater seepage in the vicinity of present-day Carbonate springs (fig. 16), possibly owing to a breaching of a small lake that formed

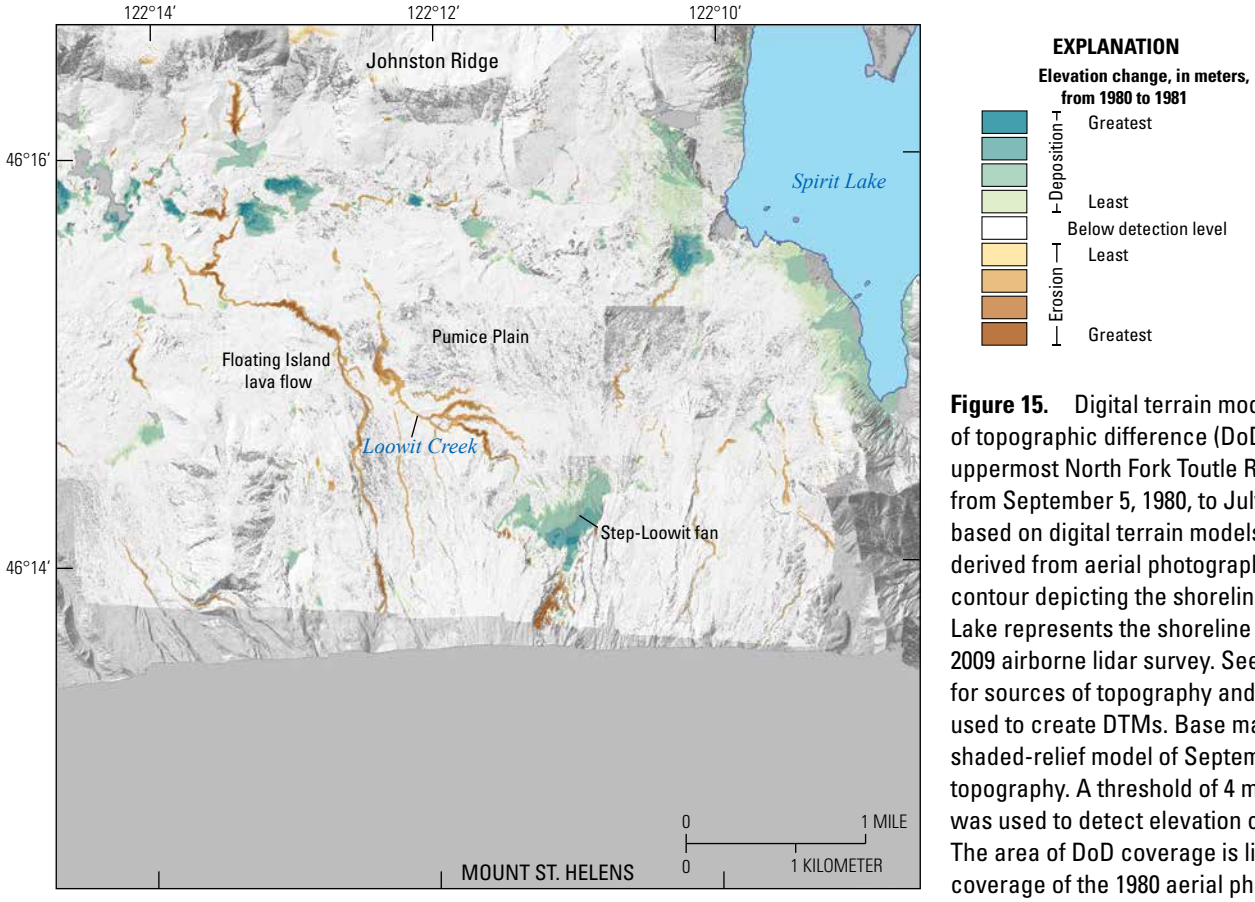

Figure 15. Digital terrain model of topographic difference (DoD) of uppermost North Fork Toutle River basin from September 5, 1980, to July 27, 1981, based on digital terrain models (DTMs) derived from aerial photography. The contour depicting the shoreline of Spirit Lake represents the shoreline from a 2009 airborne lidar survey. See table 2 for sources of topography and methods used to create DTMs. Base map is a shaded-relief model of September 1980 topography. A threshold of 4 meters was used to detect elevation change. The area of DoD coverage is limited by coverage of the 1980 aerial photographs.

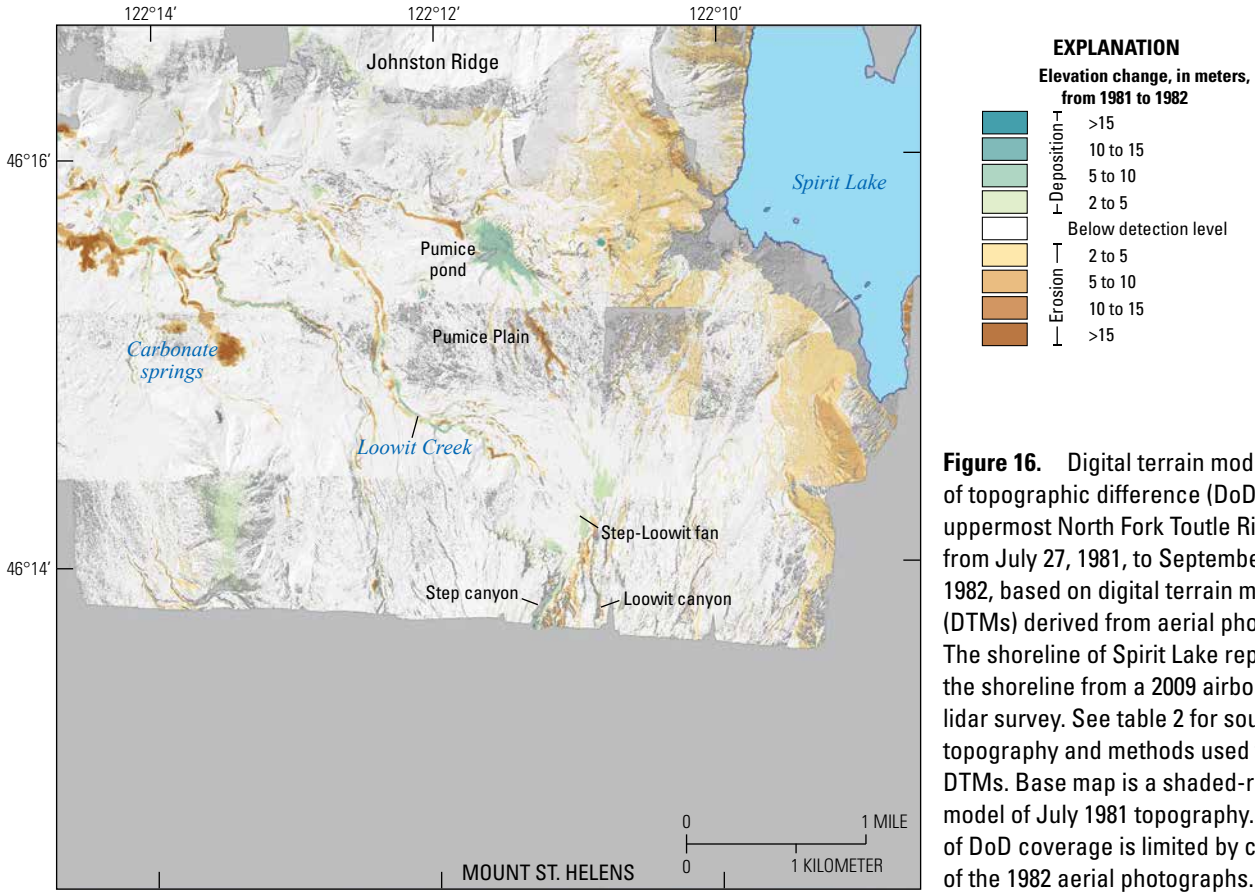

Figure 16. Digital terrain model of topographic difference (DoD) of uppermost North Fork Toutle River basin from July 27, 1981, to September 22, 1982, based on digital terrain models (DTMs) derived from aerial photography. The shoreline of Spirit Lake represents the shoreline from a 2009 airborne lidar survey. See table 2 for sources of topography and methods used to create DTMs. Base map is a shaded-relief model of July 1981 topography. The area of DoD coverage is limited by coverage of the 1982 aerial photographs.

there (Simon, 1999). Although the March 1982 lahar was a significant hydrologic event (fig. 17), and it left an imprint on the topography as noted above, it generally had little detectable impact, within our threshold limits, other than noted above on the landscape evolution of upper NFTR basin. In general, its deposit is less than 2 m thick (Waitt and others, 1983; Pierson, 1999), and thus the depositional imprint of that event, except perhaps in the pumice pond, is below the level of detectable change achieved in this DoD.

Geomorphic changes represented by the 1980–81 and 1981–82 DoDs occurred during a period when the basin experienced significant and varied hydrologic adjustments. As noted previously, a daily mean streamflow of 150 m^3/s (as estimated on NFTR below the SRS), a streamflow having an approximately 0.27 annual exceedance probability (a 4-year recurrence-interval flow; fig. 9), was exceeded 7 times from 1981 to 1983. Thus, this initial phase of network development occurred under conditions of distinctly enhanced runoff (as well as being affected by volcanically induced hydrologic events). Although this period encompasses one of the largest floods recorded (960 m^3/s on February 20, 1982; table 1) on NFTR (NFTR at Kid Valley, streamgage 14241100; KID in fig. 2), that flood resulted mainly from breaching of Jackson Lake—a lake impounded at the debris-avalanche-deposit margin downstream from Castle Lake (Simon, 1999). Hence, that event had no direct impact on fluvial-network evolution in upper NFTR basin above Castle and Coldwater Lakes.

1982–84

Some of the most extensive evolution of the channel network in upper NFTR basin occurred between late 1982 and summer 1984, especially along Truman channel (fig. 18). This period encompasses the pumping operations enacted to lower and stabilize Spirit Lake while a suitable outlet was designed and constructed. Water from Spirit Lake was pumped through a conduit shallowly buried within the debris-avalanche deposit to a stilling basin west of the crest of the Spirit Lake blockage, from which it then flowed across the blockage surface. Full pumping operations began November 5, 1982, and ended in late April 1985 when the present-day outlet tunnel became fully operational. Extensive erosion by continuous flow of 5.1 m^3/s—including more than 10 m of incision and many tens of meters widening—is evident in the DoD (see also fig. 11). Much of the erosion along Truman channel occurred within weeks to a few months of the start of full pumping operations.

By summer 1984, the geometry of Truman channel had largely stabilized and equilibrated to the steady water discharge delivered (fig. 11), and since then extensive riparian vegetation has established.

The 1982–84 DoD also shows significant erosion, deposition, and sculpting of channels across the blockage landscape. During this 2-year period, Loowit Creek channel became more prominently defined, both incising and eroding laterally (figs. 10*B*, *C*). The mainstem NFTR channel downstream from the Loowit Creek-Truman channel confluence eroded and enlarged, but also aggraded and accumulated sediment below the erosional reach. The channel formed by streamflow emanating from the Carbonate springs area accumulated sediment, and sediment continued to aggrade the Step-Loowit fan at the foot of the volcano. Hydrologically, daily mean streamflow greater than 150 m^3/s occurred in water year[1] 1983 and approached that magnitude of streamflow in water year 1984 (fig. 7), but there were no exceptional hydrologic events. Nevertheless, basin hydrology remained in a state of disequilibrium compared to pre-eruption hydrology (Major and Mark, 2006). In addition, the volcano remained in a state of active eruption and triggered melt-induced floods and debris flows that affected upper NFTR basin. Relatively small eruptions in February 1983 and May 1984 triggered slushflows, debris flows, and small-magnitude floods that emanated from the crater and swept across Step-Loowit fan and through channels across the Pumice Plain (Pierson and Janda, 1994; Pierson and Waitt, 1999; Pringle and Cameron, 1999; Major and others, 2005). Narrow fingers of flow from these events reached Spirit Lake. These flows contributed to further aggradation of the Step-Loowit fan and likely helped sculpt Loowit Creek channel through lateral erosion (see cross sections LO033 and LO040, fig. 10*B, C*).

[1]A water year is the 12-month period from October 1 through September 30 and is designated by the calendar year in which it ends.

Figure 17. Lahar generated by melting of crater snow during a small explosion on March 19, 1982. Spirit Lake is in the lower left corner of the image. U.S. Geological Survey photograph by T. Casadevall.

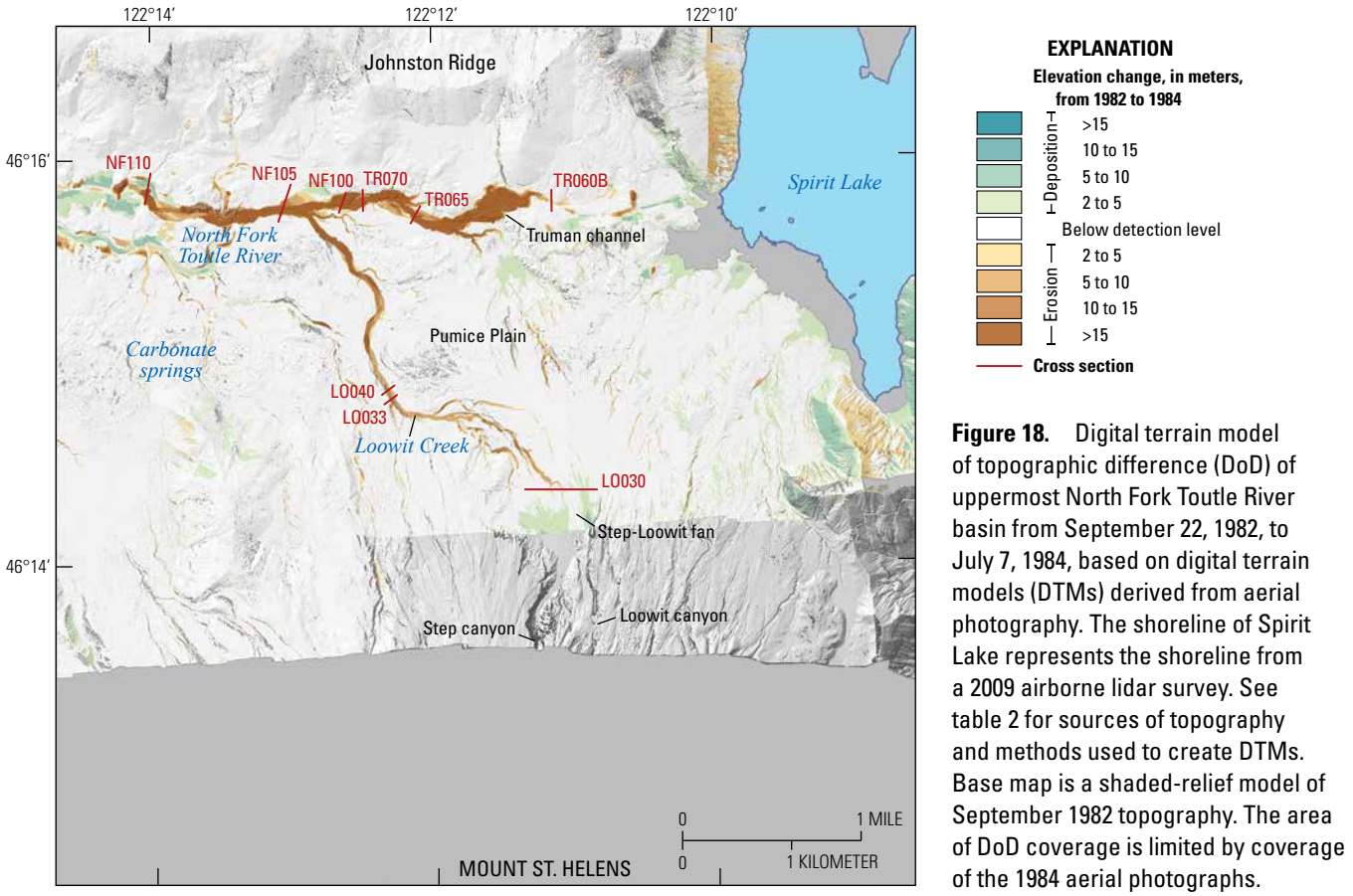

Figure 18. Digital terrain model of topographic difference (DoD) of uppermost North Fork Toutle River basin from September 22, 1982, to July 7, 1984, based on digital terrain models (DTMs) derived from aerial photography. The shoreline of Spirit Lake represents the shoreline from a 2009 airborne lidar survey. See table 2 for sources of topography and methods used to create DTMs. Base map is a shaded-relief model of September 1982 topography. The area of DoD coverage is limited by coverage of the 1984 aerial photographs.

1984–85

Little geomorphic change is detected in the DoD from July 7, 1984 to July 25, 1985 (fig. 19). This lack of detectable change results in part because water years 1984 and 1985 were hydrologically muted, with few daily mean streamflows approaching 150 m^3/s (fig. 7), and because the DoD for this period has a large (4 m) threshold of detection. Aside from a minor eruption-triggered debris flow in May 1984 (Pringle and Cameron, 1999), only modest amounts of streamflow (largely less than 1.5 m^3/s) issued from the crater. Cross sections along Loowit Creek channel (LO033, LO040) show localized sediment deposition (figs. 10*B*, *C*), whereas farther downstream, at cross sections NF100, NF105, and NF120, channel evolution largely involved incision and widening (figs. 10*D*, *E*, *G*). Cross section NF110, however, displays aggradation and widening (fig. 10*F*). By the mid-1980s, geomorphic evolution around the blockage and through upper NFTR basin became more event driven, requiring moderate- to large-magnitude flows (greater than 150 m^3/s as measured on NFTR below the SRS) to do much geomorphic work beyond nibbling channel margins. Relatively small flows along the major channels eroded channel banks, but otherwise left little geomorphic signal in the DoD, in part because any cumulative erosion or deposition along the channel floor was below the 4-m detection threshold; channel widening, though detectable, was neither extensive nor ubiquitous. The greatest geomorphic changes were perhaps most relevant on Step-Loowit fan, but that area is largely outside the footprint of this DoD. Although we cannot confidently detect substantive change to the fan, sediment accumulation there was likely the agent responsible for driving the avulsions of Loowit Creek visible in aerial imagery (see fig. 13).

1985–87

From July 1985 to July 1987, geomorphic modifications to the channels in upper NFTR basin were relatively minor—limited largely to modest channel enlargement promoted by channel aggradation and lateral erosion (figs. 10, 20). These minor modifications owe largely to gradually increasing landscape stability under relatively benign hydrological conditions and because flow from the crater was directed largely toward Spirit Lake rather than toward NFTR (fig. 13). Peak daily mean streamflow in water years 1985–87 was less than 150 m^3/s at NFTR below the SRS (fig. 6), and dome-building eruptions triggered only one small debris flow from the crater in May 1986, which attenuated swiftly upon reaching the flat topography of Step-Loowit fan (Cameron and Pringle, 1990).

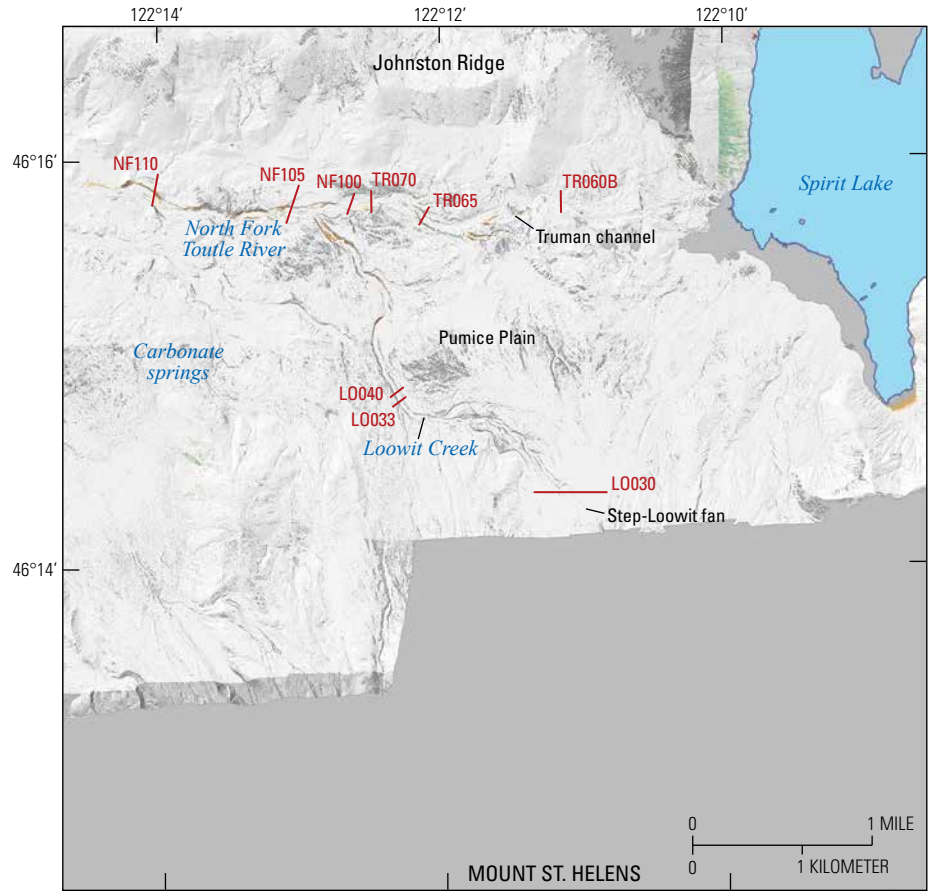

Figure 19. Digital terrain model of topographic difference (DoD) of uppermost North Fork Toutle River basin from July 7, 1984, to July 25, 1985, based on digital terrain models (DTMs) derived from aerial photography. The shoreline of Spirit Lake represents the shoreline from a 2009 airborne lidar survey. See table 2 for sources of topography and methods used to create DTMs. Base map is a shaded-relief model of July 1984 topography. A threshold of 4 meters was used to detect elevation change. The area of DoD coverage is limited by coverage of the 1984 aerial photographs.

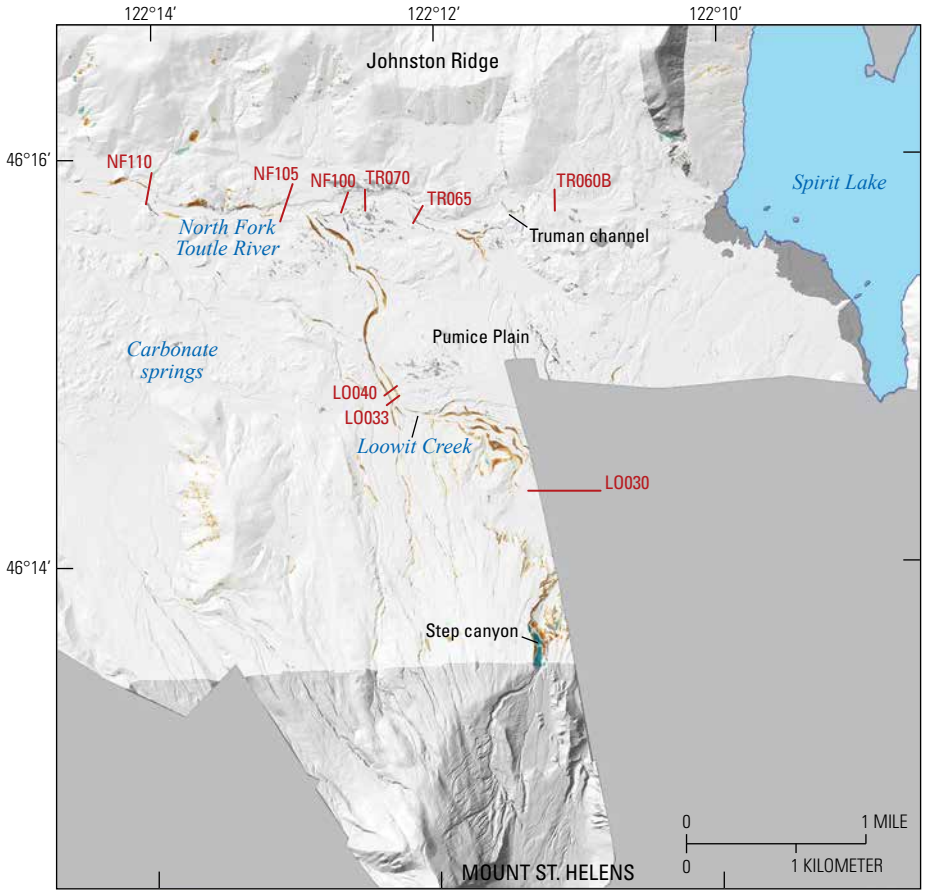

Figure 20. Digital terrain model of topographic difference (DoD) of uppermost North Fork Toutle River basin from July 25, 1985, to mid-June 1987 based on digital terrain models (DTMs) derived from aerial photography. The shoreline of Spirit Lake represents the shoreline from a 2009 airborne lidar survey. See table 2 for sources of topography and methods used to create DTMs. Base map is a shaded-relief model of July 1985 topography. The area of DoD coverage is limited by coverage of the 1987 aerial photographs.

1987–96

The frequency of remotely sensed topographic data declined sharply after 1987, and as a result our ability to holistically analyze fine-time-scale geomorphic change in upper NFTR basin diminished. By this time, however, enhanced runoff had largely diminished (Major and Mark, 2006), the long-profile of NFTR channel had begun to stabilize (Zheng and others, 2014), and the landscape had begun equilibrating to the imposed hydrologic regime. Landscape dynamics had also shifted toward an event-driven dynamic to achieve substantive geomorphic change, especially regarding further channel incision. The 1987–96 DoD (fig. 21)—documenting changes from June 1987 to August 1996—shows lateral adjustments along margins of Loowit Creek channel and renewed channel development near Carbonate springs. Cross-section surveys indicate channel refinement consisted of channel incision and widening above NF110 and aggradation and widening downstream (fig. 10).

From 1987 through 1995, basin hydrology was pedestrian and perhaps even a bit on the dry side. Daily mean streamflow below the SRS was commonly less than 100 m^3/s (fig. 6), a streamflow typically exceeded every 18 months on average (fig. 9), and peak streamflow was less than 150 m^3/s. In the early 1990s, peak daily mean streamflow approached 150 m^3/s. We note, however, that streamflow from 1988 to 1998 was regulated by culverts in the face of the SRS (fig. 8). In January 1990, substantial peak streamflows issued from Green River and South Fork Toutle River basins, but the measured peak streamflows on NFTR at KID (USGS streamgage 14241100) and FTP (USGS streamgage 14240525) (fig. 2) were muted (table 1; fig. 7). In February 1996, a strong and sustained atmospheric river delivered substantial warm rainfall onto an extensive and low-elevation snowpack (Marks and others, 1998). The combination of abundant warm rainfall and induced snowmelt generated the peak streamflow of record along lower Toutle River at Tower Road (1,750 m^3/s; USGS streamgage 14242580; labeled TOW in fig. 2) and the second largest peak streamflow, but largest daily mean streamflow, measured at NFTR below the SRS (USGS streamgage 14240525) since the gage became operational in 1989 (fig. 7; table 1).

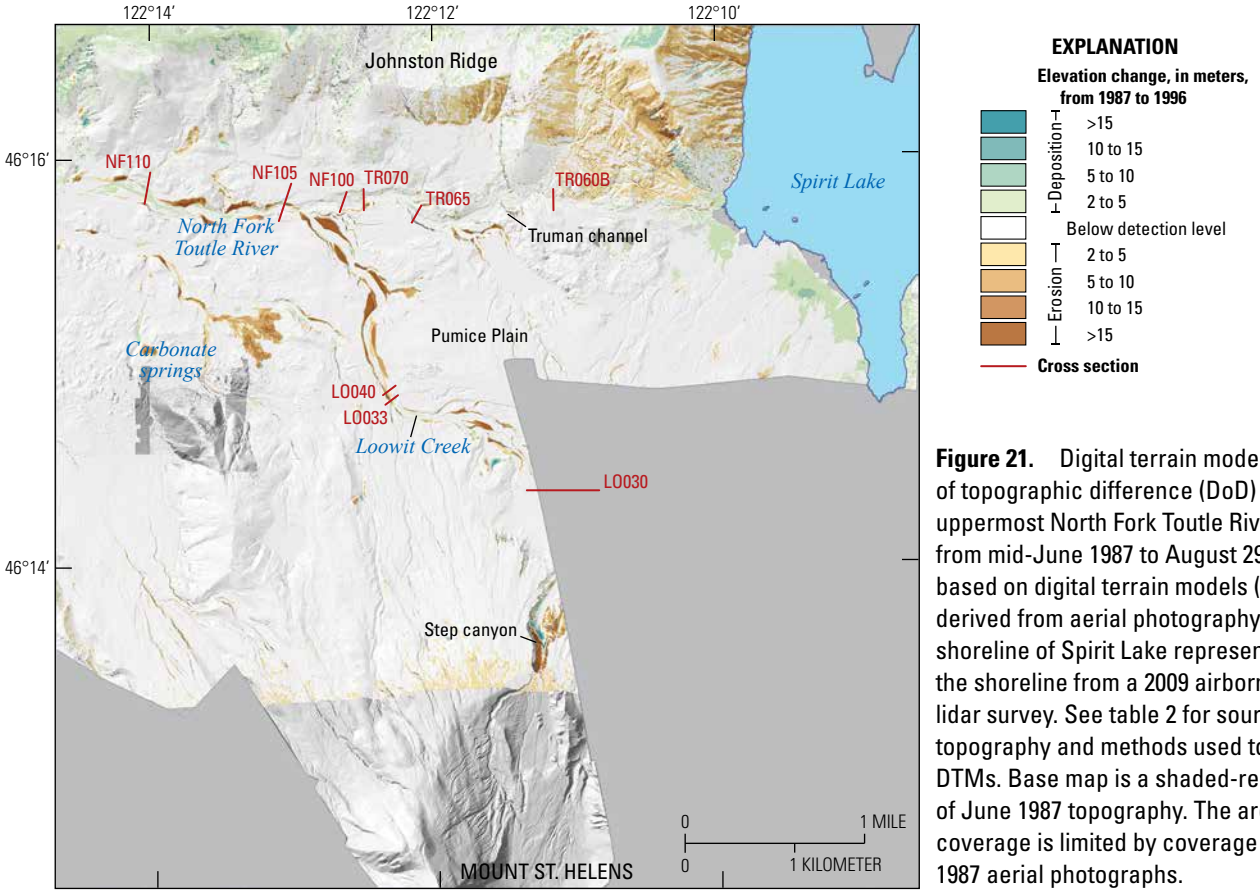

Figure 21. Digital terrain model of topographic difference (DoD) of uppermost North Fork Toutle River basin from mid-June 1987 to August 29, 1996, based on digital terrain models (DTMs) derived from aerial photography. The shoreline of Spirit Lake represents the shoreline from a 2009 airborne lidar survey. See table 2 for sources of topography and methods used to create DTMs. Base map is a shaded-relief model of June 1987 topography. The area of DoD coverage is limited by coverage of the 1987 aerial photographs.

The rare 1996 flood event is likely responsible for substantial lateral and vertical channel adjustments detected in both the DoD (fig. 21) and cross-section measurements (fig. 10), especially upstream from cross-section NF105. Renewed channel development near Carbonate springs likely owes to eastward shifting of groundwater seepage (compare the 1987–96 DoD [fig. 21] with that of 1981–82 [fig. 16]), but it is unclear whether the 1996 flood event influenced spring location or discharge magnitude. Water year 1996 recorded the greatest volume of annual runoff from upper NFTR basin since the eruption, and it was substantially larger than any other annual runoff during 1987–96 (table 3). Therefore, it is possible that abundant precipitation input to the local groundwater system invigorated and increased shallow groundwater flow, and that the increased groundwater discharge caused the channel change detected. If so, this is yet another example of the sensitivity of this landscape to changes in discharge regime.

Table 3. Annual mean streamflow and total runoff of North Fork Toutle River below sediment retention structure near Kid Valley (U.S. Geological Survey streamgage 14240525).

[m^3/s, cubic meters per second; m^3, cubic meters; E, estimated value]

Water year	Annual mean streamflow (m^3/s)[1]	Annual total runoff (million m^3)	Water year	Annual mean streamflow (m^3/s)[1]	Annual total runoff (million m^3)
1981	18.2 E	573.8 E	2000	21.0 E	663.2 E
1982	22.7 E	716.7 E	2001	13.2	415.8
1983	23.7 E	746.3 E	2002	23.6	744.6
1984	26.1 E	824.0 E	2003	17.6 E	554.9 E
1985	20.5 E	646.2 E	2004	18.3 E	578.2 E
1986	20.3 E	640.7 E	2005	17.2 E	541.2 E
1987	17.9 E	565.8 E	2006	20.9 E	660.4 E
1988	16.7 E	527.6 E	2007	21.4	673.9
1989	17.1 E	540.5 E	2008	21.9	691.6
1990	22.8	719.0	2009	18.2	573.1
1991	22.9	721.4	2010	24.8	783.6
1992	15.9	502.5	2011	30.0	944.6
1993	16.8	530.8	2012	27.4	867.7
1994	15.3	483.5	2013	22.9	723.5
1995	22.7	715.1	2014	22.6	711.3
1996	30.4	961.7	2015	18.8	594.1
1997	28.9	911.9	2016	25.8	816.0
1998	22.2	699.7	2017	32.1	1,013.1
1999	26.8 E	846.1 E	2018	19.9	629.1

[1]Values for water years 1981–89 are computed using regression relations for differences between streamflow at North Fork Toutle River at Kid Valley (USGS streamgage 14241100) and Green River above Beaver Creek, near Kid Valley (USGS streamgage 14240800). Values for water years 1999, 2000, and 2003–06 are estimated using regression relations among streamgages 14240525, 14240800, 14241100, and streamflow measured on Toutle River at Tower Road (USGS streamgage 14242580). See supplemental data file DF1 for streamflow estimates. All other water years are based on streamflow measured at North Fork Toutle River below sediment retention structure near Kid Valley (USGS streamgage 14240525).

1996–99

Except along the deeply incised canyons of Step creek and Loowit Creek on the lower north flank of the volcano, relatively minor changes are detected in the DoD that represents change from August 1996 to September 1999 (fig. 22). It is unclear if the substantial deposition detected in Step and upper Loowit canyons is real or an artifact of uncontrolled imagery near the boundaries of the terrain models, because nearly identical footprints of equivalent erosion appear in the 1999–2003 DoD (fig. 23). Major channels (Loowit Creek, mainstem NFTR) show modest lateral adjustments as channel banks continued to erode, and deposition at the head of Step-Loowit fan and along upper Loowit channel is evident. Deposition along the eastern margin of Step-Loowit fan owes mainly to small debris flows emanating from channel headwaters in September 1997 (Major and others, 2005)—a geomorphic process common in early fall when the first substantial rains strike the region. Notably, flow from Loowit Creek during this period was directed toward Spirit Lake rather than toward NFTR as it had been previously (fig. 13). Deposition detected along upper Loowit channel appears to coincide with an area of erosion just upslope, and this may reflect a small mass failure from hummocky areas on the debris avalanche, another geomorphic process commonly observed on this landscape. This period is characterized by hydrologic conditions typical of the long-term average along lower NFTR (fig. 7)—neither extreme events nor notably dry conditions (though water year 1998 appears to be below average).

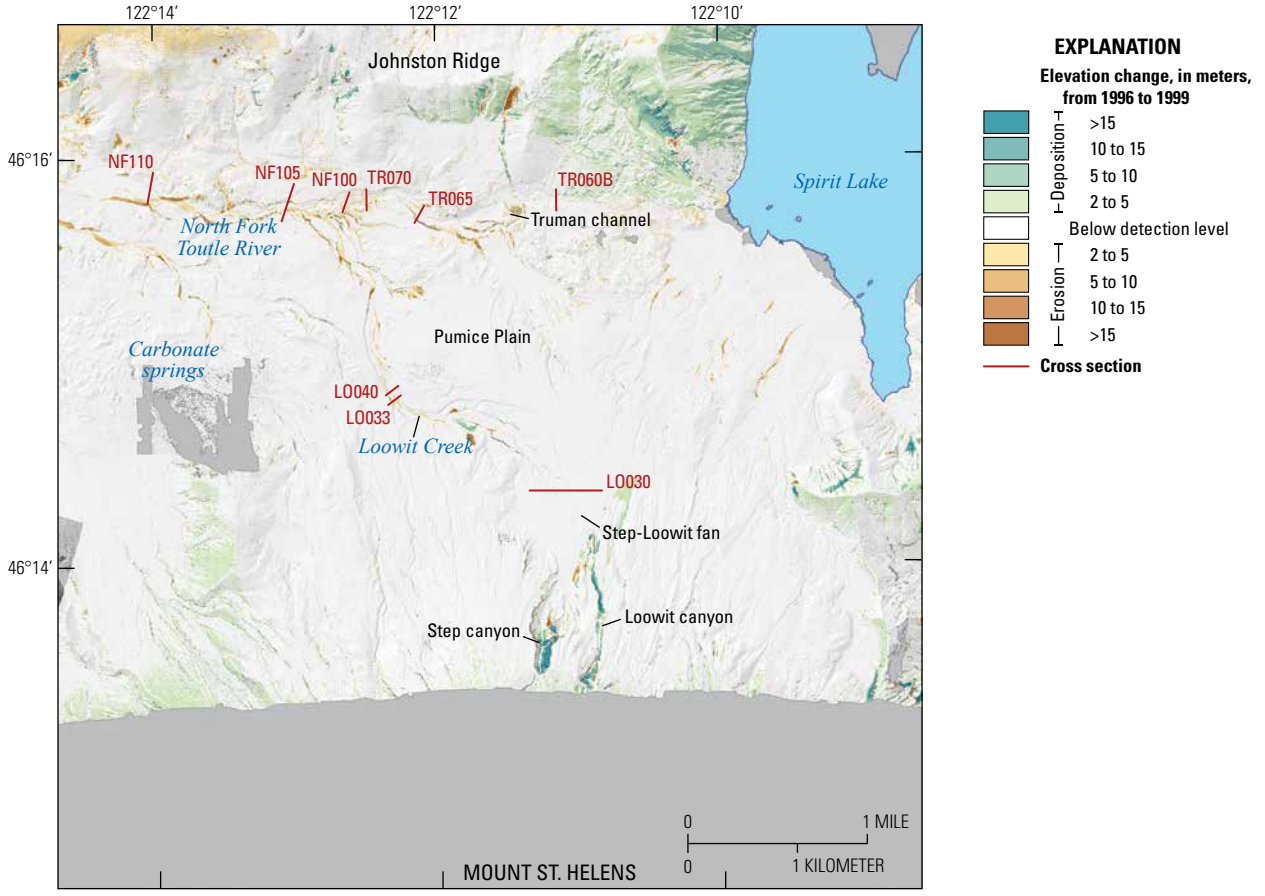

Figure 22. Digital terrain model of topographic difference (DoD) of uppermost North Fork Toutle River basin from August 29, 1996, to September 3, 1999, based on digital terrain models (DTMs) derived from aerial photography. The shoreline of Spirit Lake represents the shoreline from a 2009 airborne lidar survey. See table 2 for sources of topography and methods used to create DTMs. Base map is a shaded-relief model of August 1996 topography. The area of DoD coverage is limited by coverage of the 1996 aerial photographs.

1999–2003

Relatively benign hydrologic conditions characterize the period from September 1999 to September 2003 (fig. 7). Consequently, little except local geomorphic change is detected (fig. 23). Peak daily mean streamflow of NFTR below the SRS approached or exceeded 150 m^3/s on few occasions, and during a few water years was largely less than 50 m^3/s. Average annual mean streamflow (and average total annual runoff) from NFTR basin during this period is 25 percent lower than that from 1996–99 (table 3). The greatest geomorphic changes occurred in headwater areas of Step and Loowit canyons, where apparent erosion of tall banks is evident, although as noted previously, this footprint of erosion may be an artifact of the terrain-model processing. Nevertheless, sediment was deposited locally along Step creek channel, the eastern margin of Step-Loowit fan, and thinly along channels draining toward Spirit Lake (fig. 23). Through much of this period, flow from the crater was directed toward Spirit Lake and not along Loowit Creek (fig. 13). Apparent hillside erosion around the margins of the DoD is an artifact of differencing a photogrammetry-derived DTM (that includes vegetation) (1999) and a bare-earth, lidar-derived DTM (2003). But this does not fully explain the substantial changes apparent within the steep confines of Step and Loowit canyons.

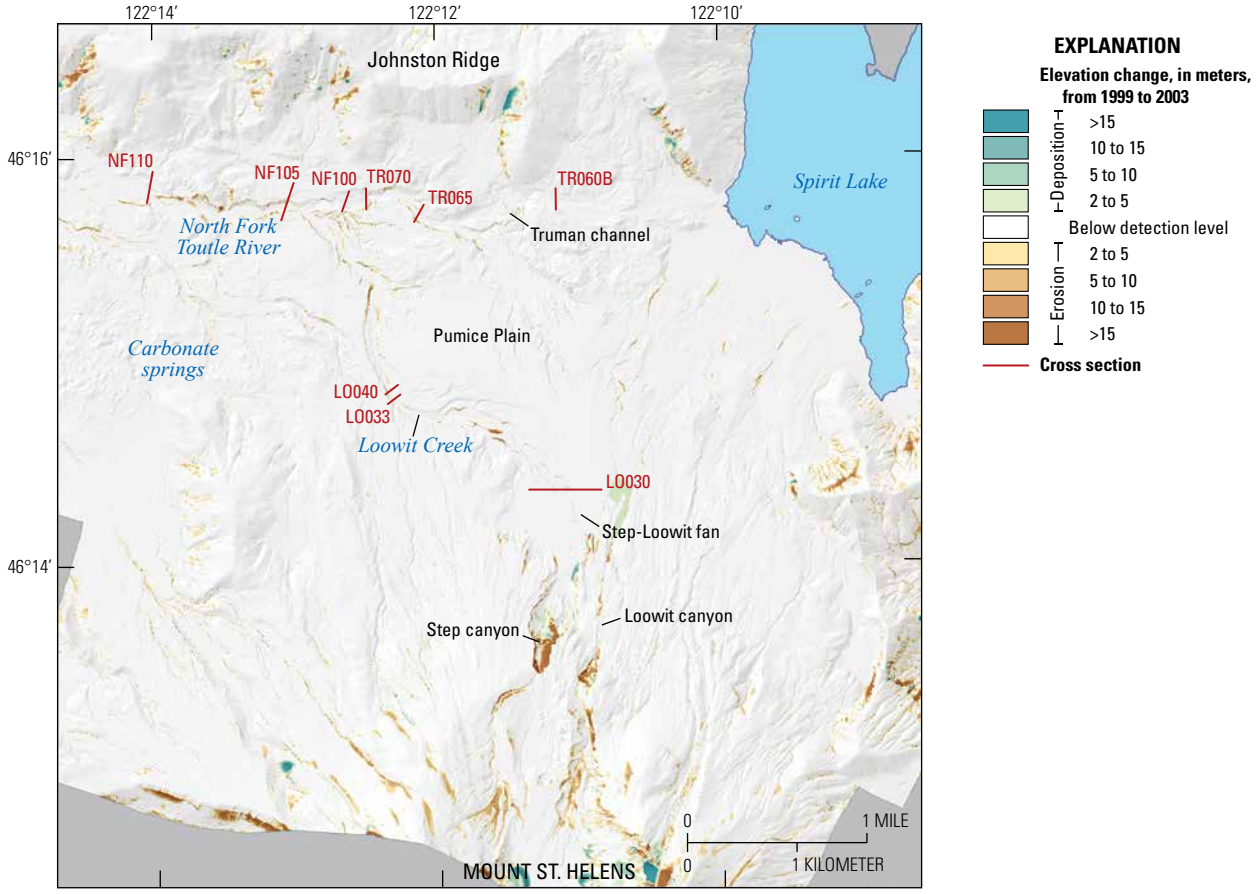

Figure 23. Digital terrain model of topographic difference (DoD) of uppermost North Fork Toutle River basin from September 3, 1999, to late September 2003 based on digital terrain models (DTMs) derived from aerial photography and airborne lidar. The shoreline of Spirit Lake represents the shoreline from a 2009 airborne lidar survey. See table 2 for sources of topography and methods used to create DTMs. Base map is a shaded-relief model of September 1999 topography. The area of DoD coverage is limited by coverage of the 1999 aerial photographs.

2003–07

Extensive geomorphic adjustments associated with substantial channel incision, widening, and mass-movement sculpted the fluvial network from September 2003 to October 2007 (figs. 10, 24). Locally, 10 m of incision and tens of meters of channel widening occurred, mainly along Loowit Creek channel but extending downstream from the Truman channel-Loowit Creek channel confluence. Mass failure of debris-avalanche sediment perched on the south face of Johnston Ridge in January 2006 (Major and others, 2018) deposited several meters of sediment in the NFTR channel and forced the river to migrate and laterally erode its bank (fig. 10*F*). Although this period is characterized by relatively normal hydrologic conditions (fig. 7), and annual mean streamflow is 6 percent less than that from 1999–2003 (table 3), a substantial storm in November 2006 produced the third greatest peak streamflow and third greatest daily mean streamflow measured on NFTR below the SRS since the gage became operational in 1989 (figs. 7, 9). This flood and an associated debris flow (Mosbrucker and others, 2019) are largely responsible for the geomorphic response detected during this period. This event, and its consequent geomorphic response, illustrate not only the important role that substantial hydrologic events have on evolution of this landscape, but also reinforce the notion that this landscape remains sensitive to infrequent, but not extreme, hydrologic events (see, for example, cross sections LO033, LO040, and NF100, fig. 10*B, C, D*).

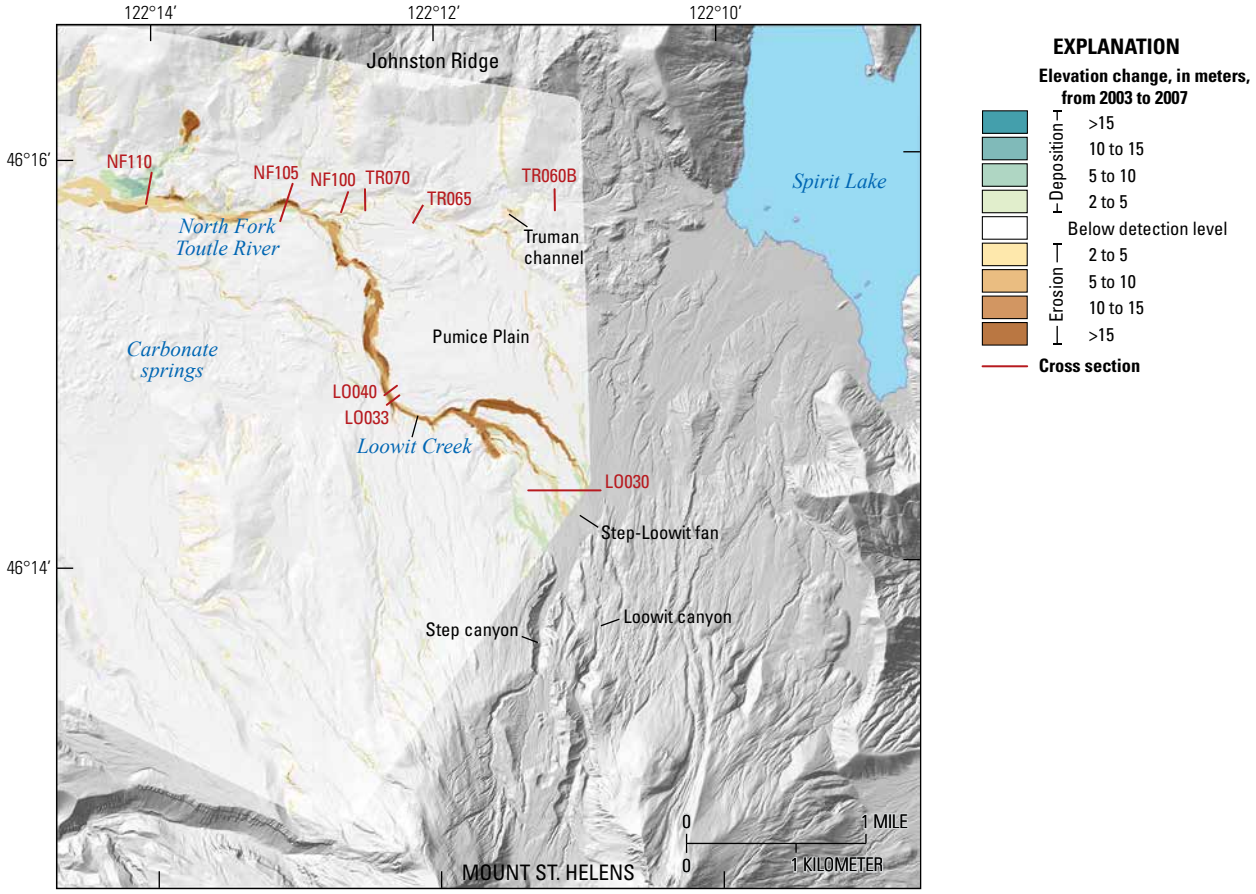

Figure 24. Digital terrain model of topographic difference (DoD) of uppermost North Fork Toutle River basin from late September 2003 to late October 2007 based on digital terrain models (DTMs) derived from airborne lidar. The shoreline of Spirit Lake represents the shoreline from a 2009 airborne lidar survey. See table 2 for sources of topography and methods used to create DTMs. Base map is a shaded-relief model of September 2003 topography. The area of DoD coverage is limited by coverage of the 2007 lidar survey.

2007–09

The 2007–09 DoD, reflecting change from October 2007 to September 2009, reveals persistent, lateral sculpting of the drainage system (fig. 25), especially along Loowit Creek, consistent with local observations from surveys of channel cross sections (fig. 10). Deposition along the valley floor is also evident and widely dispersed along the channel network. Substantial deposition (~5m) is evident, however, along a flat reach of lower Step creek at its confluence with Loowit Creek between cross sections LO030 and LO033. That sediment deposition appears to have filled an area of erosion caused by the November 2006 event (see fig. 24), and its magnitude appears to exceed that of bank erosion immediately upstream. We suggest this sediment deposition may be due to a debris flow from the Step canyon headwaters, although we have no solid evidence of such an event at this time. Although water years 2008 and 2009 appear to have been hydrologically modest (see fig. 7), with only brief instances of daily mean streamflow approaching 150 m^3/s at the NFTR streamgage below the SRS, there was a substantial storm in January 2009. Unfortunately, a gage malfunction prevented measurement of peak streamflow below the SRS. But data from the Natural Resources Conservation Service Spirit Lake snow telemetry (SNOTEL) station (site number 777) document 185 mm of rainfall at temperatures well above freezing (1–6 degrees C) during January 6–8, 2009. This rainfall, 60 percent of which fell on January 7, could have triggered a small debris flow. Data from acoustic flow monitors on the Pumice Plain downstream from cross-section LO033 are inconclusive (K.R. Spicer, U.S. Geological Survey, written commun., 2019). Water years 2008 and 2009 were otherwise rather benign hydrologically, with average annual mean streamflow less than the long-term average from 1981 to 2018 (table 3).

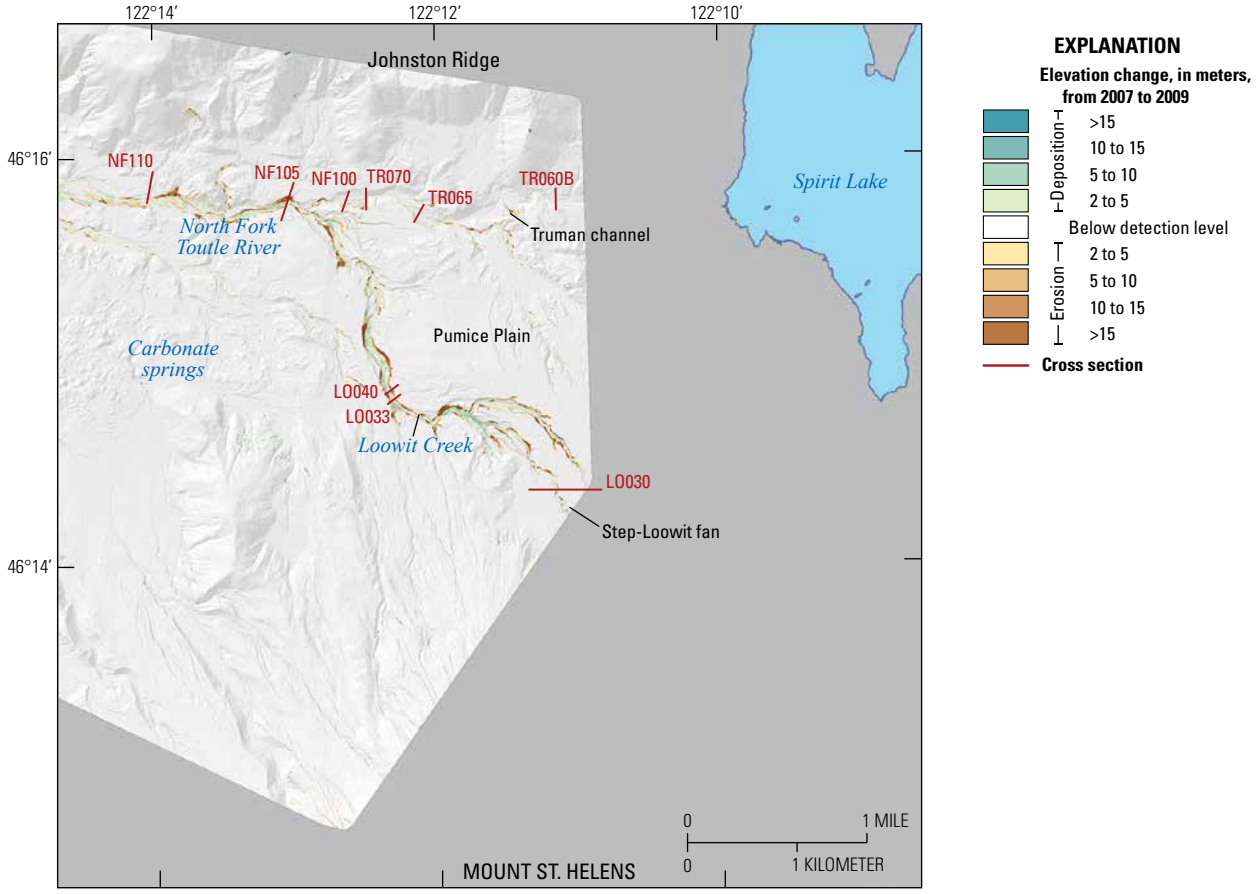

Figure 25. Digital terrain model of topographic difference (DoD) of uppermost North Fork Toutle River basin from late October 2007 to late September 2009 based on digital terrain models (DTMs) derived from airborne lidar. The shoreline of Spirit Lake represents the shoreline from the 2009 lidar survey. See table 2 for sources of topography and methods used to create DTMs. Base map is a shaded-relief model of October 2007 topography. The area of DoD coverage is limited by coverage of the 2007 lidar survey.

2009–15

From September 2009 to September 2015, channel margins continued to enlarge, particularly at channel bends (figs. 10, 26). The greatest sculpting occurred just downstream from the Step creek-Loowit Creek confluence upstream from cross section LO033. That flat reach continued to accumulate sediment supplied from upstream, and this aggradation likely drove the documented channel widening. Modest sculpting within Loowit and Step canyons is evident, as is moderate deposition near the head of Step-Loowit fan. Bank erosion is evident along small channels leading into Spirit Lake. The most obvious change over this period is advancement of Crater Glacier in the headwater reaches of Step and Loowit canyons. Apparent deposition in the Carbonate springs area is an artifact of vegetation. The 2009 DTM is a bare-earth, lidar-derived model, whereas the 2015 DTM is a photogrammetry-derived model that includes vegetation. These "deposition artifacts" owing to vegetation appear on several hillsides in this DoD. The modest, but inexorable, channel changes detected over this 6-year period attest to the modest hydrologic conditions characteristic of the period (fig. 7). There were no substantial floods or debris flows and daily mean streamflow remained below 150 m^3/s. However, average annual mean streamflow was 8 percent greater than the long-term average, and annual mean streamflow (and total annual runoff) in water year 2011 was the third greatest recorded or estimated for the NFTR below the SRS (table 3). Thus, geomorphic sculpting was done largely under conditions characterized by low-magnitude, but long-duration, high-volume streamflow.

2015–17

The largest peak streamflow measured on NFTR below the SRS (FTP in fig. 2), since it became operational in 1989, occurred in early December 2015 (fig. 7). This flood also generated the second greatest daily mean streamflow measured at or estimated for that gage (figs. 7, 9). Based on the hypothesis that substantive geomorphic work in upper NFTR basin is now event-driven, we anticipated that the DoD reflecting

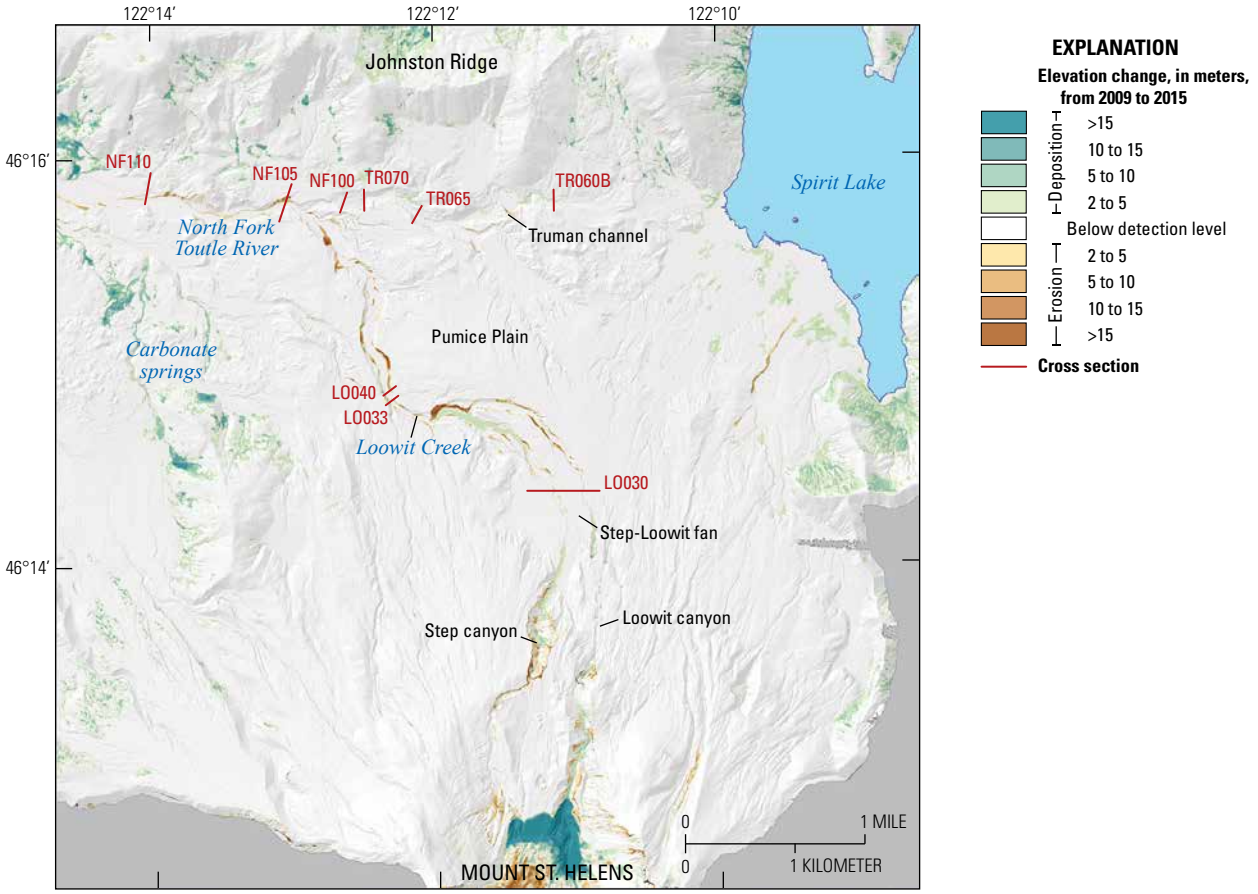

Figure 26. Digital terrain model of topographic difference (DoD) of uppermost North Fork Toutle River basin from late September 2009 to September 27, 2015, based on digital terrain models (DTMs) derived from airborne lidar and aerial photography. The shoreline of Spirit Lake represents the shoreline from a 2009 airborne lidar survey. See table 2 for sources of topography and methods used to create DTMs. Base map is a shaded-relief model of September 2009 topography. The area of DoD coverage is limited by coverage of the 2015 aerial photographs. Apparent deposition in the Carbonate springs area results from differencing a DTM derived from aerial photography (which is influenced by dense vegetation) (2015) and a bare-earth, lidar-derived DTM (2009).

change from September 2015 to September 2017 would show another period of significant erosion. Although the DoD and surveyed cross sections (figs. 10, 27) show channel widening (for example, at cross sections NF100 to NF120), particularly at channel bends, the modest extent of widening and general lack of incision belie the anticipated response based on prior geomorphic responses to large flood events. (The apparent erosion in the Carbonate springs area is again an artifact of vegetation.) Reasons for this relatively muted response are unclear. It may be that although the storm was significant and generated substantial runoff, the duration of that runoff was relatively short-lived in the upper basin. Runoff from upper NFTR basin during the 5-day period that encompasses the bulk of that storm (December 7–11) accounted for only about 7 percent of the annual runoff for water year 2016. Although the February 1996 and November 2006 storms also delivered 7 to 8 percent of their respective annual runoff over five days each, the December 2015 storm delivered the least amount of precipitation to upper NFTR basin as measured at Spirit Lake (Natural Resources Conservation Service SNOTEL site 777, Spirit Lake). Total precipitation during December 7–11, 2015, was 268 mm, compared to 328 mm during February 6–10, 1996, and 338 mm during November 5–9, 2006. Furthermore, the 1996 and 2006 storms remained warm and delivered rainfall throughout, whereas the December 2015 storm swiftly transitioned to snowfall shortly after peak streamflow occurred. It is likely that the trajectories of storm tracks and spatial distributions of precipitation among those three storms differed substantially. Even though the 2015 storm generated substantial peak and daily mean streamflow on the NFTR below the SRS, that storm apparently did not affect upper NFTR basin as strongly as did the other two storms. As a result, the December 2015 storm had a lesser geomorphic impact on the upper NFTR basin even though 40 km downstream from the volcano it generated one of the most substantial floods since the 1980 eruption.

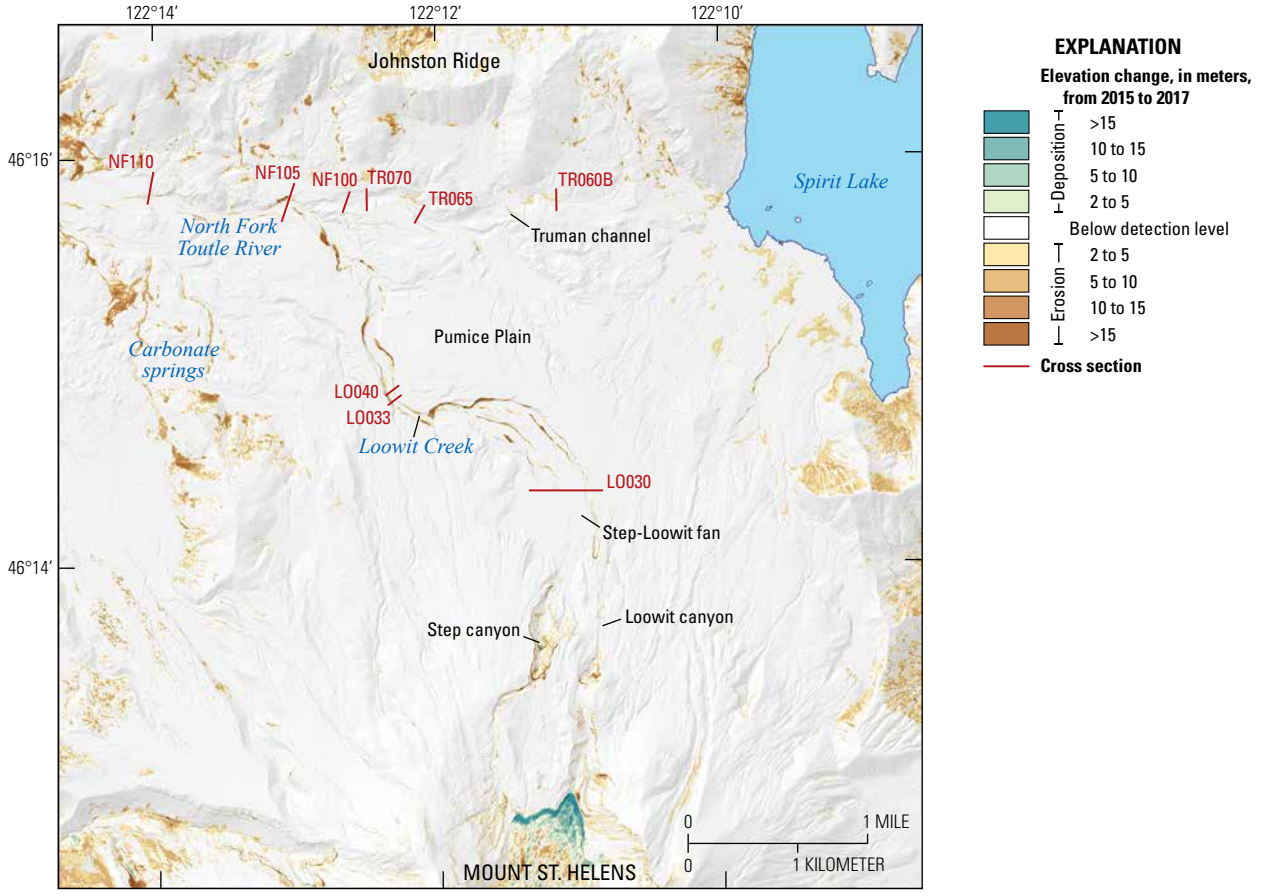

Figure 27. Digital terrain model of topographic difference (DoD) of uppermost North Fork Toutle River basin from September 27, 2015, to late September 2017 based on digital terrain models (DTMs) derived from aerial photography and airborne lidar. The shoreline of Spirit Lake represents the shoreline from a 2009 airborne lidar survey. See table 2 for sources of topography and methods used to create DTMs. Base map is a shaded-relief model of September 2015 topography. Apparent erosion in the Carbonate springs area results from differencing a bare-earth, lidar-derived DTM (2017) and a DTM derived from aerial photography (which is influenced by dense vegetation) (2015).

2017–18

To determine whether single-year change is detectable during a typical water year nearly 40 years after the 1980 eruption, we generated a DoD representing changes from September 2017 to September 2018 (fig. 28). In October 2017, small debris flows triggered by one of the first heavy autumn rainstorms issued from the crater and swept along Step-Loowit fan. That storm also generated the peak streamflow for water year 2018 measured at NFTR below the SRS (table 1). Other than this early rainstorm causing a flush of sediment, the remainder of water year 2018 was benign, with no large storms or flood events. Peak streamflow at NFTR below the SRS was less than 150 m^3/s, and peak daily mean streamflow was less than 100 m^3/s (fig. 7). As a result, we find little change on the landscape other than minor erosion along channel margins and some detectable deposition along Step-Loowit fan. These results emphasize and reinforce our hypothesis that the channel system of upper NFTR basin has largely equilibrated to the long-term average hydrologic condition that now characterizes the basin, and that large storms, and consequent large floods and debris flows (perhaps coincident with ≥10-year return interval peak streamflow), are now required to generate significant geomorphic change along the evolving drainage network. Nevertheless, inexorable bank erosion continues and helps maintain abnormally elevated sediment delivery from this basin relative to pre-eruption conditions (see Major and others, 2019).

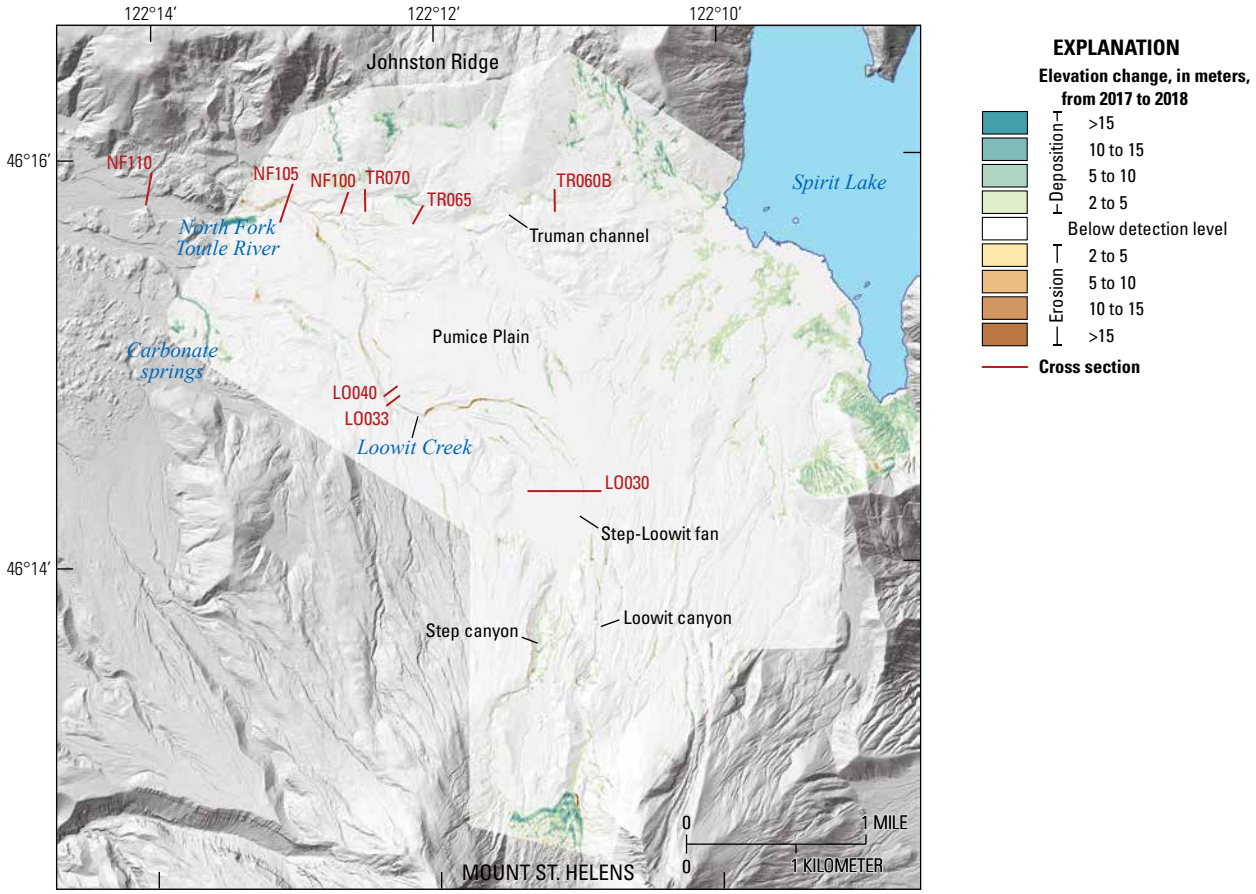

Figure 28. Digital terrain model of topographic difference (DoD) of uppermost North Fork Toutle River basin from late September 2017 to September 26, 2018, based on digital terrain models (DTMs) derived from airborne lidar and aerial photography. The shoreline of Spirit Lake represents the shoreline from a 2009 airborne lidar survey. See table 2 for sources of topography and methods used to create DTMs. Base map is a shaded-relief model of September 2017 topography. The area of DoD coverage is limited by coverage of the 2018 oblique aerial photographs. Apparent deposition on hillsides, near the shore of Spirit Lake, and near Truman channel results from differencing a bare-earth, lidar-derived DTM (2017) and a DTM derived from aerial photography (which is influenced by dense vegetation) (2018).

Geomorphic Processes and Relations with Topography and Surface Geology

To examine the extent to which surface geology of the blockage affected drainage development between 1980 and 1985, we examined spatial relations between DoDs and surface geology mapped in 1980 (Lipman and Mullineaux, 1981). Mapped surface geology, however, does not capture the three-dimensional depositional sequences (for example, Brand and others 2014, 2016) that certainly influence geomorphic development, particularly after initial channel development ensued. For example, pyroclastic-flow deposits overlie the debris-avalanche deposit, have variable stratigraphic texture, and contain many internal structures having variable erosional resistance. In places where it appears that surficial pyroclastic deposits may have influenced channel evolution, it is possible that the debris-avalanche deposit also, or perhaps predominantly, influenced channel evolution. With that limitation in mind, we examine example areas where we might anticipate that surface geology may influence the location and extent of geomorphic change (fig. 29).

Surface geology of the blockage is composed of exposures of debris-avalanche, blast, and pyroclastic-flow deposits (figs. 4, 5, 29). The irregular, hummocky topography of the debris-avalanche deposit appears to have steered initial network development through fill-and-spill among depressions and by headward incision around hummocks (Rosenfeld and Beach, 1983; Janda and others, 1984; Parsons, 1985; fig. 30). These observations indicate surface topography may be a dominant influence on channel position rather than deposit geology. In the blockage, hummocks are composed largely of stratigraphically intact, but shattered, pieces of the mountain, whereas inter-hummock areas are composed of both intact and blended pieces of the mountain rarely larger than coarse gravel. Although it may be tempting to also interpret this steering as a result of an erodibility contrast between hummock and inter-hummock areas, the co-location of topographic gradients and geologic variation precludes fully disentangling the effect of substrate composition from the effect of deposit topography. Once a channel established, bank erosion and channel widening carved into hummocks, suggesting that these features are certainly erodible (fig. 31). Indeed, as of 2019, many hummocks have been sculpted or removed by fluvial erosion that has triggered slumping of hummock sediment. The surfaces of the blast and pyroclastic-flow deposits are very susceptible to erosion and were dominated by channel incision during initial channel development. Although channel locations are close to contacts between blast and pyroclastic-flow deposits, indicating a possible erodibility contrast, in some cases they crosscut contacts, indicating that channel initiation was more strongly influenced by topographic slope (fig. 32). Despite a lack of clear control on geomorphic evolution of the blockage by the geologic composition of the 1980 deposits, pre-existing geologic features, such as Floating Island lava flow, did influence location of drainage development (fig. 15).

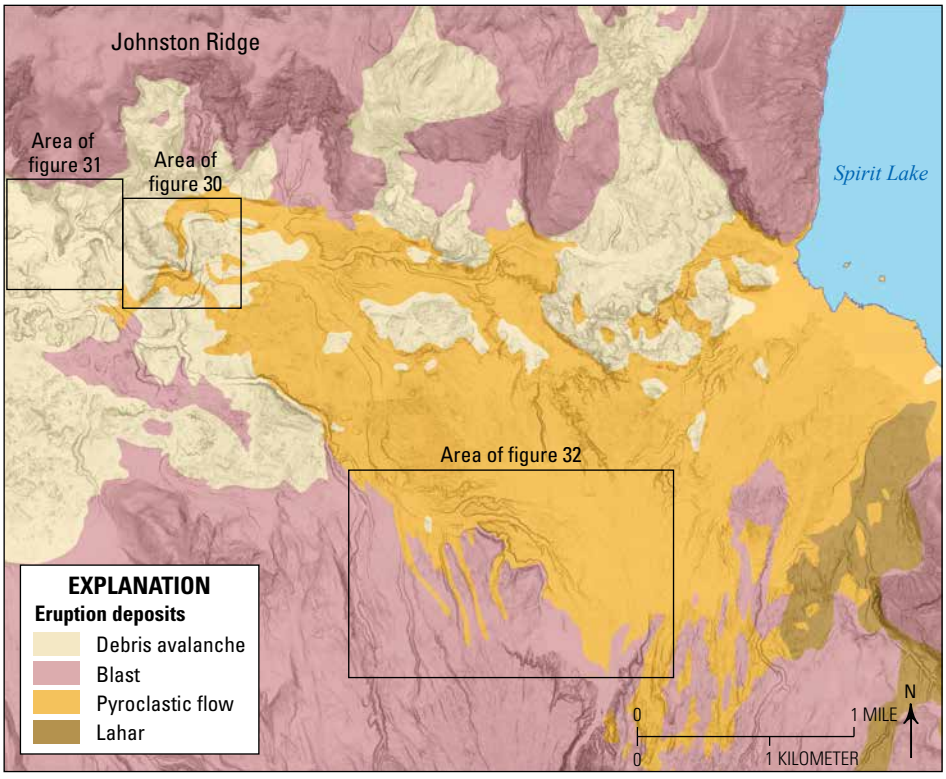

Figure 29. Simplified surface geology of the Spirit Lake blockage (adapted from Lipman and Mullineaux, 1981). The geology has been draped over a shaded-relief topographic model derived from 1982 aerial photography (see table 2). Boxes delineate detailed areas shown in figures 30–32.

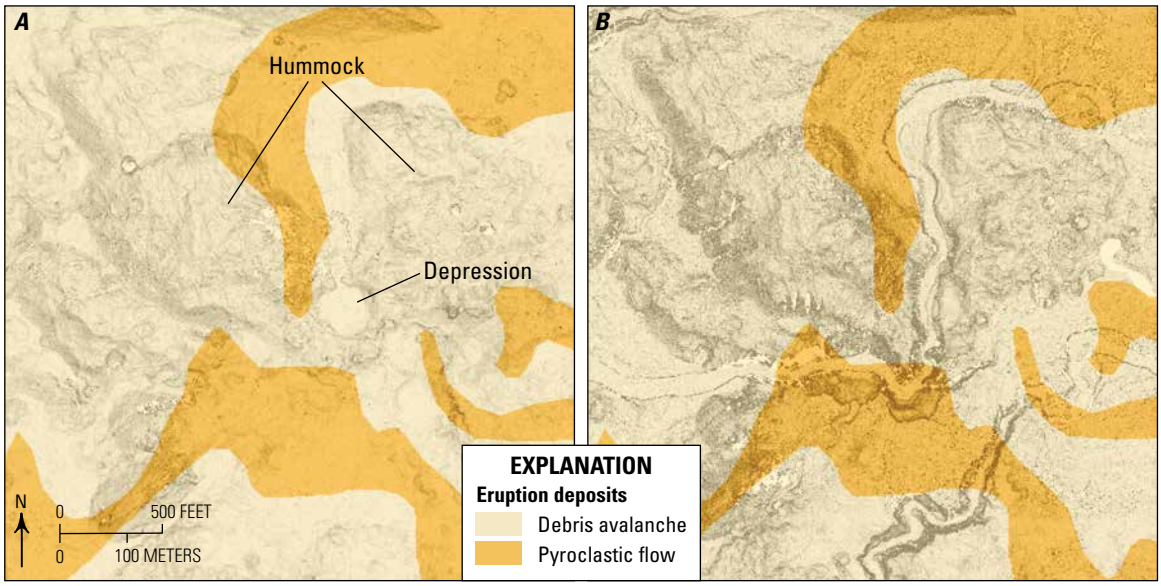

Figure 30. Example of topographic influence on location of channel development by the rugged surface texture of the debris-avalanche deposit. Two hummocks of rugged debris-avalanche topography in 1980 (*A*) dictate location of channel incision in 1981 (*B*). Simplified surface geology adapted from Lipman and Mullineaux (1981). See figure 29 for location. Base images are digital terrain models derived from aerial photographs (see table 2).

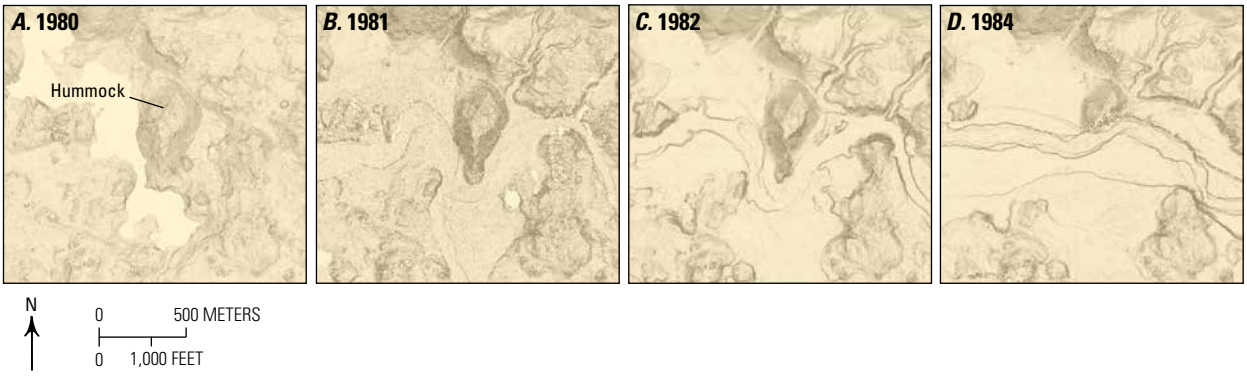

Figure 31. Examples of initial topographic influence on location of channel development by a hummock and depression, followed by lateral erosion in the debris-avalanche deposit. This image sequence, from 1980 (*A*) to 1984 (*D*), shows channel development was more strongly influenced by topography than by deposit geology. As the channel became more fully formed and a stronger topographic gradient emerged, the river easily eroded hummock material. Simplified surface geology adapted from Lipman and Mullineaux (1981). See figure 29 for location. Base images are digital terrain models derived from aerial photographs (see table 2).

Location of the drainage network is largely settled, and the overall rate and magnitude of landscape change since the mid-1980s has decreased (see also Major and others, 2018, 2019). Hence, it is unclear whether the geology of the Spirit Lake blockage has played a role in more recent geomorphic evolution. Specifically, it is not entirely obvious whether exhumed contacts (for example, that between the pyroclastic-flow and debris-avalanche deposits) provide a local base level that regulates channel incision, or whether the overall topographic regime has set the most influential base-level control. Observations east of the blockage crest (C. Crisafulli, U.S. Forest Service, written commun., 2019) indicate that small channels have cut through pyroclastic deposits but not deeply into the debris-avalanche deposit, suggesting that both geology and local topographic base level (in this case Spirit Lake) may be influencing geomorphic evolution of those channels. West of the blockage crest, however, the base-level control (the SRS) is well below the elevation of geologic contacts, and both Loowit Creek and NFTR have incised below geologic contacts and into debris-avalanche deposit. This indicates that

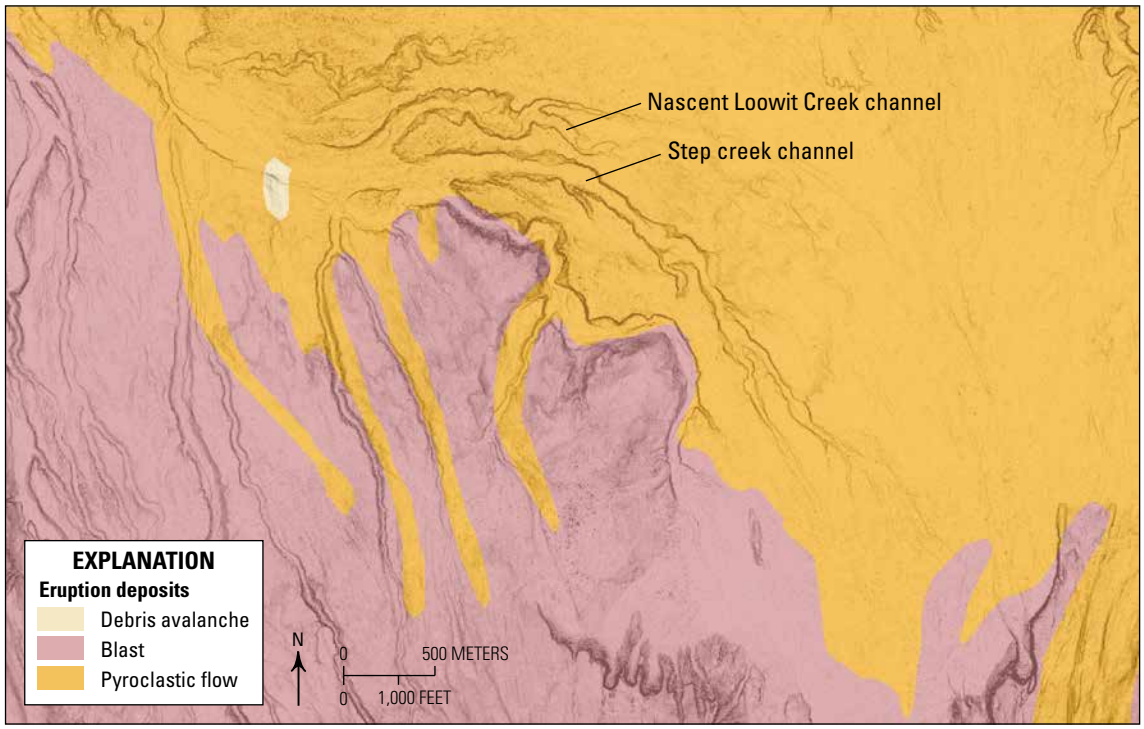

Figure 32. Example of how channel development may be influenced by location of geologic contacts between the blast pyroclastic density current deposit and pyroclastic-flow deposits. Nascent channels that ultimately became main drainages for Loowit Creek and Step creek largely followed topographic gradients within pyroclastic-flow deposits. Headwater extensions of other channels draining the lower north flank of the volcano, however, have steered around outcroppings of blast deposit and preferentially eroded pyroclastic-flow deposits. See figure 29 for location. Simplified surface geology adapted from Lipman and Mullineaux (1981). The geology has been draped over a shaded-relief topographic model derived from 1982 aerial photography (see table 2).

topographic control, rather than geologic control, exerts a stronger influence on channel incision and evolution. Future work refining the influence of blockage geology on proximal channel evolution may benefit from more detailed consideration of correlations among individual units mapped within the debris-avalanche deposit (Glicken, 1996) and channel evolution.

The greater spatial extent of geomorphic change in the 1980–81 DoD compared to later 1980s DoDs demonstrates how erosion differs between the early and later stages of drainage development. As the drainage network established, the locations of channels appear to be dictated by the overall topographic gradient (for example, subparallel channels on the Pumice Plain, which slopes to the north-northwest; see figs. 3, 6) except where surface roughness elements are significant enough to steer channel incision (figs. 31, 32). But once the drainage network became established, most landscape change occurred through channel modification and sculpting rather than additional channel initiation or integration. The nature of subsequent enlargement and evolution of the channel network, rather than initiation of additional channels, indicates that geologic properties and erodibility contrasts along with individual hydrological events, which greatly influence sediment supply and channel equilibrium, subsequently played a more substantial role in later-stage channel evolution (although topographic influence, such as avulsion on Step-Loowit fan, persists).

Our analyses indicate that overall topographic gradient (fig. 6) and pre-existing geologic controls, such as the Floating Island lava flow, largely set the location of the drainage network. But we suggest that once channels were established, the pattern of channel evolution was influenced by an interplay between channel depth, substrate geology, and the spatial organization of geomorphic processes. For example, at the head of Step-Loowit fan where channel depths are about 1 m and debris flows of similar depth frequently pass, multiple avulsions have occurred (fig. 13). In contrast, channels farther down the network are more deeply incised (fig. 10) and have a lower frequency of hydrologic events of sufficient scale to fill them and trigger avulsion. Nevertheless, event-driven erosion, such as that near cross section NF110 caused by the 2006 landslide from Johnston Ridge (fig. 10*F*) or that along Loowit Creek channel driven by the November 2006 flood event, can significantly influence the evolution of existing channel geometry. Importantly, these forms of channel evolution are influenced strongly by composition of the channel banks within the context of overall base-level control and transport capacity relative to sediment supply.

Implications for Future Geomorphic Development in Response to Management Options

The approximately 40-year history of fluvial response of upper NFTR to volcanic events, storms, lake breakouts, and pumping of Spirit Lake provides a strong foundation for forecasting future geomorphic behavior of this landscape. Here we consider how landscape evolution of upper NFTR basin provides insight useful for forecasting likely trajectories of future change in response to various potential outlets for Spirit Lake. We consider two potential management scenarios: (1) operation of some form of closed conduit outlet (the existing or an upgraded outlet tunnel, or a conduit buried across the debris blockage); and (2) an open channel across the blockage. Other management options are possible. For example, a conduit draining water to the Muddy River basin would remove any future influence of Spirit Lake outflow on geomorphic evolution and sediment transport in NFTR basin, but such loss of water could affect fish recovery in the Toutle watershed and the increase in flow to the Muddy River basin would temporarily increase its sediment delivery. Our goal here is not to be exhaustive, but rather to consider the hydrogeomorphic implications of either an open-channel or closed-conduit outlet through the lens of what we know about the historical hydrogeomorphic behavior of the landscape. Furthermore, the following discussion is not tied to any specific outlet designs. It is possible that proper design could mitigate many of the issues we highlight. Our purpose here is to emphasize the hydrogeomorphic functioning of the Spirit Lake blockage and surrounding terrain in its present state to provide geologic, hydrologic, and geomorphic context for design and long-term management of an outlet for Spirit Lake. A more extensive assessment of risks and vulnerabilities associated with various possible outlet options is provided by Grant and others (2017).

Closed-Conduit Outlet

If the outlet to Spirit Lake is managed using some form of closed conduit, we expect that the trajectories of landscape change that have occurred in upper NFTR basin since 1980, as documented here, will continue along current trajectories. Specifically, we anticipate that the dominant erosional processes will continue to be persistent lateral adjustment and localized widening of the existing channel network, with limited vertical downcutting except perhaps during exceptional hydrological events. The gradual shift from dominance of vertical to lateral erosion that we and others have documented (Simon and Klimetz, 2012; Zheng and others, 2014; Major and others, 2018; 2019) results from both the overall adjustment of channel grade (Zheng and others, 2014) to the prevailing streamflow regime and sediment supply in upper NFTR, and to the coarsening of the bed over time (Simon and Thorne, 1996). Provided streamflow and sediment supply remain relatively consistent with what they are today, we do not expect dramatic, widespread vertical incision, although continued local incision is likely (see Major and others, 2019). As documented in November 2006, however, episodic storm events that generate substantial floods and debris flows still retain the capacity to promote vertical incision of many meters (figs. 10*B*, *C*, 24). This forecasted behavior assumes no other direct human modifications or infrastructure that would change the fundamental hydrogeomorphic functioning of the landscape; it also assumes that volcanic activity continues to be modest and in keeping with the types of events that have occurred since the end of major explosive activity in 1980—namely relatively benign dome growth and infrequent eruption-triggered lahars.

Future erosion that produces substantial geomorphic response will likely be event-based rather than resulting from a regime of continuous erosion over a broad range of streamflows like the hydrogeomorphic behavior that characterized the first decade of response following the 1980 eruption (Major, 2004). As discussed, streamflow and debris flows associated with floods having daily mean magnitude exceeding 150 m^3/s (as measured on NFTR below the SRS) are now typically required to perform notable geomorphic work during a single event. Daily mean streamflow of this magnitude has a roughly a 4-year recurrence interval (fig. 9); more frequent events of lower magnitude generally do not result in appreciable change to channel geometry. Larger hydrologic events, such as those that occurred in February 1996 and November 2006, can cause large changes in channel geometry, and we expect such behavior to continue. But not all large hydrologic events result in substantive changes in all parts of the basin. The contrasting responses between the November 2006 and December 2015 events indicate that the nature of the hydrologic event—including storm trajectory, temperature history, precipitation distribution, and generation or absence of debris flows, as well as local geological factors, can be important. It is also possible that the dimensions of the channel system may have begun adjusting and stabilizing to large discharge events. This is not to say that slow, inexorable change does not have an effect. Even in the absence of large floods and debris flows, channel banks continue to erode, and over multi-year to multidecadal time frames the cumulative slow, persistent erosion has substantial geomorphic effect.

Two major uncertainties affect this forecast: future volcanic activity and climate change. Any volcanic activity that loads the channel system with sediment, including pyroclastic flows, lahars, landslides, or abundant tephra fall, would likely result in channel aggradation, although steep channel headwaters closest to the volcano could erode. Such events have occurred episodically since the 1980 eruptions (Waitt and others, 1983; Cameron and Pringle, 1990; Pringle and Cameron, 1999; Pierson, 1999; Major and others, 2005) and may occur again when the volcano reawakens. The effects of relatively small channel-loading events, such as small debris flows from the crater, tend to be concentrated in the uppermost reaches of NFTR basin, particularly along the Step-Loowit fan and immediately downstream. Larger and more mobile flows (such

as eruption-triggered lahars or large glacier-outburst floods) can travel much farther, to tens of kilometers. In addition, Crater Glacier now poses a source of abundant water that could be released during a future eruption, especially during an explosive eruption. Should an eruption melt glacier ice and liberate a large volume of water, such a flood would likely erode sediment across the blockage and potentially initiate geomorphic instabilities along perennial and ephemeral channels, which could have significant impact on channel stabilities.

Climate change may alter streamflow and sediment supply in NFTR basin, and thus its hydrogeomorphic functioning. Landscape-evolution modeling that considered climate variations showed that substantive valley erosion of the basin is likely to persist for many more decades (Meadows, 2014). Furthermore, a key factor of the November 2006 event was heavy precipitation falling as rainfall at high elevations on barren volcanic slopes lacking seasonal snowpack. That lack of snowpack allowed heavy precipitation to fall directly on loose volcaniclastic sediment, permitting rapid runoff and sediment mobilization. Most climate predictions do not call for significantly increased precipitation in the Pacific Northwest, but they do call for warmer temperatures, more intense rainfalls, and a shift from snow to rain at high elevations (International Panel on Climate Change [IPCC], 2014). Therefore, conditions that characterized the November 2006 event may become more frequent. If so, notable dynamic adjustments to the channel system may also become more frequent.

As time passes, vegetation will continue to expand across the valley. But growth and expansion of vegetation coverage is likely to have mixed results on short-term channel evolution and stability. Many valley banks along NFTR drainage network are several meters to a few tens of meters tall. Consequently, valley bank heights exceed rooting depths, and thus vegetation established atop those high surfaces will have little effect on channel erosion and bank stability. Until channel and valley widths exceed the active channel migration zone, vegetation will be unlikely to anchor the bases of valley banks and impede erosion. Thus, until the channel network achieves a sufficient degree of geomorphic stability, ecological recovery along channel margins is unlikely to develop sufficiently to impede lateral channel erosion (see Gran and others, 2015; Major and others, 2019).

We anticipate future switching of the channel course across the Step-Loowit fan, like what has occurred multiple times in the past. Although the channels draining the crater currently flow northwesterly into NFTR, the low relief of the fan and high sediment loads supplied from the crater will likely cause future avulsions and channel changes and result in drainage flowing northeast toward Spirit Lake as it has in the past. Overall, such channel avulsions should not pose substantial risks to a closed-conduit outlet, though it could expose an outlet intake to a higher degree of risk when flow is directed toward the lake. Under these forecast conditions it is unlikely that the lake would be "captured" by channel switching across the fan and cause a breach of the blockage.

Open-Channel Outlet

An open-channel outlet across the blockage introduces greater uncertainty with respect to hydrogeomorphic behavior of the drainage system than does a closed-conduit outlet. First, there is currently no developed design, engineering scheme, or location for an open channel identified, so specific issues that might accompany any such plan are unknown. Second, aside from the Truman channel, which was active in the mid-1980s when pumping was used to maintain a safe lake level and which partly crosses the blockage, no channel has crossed the blockage, so the geomorphic consequences must be inferred. Finally, future volcanic or geomorphic events have the potential to more directly impact an open channel than a closed conduit, yet the type, location, and magnitude of such events can only be broadly generalized and consequent risks hypothesized. Such uncertainties are intrinsic to introducing a new outlet technology into a dynamic landscape. Grant and others (2017) summarize specific risks to an open-channel outlet.

Despite the greater uncertainty associated with an open-channel outlet compared to that associated with a closed conduit, the geomorphic history of upper NFTR basin offers insight into potential issues surrounding an open channel. Accordingly, we assume that all geomorphic issues and trajectories associated with a closed conduit, as discussed above, are also associated with an open channel. The channel would presumably be designed solely to provide an outlet for Spirit Lake and maintain safe lake levels, and no other source of water would feed into it other than the lake. Further, we assume that the channel would deliver water to upper NFTR much as the Truman channel did. Indeed, we anticipate that a reasonable alignment for an open channel would follow that of Truman channel for several reasons. First, such an alignment broadly follows the topographically lowest ground across the blockage and is the location where a natural channel would likely have established had it been allowed to do so. Second, that alignment is located as far as possible from Mount St. Helens, providing the least possible exposure to future volcanic events. Third, excavation of an open channel would require removal of large amounts of sediment from the blockage. If an open channel followed the incised Truman channel, the amount of sediment removal may be minimized, possibly reducing construction costs and effects. Further geophysical analyses are required to determine if this is the most feasible alignment for an open-channel outlet.

A key aspect of an open channel across the blockage is that it would inject a large source of flowing water into a highly erodible landscape. The geomorphic history of the blockage shows that whenever large, or even modest, volumes of moving water have access to the material comprising the blockage, very rapid erosion can occur. This was evident throughout the 1980s during the initial phase of channel adjustments, when even streamflow less than or equal to a 2-year recurrence-interval streamflow caused extensive channel erosion and sediment transport (Major, 2004). Rapid

erosion of the Truman channel from 1982 to 1984 (fig. 11) exemplifies the processes and timescales involved. Moreover, the entire stratigraphic sequence of the blockage, and not just the upper pyroclastic-flow and ashcloud deposits, is susceptible to rapid fluvial erosion. Although the debris-avalanche deposit appears to offer greater resistance to erosion locally than do the overlying pyroclastic deposits, it is nevertheless a highly erodible deposit as is evident by extensive incision and widening along NFTR downstream from cross-section NF100 and along Truman channel (see figs. 10–12; Major and others, 2019).

Implications of our analysis are that an open channel will likely have to be heavily armored, and that any water flowing in an open channel must be fully isolated from the surrounding debris-blockage deposits, otherwise rapid and uncontrolled erosion may occur. Isolation includes hardened bed and banks, sufficient freeboard to prevent overtopping of channel walls, and measures to prevent water from discharging around the channel entrance rather than through it. An unarmored, naturalized open channel is not a viable option considering the steep gradient across the blockage, the mobility of blockage sediment, and the potential consequences of an uncontrolled release of water from the lake (see Scott, 1988; Grant and others, 2017).

Full or partial blockage of an open channel, either by volcanic events such as lahars or pyroclastic flows, or by weather-induced geomorphic events such as debris flows or landslides, poses specific risks (Grant and others, 2017). A channel-filling blockage and consequent ponding of water could possibly lead to overtopping of the channel walls or an "end run" around the channel entrance, thereby diverting water across the blockage. Resultant erosion and probable geomorphic instabilities, such as knickpoint development and migration, could potentially destabilize the channel through undercutting, or bypass it completely, resulting in uncontrolled fluvial erosion.

An extreme-case scenario is that an uncontrolled release of water and subsequent erosion could result in knickpoints retrogressively migrating toward Spirit Lake and releasing lake water in a runaway break-out event. Although such a scenario has a low (but unquantified) probability of occurrence, the consequences of such an event would be catastrophic because of the very large volumes of water involved and because the timescales for intervention (assuming one could be mounted) would be measured in hours to days. In contrast, failure of a closed conduit, such as a tunnel or a buried conduit, would have a much longer timescale for intervention (weeks to months), because failure of the blockage following failure of a conduit outlet requires lake level to rise to the contact between the debris avalanche and overlying pyroclastic deposits (Grant and others, 2017).

Tradeoffs Among Outlet Alternatives

Scientific, engineering, and social complexities and values must be evaluated when considering a long-term management solution for the security of Spirit Lake. These complexities and values revolve around engineering performance, scientific understanding of hazards, timescales for potential intervention in the event of outlet failure, social values particularly as regard fish, wildlife, environmental and cultural significance, and public safety. Tradeoffs among these complexities are summarized in table 4. The ultimate long-term management solution is the one that best minimizes risk of outlet failure and breaching of the blockage within the context of values that society prizes most.

Our intent here is not to argue for or against any singular management decision, but rather to emphasize insights that analysis of channel evolution on and around the blockage reveals in terms of the intrinsic erodibility of this landscape. Any decision regarding long-term management of outflow from Spirit Lake should be made with the historical context of channel evolution in mind, as it is an important guide to potential future geomorphic behavior and functioning of this dynamic landscape.

Table 4. Summary of scientific, engineering, and societal tradeoffs among outlet alternatives.

Outlet performance	Conduit-style outlet	Open-channel outlet
Known engineering design and performance	Yes	No
Potential for mechanical failure	Yes	No
Outflow scales with inflow	No	Yes
Vulnerability to principal regional hazards[1]		
Hydrologic	High	Moderate
Volcanic	Low[2]	High
Seismic	Low[2]	High
Geomorphic	Very low	Moderate to high
Timescales of lake-level recession post-hydrologic event[1]	Weeks to months	Days
Timescale for intervention in event of failure[1]	Weeks to months	Hours to days
Passes fish	No	Yes

[1]See Grant and others (2017).

[2]Vulnerability of a conduit buried across the blockage is greater than that of a tunnel bored through bedrock.

Summary and Conclusions

The cataclysmic 1980 eruption of Mount St. Helens reset the topography of upper North Fork Toutle River (NFTR) basin. Sediment from a colossal debris avalanche, a laterally directed ("blast") pyroclastic density current, and later pyroclastic flows thickly filled basin headwaters, raised the bed and surface of Spirit Lake and transformed its basin, blocked its outlet, and severed hydrologic connection between the upper and lower parts of the basin. Reconnection required establishment of a new drainage network. To prevent catastrophic breaching of Spirit Lake, a tunnel outlet was bored through bedrock, and water from Spirit Lake now bypasses basin headwaters and enters NFTR downstream from Coldwater Lake. In this study, we documented initiation and nearly 40 years of geomorphic evolution of the fluvial channel network on and around the Spirit Lake blockage without overland flow from Spirit Lake. Our analyses show the post-eruption drainage network bears a strong resemblance to the pre-eruption drainage network, and thus we infer that gross topography exerts a first-order control on channel location within the network. In addition, blockage geology—to first approximation the mapped surface distributions of debris-avalanche, blast, and pyroclastic-flow deposits—has also influenced channel location. In particular, the location of Loowit Creek channel, which drains the Mount St. Helens crater and traverses the Pumice Plain west of the blockage crest, may have been influenced by contrasts in erosional resistance between the blast and pyroclastic-flow deposits or contrasts within the pyroclastic-flow deposits themselves. The mounded topography of the debris-avalanche deposit (hummocks) and possible erosional heterogeneity of its composition also guided channel location locally.

The basic architecture of the developing fluvial network established within a few years after the cataclysmic eruption. Initial channel development occurred during a time of enhanced runoff owing to transient hydrologic changes to the landscape. During this time, streamflow peaks (both primary and secondary) were a few percent to many tens percent greater for a given precipitation input than they were before the eruption, and a range of streamflows, from small-magnitude (less than 2-year return-interval) to large-magnitude (greater than 10-year return-interval) discharges, played fundamental roles eroding and transporting sediment and establishing the fluvial network. Some of the most dramatic channel evolution was caused by modest streamflow (5.1 m^3/s) pumped from Spirit Lake while the present tunnel outlet was designed and constructed.

Within several years of the 1980 eruption, the established fluvial network began equilibrating to average hydrologic conditions and the consequent upstream sediment delivery. As a result, geomorphic evolution of the drainage network switched gradually from a regime of modification by a broad range of streamflow to one that is more event-driven. Since the mid-1980s, moderate- to large-magnitude streamflows, particularly those generating daily mean streamflows greater than about 150 m^3/s—as measured on NFTR below the sediment retention structure (USGS streamgage 14240525)—are needed to do much geomorphic work beyond modest erosion of channel margins. Though relatively small-magnitude streamflows (those having daily mean discharges less than 150 m^3/s) were important during the initial phase of channel development, by the mid-1980s they had largely become agents of channel refinement rather than agents of major channel change. Nevertheless, inexorable erosion of channel banks, and not just major geomorphic changes driven by large-magnitude floods and debris flows, continues to maintain sediment delivery from this basin at levels that are elevated compared to pre-eruption conditions.

Documentation of acute erosion, channel avulsion, and persistent channel refinement on and around the Spirit Lake blockage illustrates the sensitive and dynamic nature of upper NFTR fluvial system. It is clear from analyses presented here that the blockage sediments are highly susceptible to erosion, especially when water is introduced to parts of the landscape lacking well-established channels or when channels are subject to streamflow to which they are not well-adjusted. Considerable sediment mobility, now driven largely by floods and debris flows generated by large storms, may establish geomorphic instabilities such as knickpoints or knickzones that can migrate headward rapidly and potentially trigger additional instabilities in smaller channels tributary to main trunk channels.

The erosional susceptibility documented here has significant implications—and cautionary ramifications—for an open-channel outlet for Spirit Lake. The most logical placement of an open-channel outlet is along or near the present alignment of Truman channel. But that channel is adjusted to a mean discharge of 5.1 m^3/s. Streamflow of substantially greater magnitude, almost certain through an open channel because discharge would be unregulated and vary with lake level, is very likely to induce additional channel incision and widening unless the channel is heavily fortified, especially given the overall 3-percent gradient (125-m elevation drop over 4 km) from Spirit Lake to the Truman channel-NFTR confluence. Furthermore, if water somehow escaped an open channel and breached the blockage drainage divide, it would flow largely over landscape lacking channels adjusted to such flow. Because the un-channelized landscape is very susceptible to erosion, an intense overland flow could generate geomorphic instabilities with possibly catastrophic consequences. These risks could be reduced by careful design and engineering that accounts for the hydrogeomorphic behavior of this landscape.

Acknowledgments

This work was conducted in cooperation with the U.S Forest Service Gifford Pinchot National Forest. We thank Liz Safran, Matt Collins, Fred Swanson, Charlie Crisafulli, Rene Renteria, Jonathan Berry, Claire Landowski, and Regan Austin for comments and discussions that sharpened our thinking and presentation. A U.S Geological Survey Mendenhall Postdoctoral fellowship provided partial funding for Kristin Sweeney.

References Cited

Anderson, S.W., 2019, Uncertainty in quantitative analyses of topographic change—error propagation and the role of thresholding: Earth Surface Processes and Landforms, v. 44, p. 1015–1033.

Bakker, M., and Lane, S.N., 2017, Archival photogrammetric analysis of river–floodplain systems using Structure from Motion (SfM) methods: Earth Surface Processes and Landforms, v. 42, p. 1274–1286.

Brand, B.D., Bendaña, S., Self, S., and Pollock, N., 2016, Topographic controls on pyroclastic density current dynamics—Insight from 18 May 1980 deposits at Mount St. Helens, Washington (USA): Journal of Volcanology and Geothermal Research, v. 321, p. 1–17.

Brand, B.D., Mackaman-Lofland, C., Pollock, N.M., Bendaña, S., Dawson, B., and Wichgers, P., 2014, Dynamics of pyroclastic density currents—Conditions that promote substrate erosion and self-channelization—Mount St. Helens, Washington (USA): Journal of Volcanology and Geothermal Research, v. 276, p. 189–214.

Brasington, J., Langham, J., and Rumsby, B., 2003, Methodological sensitivity of morphometric estimates of coarse fluvial sediment transport: Geomorphology, v. 53, p. 299–316.

Britton, J.P., Askelson, S.K., Budai, C.M., and Scofield, D.H., 2016, Repair of failing Spirit Lake outlet tunnel at Mount St. Helens, *in* Crookston, B., and Tullis, B., eds., Hydraulic Structures and Water Systems Management, 6th IAHR International Symposium on Hydraulic Structures, accessed June 2019 at https://doi.org/10.15142/T3170628160853.

Cameron, K.A., and Pringle, P.T., 1990, Avalanche-generated debris flow on 9 May 1986, at Mount St. Helens, Washington: Northwest Science, v. 64, p. 159–164.

Cluer, B., and Thorne, C., 2014, A stream evolution model integrating habitat and ecosystem benefits: River Research and Applications, v. 30, p. 135–154.

Clynne, M.A., Ramsey, D.W., and Wolfe, E.W., 2005, Pre-1980 eruptive history of Mount St. Helens, Washington: U.S. Geological Survey Fact Sheet 2005–3045, 4 p.

Clynne, M.A., Calvert, A.T., Wolfe, E.W., Evarts, R.C., Fleck, R.J., and Lanphere, M.A., 2008, The Pleistocene eruptive history of Mount St. Helens, Washington, from 300,000 to 12,800 years before present, chap. 28 *of* Sherrod, D.R., Scott, W.E., and Stauffer, P.H., eds., A volcano rekindled—The renewed eruption of Mount St. Helens, 2004–2006: U.S. Geological Survey Professional Paper 1750, p. 593–627.

Collins, B. D., and Dunne, T., 1986, Erosion of tephra from the 1980 Eruption of Mount St Helens: Geological Society of America Bulletin, v. 97, p. 896–905.

Collins, B.D., and Dunne, T., 2019, Thirty years of tephra erosion following the 1980 eruption of Mount St. Helens: Earth Surfaces Processes and Landforms, v. 44, p. 2780–2793.

Crandell, D.R., 1987, Deposits of pre-1980 pyroclastic flows and lahars from Mount St. Helens volcano, Washington: U.S. Geological Survey Professional Paper 1444, 91 p.

de Haas, T., Densmore, A.L., Stoffel, M., Suwa, H., Imaizumi, F., Ballesteros-Cánovas, J.A., Wasklewicz, T., 2018a, Avulsions and the spatio-temporal evolution of debris-flow fans: Earth Science Reviews, v. 177, p. 53–75.

de Haas, T., Kruijt, A., and Densmore, A.L., 2018b, Effects of debris-flow magnitude-frequency distribution on avulsions and fan development: Earth Surface Processes and Landforms, v. 43, p. 2779–2793.

Densmore, A.L., de Haas, T., McArdell, B., and Schuerch, P., 2019, Making sense of avulsions on debris-flow fans: Golden, Colo., Proceedings of the 7th International Conference on Debris-Flow Hazards Mitigation, 8 p., accessed December 2019 at https://doi.org/10.25676/11124/173161.

Dunne, T., and Leopold, L.B., 1981, Flood and sedimentation hazards in the Toutle and Cowlitz River system as a result of the Mount St. Helens eruption: Federal Emergency Management Agency, Region X, 92 p.

Fairchild, L.H., 1987, The importance of lahar initiation processes: Reviews of Engineering Geology, v. 7, p. 51–62.

Glicken, H., 1996, Rockslide–debris avalanche of May 18, 1980, Mount St. Helens Volcano, Washington: U.S. Geological Survey Open-File Report 96–677, 90 p.

Glicken, H., Meyer, W., and Sabol, M., 1989, Geology and groundwater hydrology of Spirit Lake blockage, Mount St. Helens, Washington, with implications for lake retention: U.S. Geological Survey Bulletin 1789, 33 p.

Gomez, C., Hayakawa, Y., and Obanawa, H., 2015, A study of Japanese landscapes using structure from motion derived DSMs and DEMs based on historical aerial photographs—New opportunities for vegetation monitoring and diachronic geomorphology, Geomorphology, v. 242, p. 11–20.

Gran, K.B., and Montgomery, D.R., 2005, Spatial and temporal patterns in fluvial recovery following volcanic eruptions—channel response to basin-wide sediment loading at Mount Pinatubo, Philippines: Geological Society of American Bulletin, v. 117, p. 195–211.

Gran, K.B., Montgomery, D.R., and Halbur, J.C., 2011, Long-term elevated post-eruption sedimentation at Mount Pinatubo, Philippines: Geology, v. 39, p. 67–70.

Gran, K.B., Tal, M., and Wartman, E.D., 2015, Co-evolution of riparian vegetation and channel dynamics in an aggrading braided river system, Mount Pinatubo, Philippines: Earth Surface Processes and Landforms, v. 40, p. 1101–1115.

Grant, G.E., Major, J.J., and Lewis, S.L., 2017, The geologic, geomorphic, and hydrologic context underlying options for long-term management of the Spirit Lake outlet near Mount St. Helens, Washington: U.S. Department of Agriculture, Forest Service, Pacific Northwest Research Station General Technical Report PNW-GTR-954, 151 p., accessed December 2019 at https://www.fs.usda.gov/treesearch/pubs/54429.

Gudmundsson, M.T., 2015, Hazards from lahars and jökulhlaups, *in* Sigurdsson, H., Houghton, B., Rymer, H., Stix, J., and McNutt, S., eds., The Encyclopedia of Volcanoes: Academic Press, p. 971–984.

Hausback, B.P., and Swanson, D.A., 1990, Record of prehistoric debris avalanches on the north flank of Mount St. Helens volcano, Washington: Geoscience Canada, v. 17, p. 142–145.

Hayes, S.K., Montgomery, D.R., and Newhall, C.G., 2002, Fluvial sediment transport and deposition following the 1991 eruption of Mount Pinatubo: Geomorphology, v. 45, p. 211–224.

Intergovernmental Panel on Climate Change [IPCC], 2014, Climate change 2014—Synthesis Report: Geneva, Switzerland, IPCC, Contributions of Working Groups I, II, III to the Fifth Assessment Report of the Intergovernmental Panel on Climate Change, 151 p, accessed December 2019, at https://www.ipcc.ch/report/ar5/syr/.

Janda, R.J., Meyer, D.F., and Childers, D., 1984, Sedimentation and geomorphic changes during and following the 1980–1983 eruptions of Mount St. Helens, Washington: Shin-Sabo, v. 37, no. 2, p. 10–21, and v. 37, no. 3, p. 5–19.

Janda, R.J., Scott, K.M., Nolan, K.M., and Martinson, H.A., 1981, Lahar movement, effects, and deposits, *in* Lipman, P.W., and Mullineaux, D.R., eds., The 1980 eruptions of Mount St. Helens, Washington: U.S. Geological Survey Professional Paper 1250, p. 461–478.

Javernick, L., Brasington, J., and Caruso, B., 2014, Modeling the topography of shallow braided rivers using Structure-from-Motion photogrammetry: Geomorphology, v. 213, p. 166–182.

Korup, O., Seidemann, J., and Mohr, C.H., 2019, Increased landslide activity on forested hillslopes following two recent volcanic eruptions in Chile: Nature Geoscience, v. 12, p. 284–289.

Leavesley, G.H., Lusby, G.C., and Lichty, R.W., 1989, Infiltration and erosion characteristics of selected tephra deposits from the 1980 eruption of Mount St. Helens, Washington, USA: Hydrological Sciences Journal, v. 34, p. 339–353.

Lettenmaier, D.P., and Burges, S.J., 1981, Estimation of flood frequency changes in the Toutle and Cowlitz River basins following the eruption of Mt. St. Helens: University of Washington Department of Civil Engineering Water Resources Series Technical Report 69, 73 p., accessed December 2019 at https://www.ce.washington.edu/sites/cee/files/pdfs/research/hydrology/water-resources/WRS069.pdf.

Lipman, P.W., and Mullineaux, D.R., eds., 1981, The 1980 Eruptions of Mount St. Helens, Washington: U.S. Geological Survey Professional Paper 1250, 844 p.

Lisle, T.E., Major, J.J., and Hardison, J.H., 2018, Geomorphic response of the Muddy River basin to the 1980 eruptions of Mount St. Helens, 1980–2000, *in* Crisafulli, C., and Dale, V., eds., Ecological responses at Mount St. Helens—Revisited 35 years after the 1980 eruption: New York, Springer, p. 45–70.

Major, J.J., 2004, Posteruption suspended sediment transport at Mount St. Helens—Decadal-scale relationships with landscape adjustments and river discharges: Journal of Geophysical Research, v. 109, art. no. F01002, https://doi.org/10.1029/2002JF000010.

Major, J.J., Bertin, D., Pierson, T.C., Amigo, Á., Iroumé, A., Ulloa, H., and Castro, J., 2016, Extraordinary sediment delivery and rapid geomorphic response following the 2008–2009 eruption of Chaitén Volcano, Chile: Water Resources Research, v. 52, p. 5075–5094.

Major, J.J., and Mark, L.E., 2006, Peak flow responses to landscape disturbances caused by the cataclysmic 1980 eruption of Mount St. Helens, Washington: Geological Society of America Bulletin 118, p. 938–958.

Major, J.J., Mosbrucker, A.R., and Spicer, K.R., 2018, Sediment erosion and delivery from Toutle River basin after the 1980 eruption of Mount St. Helens—A 30-year perspective, *in* Crisafulli, C., and Dale, V., eds., Ecological responses at Mount St. Helens—Revisited 35 years after the 1980 eruption: New York, Springer, 19–44.

Major, J.J., Pierson, T.C., Dinehart, R.L., and Costa, J.E., 2000, Sediment yield following severe volcanic disturbance—a two-decade perspective from Mount St. Helens: Geology, v. 28, p. 819–822.

Major, J.J., Pierson, T.C., and Scott, K.M., 2005, Debris flows at Mount St. Helens, Washington, USA, *in* Jakob, M., and Hungr, O., eds., Debris-flow hazards and related phenomena: Berlin, Springer-Praxis, p. 685–731.

Major, J.J., Zheng, S., Mosbrucker, A.R., Spicer, K.R., Christianson, T., and Thorne, C.R., 2019, Multi-decadal geomorphic evolution of a profoundly disturbed gravel bed river system—a complex, nonlinear response and its impact on sediment delivery: Journal of Geophysical Research Earth Surface, v. 124, https://doi.org/10.1029/2018JF004843.

Manville, V., Hodgson, K.A., and Nairn, I.A., 2007, A review of break-out floods from volcanogenic lakes in New Zealand: New Zealand Journal of Geology and Geophysics, v. 50, p. 131–150.

Marks, D., Kimball, J., Tingey, D., and Link, T., 1998, The sensitivity of snowmelt processes to climate conditions and forest cover during rain-on-snow—A case study of the 1996 Pacific Northwest flood: Hydrological Processes, v. 12, p. 1569–1587.

Meadows T., 2014, Forecasting long-term sediment yield from the upper North Fork Toutle River, Mount St. Helens, USA: Nottingham, England, University of Nottingham, Ph.D. dissertation, accessed December 2019 at http://eprints.nottingham.ac.uk/27800/1/Thesis_FINAL_TM.pdf.

Meyer, D.F., 1995, Stream-channel changes in response to volcanic detritus under natural and augmented discharge, South Coldwater Creek, Washington: U.S. Geological Survey Open-File Report 94–519, 137 p.

Meyer, D.F., and Dodge, J.E., 1988, Post-eruption changes in channel geometry of streams in the Toutle River drainage basin, 1983–85, Mount St. Helens, Washington: U.S. Geological Survey Open-File Report 87–549, 226 p.

Meyer, D.F., and Martinson, H.A., 1989, Rates and processes of channel development and recovery following the 1980 eruption of Mount St. Helens, Washington: Hydrological Sciences Journal, v. 34, p. 115–127.

Meyer, D.F., Nolan, K.M., and Dodge, J.E., 1986, Post-eruption changes in channel geometry of streams in the Toutle River drainage basin, 1980–82, Mount St. Helens, Washington: U.S. Geological Survey Open-File Report 85–412, 128 p.

Meyer, W., Sabol, M.A., and Schuster, R., 1986, Landslide dammed lakes at Mount St. Helens, Washington, *in* Schuster, R.L., ed., Landslide dams—Processes, risks, and mitigation: American Society of Civil Engineers Geotechnical Special Publication 3, p. 21–41.

Mosbrucker, A., 2014, High-resolution digital elevation model of Mount St. Helens crater and upper North Fork Toutle River basin, Washington, based on an airborne lidar survey of September 2009: U.S. Geological Survey Data Series 904, accessed December 2019 at https://doi.org/10.3133/ds904.

Mosbrucker, A.R., 2015, High-resolution digital elevation model of lower Cowlitz and Toutle River, adjacent to Mount St. Helens, Washington, based on airborne lidar survey of October 2007: U.S. Geological Survey Data Series 936, accessed December 2019 at https://doi.org/10.3133/ds936.

Mosbrucker, A.R., 2019, Digital elevation models of Mount St. Helens crater and upper North Fork Toutle River basin, based on 1987 and 1999 photogrammetry surveys: U.S. Geological Survey data release, accessed December 2019 at https://doi.org/10.5066/P96B0IEC.

Mosbrucker, A.R., 2020, High-resolution digital elevation model of Mount St. Helens and upper North Fork Toutle River basin, based on airborne lidar surveys of July–September, 2017: U.S. Geological Survey data release, accessed March 2020 at https://doi.org/10.5066/P9H16RC7.

Mosbrucker, A.R., Major, J.J., Spicer, K.R., and Pitlick, J., 2017, Camera system considerations for geomorphic applications of SfM photogrammetry: Earth Surface Processes and Landforms, v. 42, p. 969–986.

Mosbrucker, A.R., Spicer, K.R., and Major, J.J., 2019, North Fork Toutle River debris flows initiated by atmospheric rivers—November 2006: SEDHYD Federal Interagency Sediment and Hydrology Conference, proceedings, accessed December 2019 at https://www.sedhyd.org/2019/openconf/modules/request.php?module=oc_program&action=view.php&id=202&file=1/202.pdf

Mosbrucker, A.R., Spicer, K.R., Major, J.J., Saunders, D.R., Christianson, T.S., and Kingsbury, C.G., 2015, Digital database of channel cross-section surveys, Mount St. Helens, Washington: U.S. Geological Survey Data Series 951, accessed December 2019 at http://doi.org/10.3133/ds951.

Mosbrucker, A.R., and Sweeney, K.E., 2019, Digital terrain models of Spirit Lake blockage and Mount St. Helens debris avalanche deposit, based on 1980–2018 airborne photogrammetry surveys: U.S. Geological Survey data release, accessed December 2019 at https://doi.org/10.5066/P96OCPSQ.

Mullineaux, D.R., and Crandell, D.R., 1962, Recent lahars from Mount St. Helens, Washington. Geological Society of America Bulletin, v. 73, p. 855–870.

National Academies of Sciences, Engineering, and Medicine, 2017, A decision framework for managing the Spirit Lake and Toutle River system at Mount St. Helens, Washington: Washington, D.C., The National Academies Press, 203 p., accessed December 2019 at https://doi.org/10.17226/24874.

Natural Resources Conservation Service, 2019, Spirit Lake snow telemetry (SNOTEL) site number 777: U.S. Department of Agriculture National Water and Climate Center website, accessed April 2019, at https://wcc.sc.egov.usda.gov/nwcc/site?sitenum=777.

Neiman, P.J., Ralph, F.M., Wick, G.A., Kuo, Y.-H., Wee, T.-K., Ma, Z., Taylor, G.H., and Dettinger, M.D., 2008, Diagnosis of an intense atmospheric river impacting the Pacific Northwest: Storm summary and offshore vertical structure observed with COSMIC satellite retrievals: Monthly Weather Review, v. 136, p. 4398–4420.

Neiman, P.J., Schick, L.J., Ralph, F.M., Hughes, M., and Wick, G.A., 2011, Flooding in western Washington—the connection to atmospheric rivers: Journal of Hydrometeorology, v. 12, p. 1337–1358.

Nicholas, A.P., 2013, Modelling the continuum of river channel patterns: Earth Surface Processes and Landforms, v. 38, p. 1187–1196.

Paine, A.M., Meyer, D.F., and Schumm, S.A., 1987, Incised channel and terrace formation near Mount St. Helens, Washington, *in* Beschta, R.L., Blinn, T., Grant, G.E., Ice, G.G., and Swanson, F.J., eds., Erosion and sedimentation in the Pacific Rim: International Association of Hydrological Sciences Publication 165, p. 389–390.

Parsons, M.R., 1985, Spatial and temporal changes in stream network topology—Post-eruption drainage, Mount St. Helens: Corvallis, Oregon State University, Ph.D. dissertation, 180 p., accessed December 2019 at https://ir.library.oregonstate.edu/concern/graduate_thesis_or_dissertations/qf85nf267.

Pierson, T.C., 1999, Transformation of water flood to debris flow following the eruption-triggered transient-lake breakout from the crater on March 19, 1982, *in* Pierson, T.C., ed., Hydrologic consequences of hot-rock/snowpack interactions at Mount St. Helens Volcano, Washington: U.S. Geological Survey Professional Paper 1586, p. 19–36.

Pierson, T.C., and Janda, R.J., 1994, Volcanic mixed avalanches—A distinct eruption-triggered mass-flow process at snow-clad volcanoes: Geological Society of America Bulletin, v. 106, p. 1351–1358.

Pierson, T.C., and Major, J.J., 2014, Hydrogeomorphic effects of explosive volcanic eruptions on drainage basins: Annual Review of Earth and Planetary Sciences, v. 42, p. 469–507.

Pierson, T.C., and Waitt, R.B., 1999, Dome-collapse rockslide and multiple sediment-water flows generated by a small explosive eruption on February 2–3, 1983, *in* Pierson, T.C., ed., Hydrologic consequences of hot-rock/snowpack interactions at Mount St. Helens Volcano, Washington: U.S. Geological Survey Professional Paper 1586, p. 53–68.

Poland, M.P., and Lu, Z., 2008, Radar interferometry observations of surface displacements during pre- and coeruptive periods at Mount St. Helens, Washington, 1992–2005, chap. 18 *of* Sherrod, D.R., Scott, W.E., and Stauffer, P.H., eds., A Volcano Rekindled—The renewed eruption of Mount St. Helens, 2004–2006: U.S. Geological Survey Professional Paper 1750, p. 361–382.

Pringle, P.T., and Cameron, K.A., 1999, Eruption-triggered lahar on May 4, 1984, *in* Pierson, T.C., ed., Hydrologic consequences of hot-rock/snowpack interactions at Mount St. Helens Volcano, Washington: U.S. Geological Survey Professional Paper 1586, p. 81–103.

Renshaw, C.E., Magilligan, F.J., Doyle, H.G., Dethier, E.N., and Kamtack, K.M., 2019, Rapid response of New England (USA) rivers to shifting boundary conditions—Processes, time frames, and pathways to post-flood channel equilibrium: Geology, v. 47, p. 997–1000.

Rosenfeld, C.L., and Beach, G.L., 1983, Evolution of a drainage network—Remote sensing analysis of the North Fork Toutle River, Mount St. Helens, Washington: Corvallis, Oregon State University Press, Water Resources Research Institute publication WRRI 88, 96 p.

Rowley, P.D., Kuntz, M.A., and MacLeod, N.S., 1981, Pyroclastic-flow deposits, *in* Lipman, P.W., and Mullineaux, D.R., eds., The 1980 Eruptions of Mount St. Helens, Washington: U.S. Geological Survey Professional Paper 1250, p. 489–512.

Sager, J.W., and Chambers, D.R., 1986, Design and construction of the Spirit Lake outlet tunnel, Mount St. Helens, Washington, *in* Schuster, R.L., ed., Landslide dams—Processes, risks, and mitigation: American Society of Civil Engineers Geotechnical Special Publication 3, p. 42–58.

Schumm, S.A., 1999, Causes and controls of channel incision, *in* Darby, S.E., and Simon, A., eds., Incised river channels: West Sussex, England, Wiley and Sons, p. 19–33.

Schumm, S.A., Harvey, M.D., and Watson, C.C., 1984, Incised channels—Morphology, dynamics, and control: Littleton, Colo., Water Resources Publications, 208 p.

Sclafani, P., Nygaard, C., and Thorne, C.R., 2018, Applying geomorphological principles and engineering science to develop a phased sediment management plan for Mount St. Helens, Washington: Earth Surface Processes and Landforms, v. 43, p. 1088–1104.

Scott, K.M., 1988, Origin, behavior, and sedimentology of prehistoric catastrophic lahars at Mount St. Helens, Washington: Geological Society of America Special Paper 229, p. 23–36.

Simon, A., 1999, Channel and drainage-basin response of the Toutle River system in the aftermath of the 1980 eruption of Mount St. Helens, Washington: U.S. Geological Survey Open-File Report 96–633, 130 p.

Simon, A., and Hupp, C.R., 1986, Geomorphic and vegetative recovery processes along modified Tennessee streams—An interdisciplinary approach to disturbed fluvial systems: International Association of Hydrological Sciences, Proceedings of Vancouver Symposium on Forest Hydrology and Watershed Management, IAHS-AISH Publication 167, p. 251–262.

Simon, A., and Hupp, C.R., 1987, Channel evolution in modified alluvial streams: Transportation Research Record, v. 1151, p. 16–24.

Simon, A., and Klimetz, D., 2012, Analysis of long-term sediment loadings from the upper North Fork Toutle River system, Mount St. Helens, Washington: Washington, D.C., U.S. Department of Agriculture, Agricultural Research Service, National Sedimentation Laboratory Technical Report 77, 109 p., accessed December 2019 at https://www.ars.usda.gov/ARSUserFiles/60600500/NSL%20Report%2077-Final.pdf.

Simon, A., and Rinaldi, M., 2006, Disturbance, stream incision, and channel evolution—The roles of excess transport capacity and boundary materials in controlling channel response: Geomorphology, v. 79, p. 361–383.

Simon, A., and Thorne, C.R., 1996, Channel adjustment of an unstable coarse-grained stream—opposing trends of boundary and critical shear stress, and the applicability of extremal hypotheses: Earth Surface Processes and Landforms, v. 21, p. 155–180.

Swanson, F.J., and Major, J.J., 2005, Physical events, environments, and geological-ecological interactions at Mount St. Helens—March 1980–2004, *in* Dale, V.H., Swanson, F.J., and Crisafulli, C.M., eds., Ecological responses to the 1980 eruption of Mount St. Helens: , New York, Springer, p. 27–44.

Tunnicliffe, J., Brierley, G., Fuller, I., Leenman, A., Marden, M., and Peacock, D., 2018, Reaction and relaxation in a coarse-grained fluvial system following catchment-wide disturbance: Geomorphology, v. 307, p. 50–64.

Turner, D., Lucieer, A., and Watson, C., 2012, An automated technique for generating georectified mosaics from ultra-high resolution unmanned aerial vehicle (UAV) imagery, based on Structure from Motion (SfM) point clouds: Remote Sensing, v. 4, p. 1392–1410.

University of Washington Libraries, 2018, Mount St. Helens—Lidar data: University of Washington Libraries website, accessed August 2018, at https://wagda.lib.washington.edu/data/type/elevation/lidar/st_helens/toutle03.html.

Waitt, R.B., Pierson, T.C., MacLeod, N.S., Janda, R.J., Voight, B., and Holcomb, R.T., 1983, Eruption-triggered avalanche, flood, and lahar at Mount St. Helens—effects of winter snowpack: Science, v. 221, p. 1394–1397.

Welch, M.D., and Schmidt, D.A., 2017, Separating volcanic deformation and atmospheric signals at Mount St. Helens using persistent scatterer InSAR: Journal of Volcanology and Geothermal Research, v. 344, p. 52–64.

White, J.D.L., Houghton, B.F., Hodgson, K.A., and Wilson, C.J.N., 1997, Delayed sedimentary response to the A.D. 1886 eruption of Tarawera, New Zealand: Geology, v. 25, p. 459–462.

Zheng, S., Baosheng, W., Thorne, C.R., and Simon, A., 2014, Morphological evolution of the North Fork Toutle River following the eruption of Mount St. Helens, Washington: Geomorphology, v. 208, p. 102–116.

Menlo Park Publishing Service Center, California
Manuscript approved for publication March 13, 2020
Edited by Claire Landowski and Regan Austin
Layout and design by Kimber Petersen
Illustration support by JoJo Mangano

Major and others—**A Multidecade Analysis of Fluvial Geomorphic Evolution of the Spirit Lake Blockage, Mount St. Helens, Washington**—Scientific Investigations Report 2020–5027, April 2020

ISSN 2328-0328 (online)